

DESIGN AND DEVELOPMENT OF VOLTAGE REGULATOR FOR 3-PHASE SELF EXCITED INDUCTION GENERATOR

A DISSERTATION

Submitted in partial fulfilment of the
requirements for the award of the degree

of

MASTER OF ENGINEERING

in

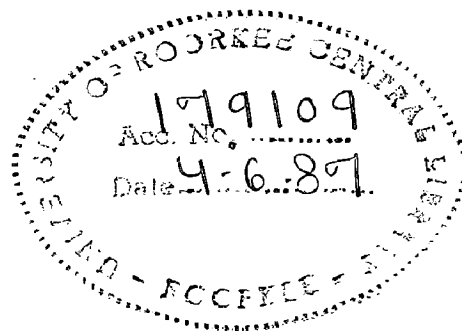
ELECTRICAL ENGINEERING

(Power Apparatus and Electric Drive)

By

DEVENDRA KUMAR SHARMA

CHECKED
1985



DEPARTMENT OF ELECTRICAL ENGINEERING
UNIVERSITY OF ROORKEE
ROORKEE-247 667 (INDIA)

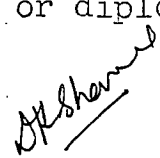
September, 1986

CANDIDATE'S DECLARATION

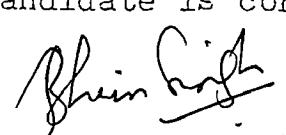
I hereby certify that the work which is being presented in the dissertation entitled "Design And Development of Voltage Regulator for 3-phase Self Excited Induction Generator" in the partial fulfilment of the requirements for the degree of MASTER OF ENGINEERING in ELECTRICAL ENGINEERING with specialisation in POWER APPARATUS AND ELECTRIC DRIVE submitted in the department of Electrical Engineering, University of Roorkee, Roorkee is an authentic record of my own work carried out during a period of 11 months, from August, 1984 to April, 1985 and from June, 1986 to July 1986 under the supervision of Dr. R.B.Saxena, Professor, Electrical Engineering Department and Dr. Bhim Singh, Lecturer, Electrical Engineering Department, University of Roorkee, Roorkee (India).

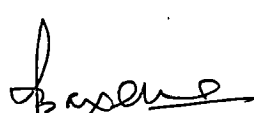
The matter embodied in this dissertation has not been submitted for the award of any other degree or diploma.

Dated:


(DEVENDRA K. SHARMA)

This is certified that the above statement made by the candidate is correct to the best of our knowledge.


(DR. BHIM SINGH)
Lecturer, Elect.Engg.Deptt.,
University of Roorkee
Roorkee


(DR. R.B.SAXENA)
Professor, Elect.Engg.Deptt.
University of Roorkee
Roorkee

Dated:

ACKNOWLEDGEMENTS

I would like to express my deep gratitude to Dr. R.B.Saxena, Professor, Electrical Engineering Department, and to Dr. Bhim Singh, Lecturer, Electrical Engineering Department, University of Roorkee, Roorkee for the magnitude of their benevolence and eternal guidance. It was their consistent encouragement without which this work could not have been carried out.

I am also grateful Dr. P.Mukhopadhyay, Prof. & Head, Electrical Engineering Department, for providing excellent facilities and most favourable working conditions.

I am indebted to Sh. Pramod Agarwal, Lecturer, Electrical Engineering Department for his invaluable suggestions.

Thanks are due to Sh. S.K.Banerjee, Research Technician and staff of P.G. Lab for their assistance throughout the tenure of my dissertation.

Last but not least, I am highly obliged to my friends, relatives and colleagues who have directly or indirectly helped me during this work.

Dated

ROORKEE



(DEVENDRA K. SHARMA)

ABSTRACT

An approach to the design of voltage regulating system for self excited induction generator is presented. The steady state analysis of self excited induction generator has been done with the help of equivalent circuit. 'Newton Raphson Method' has been adopted to solve the nonlinear simultaneous equations which appear during the analysis of the machine. The computer programs have been developed for the computation of unknown variables of nonlinear simultaneous equations and machine performance. The computed results are presented and critically discussed.

The selection of various components of voltage regulating system has been made for fabricating a practical firing control circuit. The parameters of P and PI-controllers are selected on the basis of experimental observations.

The performance study for steady state and transient response has been observed with P and PI-controllers separately to show the response and stability of the voltage regulating system.

The extensive tests have been performed to study steady state and transient performance of voltage regulating system with P and PI-controller. It is observed that in the developed voltage regulator is capable of regulating voltage for adequate load without losing self excitation.

NOMENCLATURE

Most of the symbols are already defined in the text.

However, for easy reference some important symbols are listed below:

$CVAR$	=	Capacitive VAR
F, ω	=	Output frequency and rotor speed
I_S, I_R	=	Stator, rotor current per phase
I_C	=	Capacitor current per phase
I_L	=	Load current per phase
I_{IND}	=	Inductor current per phase
P_{GEN}	=	Generated power
P_{OUT}	=	Output power
R_S, R_R	=	Stator, rotor resistance per phase
$R_L \text{ \& } X_L$	=	Load resistance and reactance per phase
V_{REF}	=	Reference voltage
V_G, V_T	=	Air gap, terminal voltage per phase
VA_{OUT}	=	Apparent output power
X_{LS}, X_{LR}	=	Stator, rotor leakage reactance per phase
X_C	=	Capacitive reactance per phase
X_m	=	Saturated magnetising reactance per phase
$X_{C \text{ Max}}$	=	Maximum capacitive reactance
$X_{M \text{ Max}}$	=	Unsaturated magnetising reactance
Z_S	=	Impedance of whole network
α	=	Firing Angle
γ	=	Conduction Angle

CONTENTS

	Page No.
CANDIDATE'S DECLARATION	(i)
ACKNOWLEDGEMENT	(ii)
ABSTRACT	(iii)
NOMENCLATURE	(iv)
CHAPTER-1 : INTRODUCTION	1-6
CHAPTER-2 : LITERATURE REVIEW	7-11
CHAPTER-3 : ANALYSIS OF SELF EXCITED INDUCTION GENERATOR	12-38
Summary	12
3.1 Introduction	12-14
3.2 Theory	14
3.2.1 Case - I	15-17
3.2.2 Case - II	17-19
3.2.3 Case - III	20-21
3.2.4 Case - IV	21-23
3.3 Digital Simulation	23-27
3.4 Experimental Set-up and Machine Parameters	27-29
3.5 Results and Discussion	29-37
3.6 Conclusion	37-38
CHAPTER-4 : DESIGN AND FABRICATION OF VOLTAGE REGULATOR	39-53
4.1 Summary	39
4.1 Introduction	39-40
4.2 Description of Closed Loop Control System	40-41
4.3 Principle of Operation	41-43
4.4 Selection of Thyristors	43-44
4.5 Selection of Inductor and Capacitor	44-46
4.6 Design of Firing Circuit	46-51
4.6.1 Design of Input Transformers	46-47

4.6.2	Attenuator Circuit	47
4.6.3	Zero Crossing Detector	47
4.6.4	Constant Current Ramp Generator	47-48
4.6.5	Comparator	48
4.6.6	AND Gate	48-49
4.6.7	High Frequency Oscillator	49
4.6.8	Pulse Amplifier	50-51
4.7	Design of Voltage Feedback Circuit	51
4.8	Design of Controller	51-53
4.9	Conclusion	53
CHAPTER-5	: PERFORMANCE OF VOLTAGE REGULATING SYSTEM	54-60
	Summary	54
5.1	Introduction	54-55
5.2	Experimentation	55
5.3	Result and Discussion	55-59
5.4	Conclusion	50-60
CHAPTER-6	: CONCLUSION AND SCOPE FOR FURTHER WORK	61-64
	Summary	61
6.1	Main Conclusion	61-64
6.2	Scope for Further Work	64
	REFERENCES	65-68
APPENDIX-A	THE CONSTANTS APPEARING IN NONLINEAR SIMULTANEOUS EQUATIONS	69-70
APPENDIX-B	DETAILS OF EXPERIMENTAL SETUP AND MACHINE PARAMETERS	71
APPENDIX-C	COMPUTER PROGRAM FOR NO LOAD	72-74
APPENDIX-D	COMPUTER PROGRAM FOR FIXED CAPACITANCE	75-79
APPENDIX-E	COMPUTER PROGRAM FOR CONSTANT TERMINAL VOLTAGE	79-82
APPENDIX-F	COMPUTER PROGRAM FOR CONSTANT V_G/F (Air gap flux)	83-86

CHAPTER - 1

INTRODUCTION

The increasing importance of fuel saving has been responsible for the revival of interest in so called alternative sources of energy. So with the drive towards the decentralization of power generation and the increasing use of non-conventional energy sources, such as wind energy, bio gas and perennial hydel potentials, it has become essential to adopt a low cost generating system which is capable of operating in remote areas and from a variety of prime movers. With the renewed interest in wind turbines as an alternative energy source, the self excited induction generators are being considered as an alternative choice to well developed synchronous generators.

The induction machine can be utilised as ^a generator in two ways. The first one is through 'regeneration' and second, is through 'self excitation'. If a squirrel cage induction motor is connected to an alternating current power source of appropriate voltage and frequency, it can operate either as a motor or as a generator. (The) regeneration is possible if the induction machine is connected to the line and its rotor is made to run above the synchronous speed. Here, the terminal voltage applied to the induction machine is 'to maintain the excitation' by producing a lagging (magnetising) current which in turn results in the rotating magnetic flux necessary for both motoring and regeneration.

If an appropriate three phase capacitor bank is connected across the terminals of a rotating induction machine, it may remain excited even after the line voltage is disconnected and machine is driven by some external source. Here an emf is induced in the machine due to the excitation provided by the capacitors. This phenomenon is termed as the 'capacitor self excitation'. Induction machine operating under this mode is referred to as self excited induction generator.

The self excited induction generators do not require any sophisticated control and can provide reliable and relatively inexpensive means to generate electricity for loads where small frequency variations are allowed up to some extent. (The) induction generators have attracted new attention due to their superior characteristics compared to synchronous generators for wind electric conversion systems (WEC's) and with recent improvements in cost, effectiveness of semiconductor devices and thus of static VAR controller, the self excited induction generators can be a cheap solution to the problem of electricity supply in remote areas where non conventional energy potentials are available.

Self excited induction generator can be used to generate power from variable speed prime movers i.e. wind turbine etc. It has become a common practice for small wind electric conversion systems and hydroplants to use induction generators instead of synchronous machines. But when an induction motor is used as generator, its efficiency is slightly lower due to higher core losses. The rotor heating is also a limiting factor for

the induction generator. Even than it can be noted that the utilization of induction generators as a source of isolated power supply in remote areas is very promising and attractive.

There are certain advantages of using squirrel cage induction machine as self excited induction generator. The squirrel cage induction machine is very robust and reliable, requiring minimum maintenance. In isolated systems, the excitation can be obtained from remanent magnetism if suitable bank of capacitors is connected across armature terminals and hence does not require separate D.C. excitation source. It has almost maintenance free operation due to absence of brushes and separate D.C. source. Induction generator can also be used as isolated or standby power source driven by constant speed prime movers such as diesel engines as well as variable speed prime movers like wind turbines etc. A distinctive advantage of such generator is the much lower cost as compared to the conventional alternators.

In the process of self excitation induction machine behaves at first as synchronous machine with a weak permanent magnet rotor and then as an asynchronous machine as the terminal voltage rises to a useful value. The induced voltages and currents would continue to rise but the magnetic saturation in induction machine results to reach an equilibrium state. The generated voltage will be dependent ^{on} (of) the value of capacitance, load current and load power factor.

For a given capacitance the induction generator starts building up voltage at a minimum speed (out-in-speed). The

minimum capacitance for self excitation is inversely proportional to the square of speed. Once the excitation has occurred, the induced voltage builds up quite rapidly and may reach dangerously high value.

To maintain the generated voltage constant with varying loads of different power factor, a fixed leading current equal to magnetism current and a variable be adding current corresponding to rotor current and load current are needed. Consequently to cope with varying load and/or speed variation of self excited induction generator, the voltage control can be suitably based on adjustable reactive power generators connected to the terminals of induction machine.

Static VAR compensators provide a continuously varying VAR to achieve desired voltage regulation at different loads and speed conditions. The static VAR compensation techniques can be categorised as follows:

1. Naturally commutated inductive VAR generators
2. Forced commutated VAR generators

The category first includes three phase fully controlled rectifier coupled to a purely inductive load, the phase controlled inductor (star or delta) and the cyclo-converter with an auxiliary high frequency bank circuit to facilitate commutation.

Anyone of the above mentioned arrangements produces lagging VAR's supplied by fixed capacitors across the induction generator terminals.

The second category includes a turn-off arrangement for the thyristors in a bridge which produces leading VAR's by controlling effective capacitance and therefore leading VAR's can also be controlled as per the load and speed.

Scope of Work - The present work includes the design and development of voltage regulator for a three phase self excited induction generator. The dissertation describes about steady state analysis, design of various components for voltage regulator and the experimental study of this voltage regulating system.

Beginning with the exhaustive literature review in second chapter the steady state analysis has been done ⁱⁿ third chapter. The literature has been reviewed in a chronological order to find out the possible gaps and their remedies. The steady state analysis of self excited induction generator has been done for different loads by considering four cases. The third chapter describes about the use of 'Newton Raphson Method' to solve the non linear equations appearing in the analysis. The flow charts for the different computer programs have been discussed and results have been presented to give a comparison of ^p computed and experimental results for different loads and to provide guide lines for the design of voltage regulator. The fourth chapter consists of the design and fabrication of voltage regulator. The details of the firing circuit, controllers and selection of capacitor and inductor are given in the same

chapter. The fifth chapter includes the steady state and transient performance of the voltage regulating system at different values of loads. The main conclusion and suggestions for the further work are narrated in the last chapter.

CHAPTER - 2

LITERATURE REVIEW

Although the phenomenon of self excitation was realized back in twenties but no proper step was taken for its practical suitability at that time. As the time is changing rapidly and energy demands are increasing day by day, the utilization of non-conventional sources of energy has become essential. In this regard people have proposed the idea to make use of self excited induction generator where non-conventional sources of energy are abundantly available.

D.W. Novotony, Gritter and Studtmann [16] have discussed regarding the excitation in inverter driveⁿ induction machines. They describe that the electrical output of the system is governed by the slip and system performance is controlled by magnetisation characteristic, stator and rotor resistances of the machines. The utilization of squirrel cage induction motor as an autonomous induction generator has been discussed by Michael B. Brennen and Abbondanti [1]. The paper describes the simple excitor^e scheme with fixed capacitors and thyristor controlled inductors suitable for balanced as well as unbalanced loads.

The problem of voltage and frequency variations is inherent in self excited induction generators. To eliminate this problem an alternative solution was given by J. Arrillaga and Watson [3] by using self excited induction generator with

controlled rectifier unit. The paper describes the operation of such ^a system for variable d.c. load at constant voltage feeding of controllable power into an existing a.c. network through a d.c. transmission link. The operation of self excited induction generator at variable speed prime mover i.e. wind Mill is described by H.R. Bolton and Nicodemou [2]. The idea adopted by J. Arrillaga and Watson [19] has been extended by Watson, Arrillaga and Densem [24] to use three phase squirrel cage induction motor with self excitation for wind power sources at variable speeds and to generate optimum power by delay angle control of rectifier. Laszlo Gyugi [6] has reviewed the possible methods of VAR generation and control by Static thyristor circuits.

Regarding the steady state analysis Murthy, Malik and Tandon [10] collectively presented an analytical technique using 'Newton Raphson Method' to identify the saturated magnetising reactance and the generated frequency of a self excited induction generator for a given capacitance, speed and load. Effects of various parameters on the steady state have also been described to provide guide lines for optimum design of such systems. The physical interpretation of self excitation in induction machines and its important parameters like shaft speed. The reduced permeability at low magnetisation and size of capacitors have been discussed by Elder, Boys and Woodward [4].

J.A.A. Melkebeek [11] describes the application of saturated model for the stability behaviour of voltage fed induction

motor and self excited induction generator. The necessity of improved model has also been pointed out due to the unrealistic predictions of classical model. The small signal stability and dynamic response for six modes of induction generator operation including both voltage and current inverter system have been examined and compared by J.A.A. Malkebeek [12]. He has introduced an improved small signal model, considering main flux saturation to study the stability properties of all six modes. The capacitive self excited case is shown to require special treatment because of the phase freedom inherent in this mode.

Malik, Divan, Murthy, Grant and Walsh [13] collectively describe a solid state voltage regulator for self excited induction generator by using fully controlled converter to compensate the capacitive VAR's of fixed capacitors across the generator terminals Patel and Dubey [20] describe a new method for the reduction of harmonic generated in the supply system due to the discontinuous current in the thyristor controlled reactor of a static VAR compensator. Elder, Boys and Woodward [5] describe the use of self excited induction generator as low cost stand alone generators, including the problem of guaranteeing excitation and its behaviour under balanced and unbalanced conditions.

John R. Parsons [7] describe the suitability of induction generator for many industrial cogeneration applications. The application of 3000 KW induction generator is compared to that of a comparably sized synchronous machine considering

their relative costs, equipment, protective relaying, utility tie-in and synchronising, maintenance and operating procedures. Under steady state analysis Murthy, Malik and Walsh [14] have discussed about the leading VAR required for the self excited induction generators at constant/variable speed. The analytical technique uses the 'Newton Raphson Method' to determine the saturated magnetising reactance. The rotor heating is the limiting factor on the power that can be obtained from the self excited induction machines. This point has been discussed by Murthy, Satyanarayan, Singh and Nagmani [15]. The steady state performance of the generator maintaining constant terminal voltage is also analysed by using 'Newton Raphson Method'. George Kontos and Lytsikas [8] describe about the effects of the harmonic currents and minimisation under the steady state operation of 3- ϕ induction generator with a 3- ϕ voltage fed autonomous inverter.

Vander Wag and Inculet [23] describe the induction generation scheme with an attempt to minimise or possibly eliminate the excitation power normally provided by a bank of capacitors. The advantages and its performance at variable speeds have been described by Nagrial and Shami [17].

Tandon, Murthy and Jha [22] have proposed a simpler approach to compute the saturated magnetising reactance and frequency under steady state operation of a self excited induction generator. S. Berchten [3] has described about the current state space form for the capacitor self excited induction generator to predict the steady state performance under

different conditions. Watson and Milner [25] describe the steady state analysis of the self excited induction generator as autonomous and parallel operated.

From the review of literature it is observed that no effort has been made till now regarding the generalised approach to analyse the steady state performance of self excited induction generator for the loads of different power factor. Here, the generalised approach has been done for the steady state analysis of the self excited induction generator which is suitable for static reactive (R-L) load, resistive (R) load and dynamic load (ac motors). Based on this analysis a voltage regulator has been designed and fabricated. The performance of this voltage regulator has been presented in terms of steady state and transient response.

CHAPTER - 3

ANALYSIS OF SELF EXCITED INDUCTION GENERATOR

Summary :-

The chapter includes the steady state analysis of self excited induction generator to extract some information for the design of voltage regulator. It presents the voltage build up at No load for different values of capacitance and effect of resistive (R) and reactive (R-L) load on the terminal voltage when the fixed capacitance is connected at the terminals of induction generator at constant/variable speeds. Further, it includes the predetermination of capacitive VAR (CVAR) requirements to keep terminal voltage (V_T) and air gap voltage to output frequency ratio (V_G/F) constant at resistive (R) and reactive (R-L) loads at constant/variable speeds. The analytical technique is based on the standard equivalent circuit and 'Newton Raphson Method' has been adopted to obtain the solution for nonlinear simultaneous equations which result from the mathematical model of equivalent circuit. Computed results have been compared with the experimental results on a 5 h.p. induction motor and a close correlation has been observed between computed and experimental values.

3.1 Introduction :-

Steady state analysis of self excited induction generator is important from the 'design and operation' point of view of

automatic voltage regulator. Knowing the parameters of the induction machine it should be possible to determine its performance for different cases at given speed and load conditions. For different cases of induction generator performance, the mathematical model results in nonlinear simultaneous equations with two unknowns namely saturated magnetising reactance and output frequency. 'Newton Raphson Method' has been found suitable to obtain the solution for these nonlinear equations. The different cases for the performance of self excited induction generator are as follows:

- Case I To find the voltage build up at no load at given capacitance and speed.
- Case II Effect of resistive (R) and reactive (R-L) load for fixed capacitance at the terminals of induction machine at given speed.
- Case III Predetermination^{of} capacitive VAR requirement to keep terminal voltage (V_T) constant at resistive (R) and reactive (R-L) load at given speed.
- Case IV Effect of resistive (R) and reactive (R-L) load on terminal voltage (V_T) and speed (ω) to keep air gap voltage to output frequency ratio (V_G/F) constant i.e. air gap flux constant.

Using 'Newton Raphson Method' the computer program has been developed to compute the unknown parameters to find out the machine performance for each case separately. Simulated results are compared with the experimental results obtained on the experimental machine under similar conditions. Both the experimental and computed results are presented graphically

and discussed to provide necessary guide-lines for the designing of voltage regulator.

3.2 Theory :-

At any speed when a suitable capacitor is connected across the terminals of induction machine the voltage starts building up due to residual magnetism in the rotor or initial charge of capacitor. As the voltage builds up, the resulting air gap flux drives the machine into saturation to get stabilised and the steady state is reached for a particular value of saturated magnetising reactance. For the present analysis the following assumptions are made:

1. In the present analysis it is assumed that all the parameters other than magnetising reactance are unaffected by the magnetic saturation.
2. Core loss in the machine is neglected.
3. Leakage reactance of stator and rotor in per unit are taken to be equalor ($X_{LS} = X_{LR} = X_1$)
4. The analysis also ignores the mmf space harmonics and the time harmonics in the generated voltage and current waveforms.

Based on the above assumptions, the steady state equivalent circuit of a self excited induction generator with resistance and inductance (R-L) series load is shown in Fig. 3.1. Where all the rotor quantities are referred to the stator and all reactances are taken on base frequency.

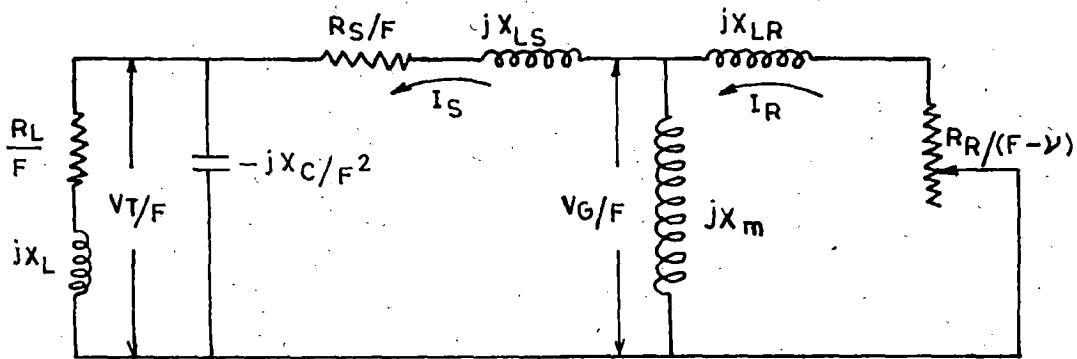


Fig. 3.1 Equivalent circuit of capacitor self excited induction generator with R-L load

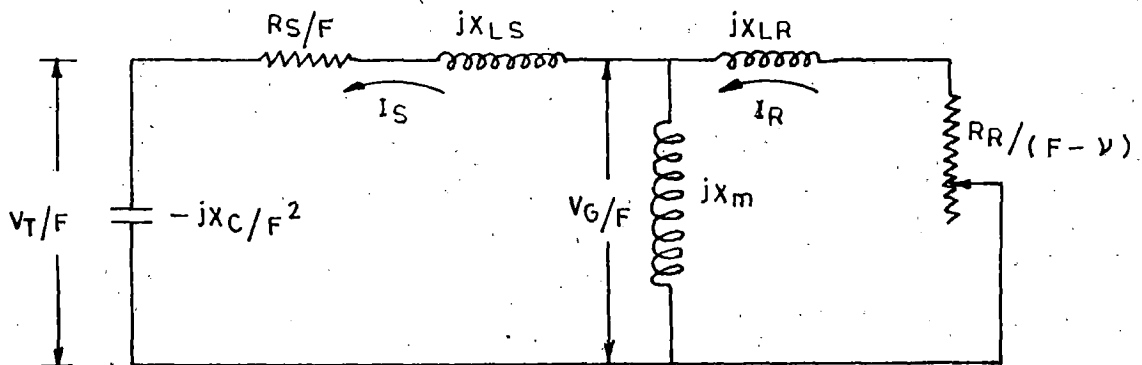


Fig. 3.2 Equivalent circuit of capacitor self excited induction generator at no load

3.2.1 Case I :-

At given speed the no load steady state equivalent circuit as shown in Fig. 3.2 can be derived from Fig. 3.1 by simply disconnecting the load from the circuit. At no load the generated voltage depends upon the speed and capacitance. At given capacitance (which fulfils the self excitation condition). The calculation can be made for generated voltage and output frequency by calculating the corresponding saturated (X_m) and frequency (F).

From the equivalent circuit in Fig. 3.2 the loop equation for current I_s can be written as:

$$Z_S I_S = 0 \quad (3.1)$$

Under steady state self excitation stator current I_s will be having some considerable value. So $I_s \neq 0$ and now from loop equation (3.1) $Z_S = 0$ (3.2)

or the impedance of the whole network is zero

where $Z_S = -j X_C/F^2 + R_S/F + j X_{LS} + j X_m + (R_R/(F-\omega) + j X_{LR})$
 Putting $X_{LS} = X_{LR} = X_1$

$$\text{Now } Z_S = -j X_C/F^2 + R_S/F + j X_1 + j X_m + (R_R/(F-\omega) + j X_1) \quad (3.3)$$

As the impedance of whole network is zero, its real and imaginary parts will be separately zero. To find X_m and F at given X_C and speed from equation (3.3), separate the real and imaginary parts as $f_1(X_m, F)$ and $g_1(X_m, F)$ respectively to put them equal to zero as nonlinear equations. So

$$f_1(X_m, F) = F^3(C_1X_m + C_2) + F^2(C_3X_m + C_4) + F(C_5X_m + C_6) + (C_7X_m + C_8) = 0 \quad (3.4)$$

$$g_1(X_m, F) = F^2(D_1X_m + D_2) + F(D_3X_m + D_4) + (D_5X_m + D_6) = 0 \quad (3.5)$$

Where $C_1, C_2 \dots C_8$ and $D_1, D_2 \dots D_6$ are constants which are defined in Appendix A.1.

The equation (3.4) and (3.5) are nonlinear algebraic equations and a suitable numerical technique is applied to calculate the value of X_m and F for different values of X_C at given speed (ω). Here 'Newton Raphson Method' has been adopted to solve these nonlinear simultaneous equations. In the 'Newton Raphson Method' the Jacobian Matrix $[J]$ is given as:

$$[J] = \begin{bmatrix} J_{11} & J_{12} \\ J_{21} & J_{22} \end{bmatrix} \quad \text{where} \quad \begin{aligned} J_{11} &= \partial f_1(X_m, F) / \partial X_m, \\ J_{12} &= \partial f_1(X_m, F) / \partial F \\ J_{21} &= \partial g_1(X_m, F) / \partial X_m \\ J_{22} &= \partial g_1(X_m, F) / \partial F \end{aligned} \quad (3.6)$$

Newton Raphson Method requires the initial guess of unknown parameters X_m and F . The initial value of output frequency F (p.u.) is equal to speed in p.u. (ω) and X_m is taken as the unsaturated magnetising reactance $X_{m \text{ Max}}$, thus

$$X_{m0} = X_{m \text{ Max}} \quad \text{and} \quad F_0 = \omega \quad (3.7)$$

Now $f_1(X_{m0}, F_0) \neq 0$ and $g_1(X_{m0}, F_0) \neq 0$

After first iteration X_m and F will assume values $(X_{m0} + h)$ and $(F_0 + K)$. In the process of satisfying equation (3.4) and (3.5), the increments h and K are given as:

$$\begin{bmatrix} h \\ k \end{bmatrix} = [J]^{-1} \begin{bmatrix} -f_1 (X_{m0}, F_0) \\ -g_1 (X_{m0}, F_0) \end{bmatrix} \quad (3.8)$$

This iterative process will remain continue until the desired accuracy is achieved i.e. $|f_1 (X_m, F)| \leq \epsilon$ and $|g_1 (X_m, F)| \leq \epsilon$. Having thus calculated X_m and F for given X_C and speed, the corresponding terminal voltage can be computed by using the equation between V_G/F and X_m . The characteristic equation between V_G/F and X_m is given in Appendix B.4.

Now knowing the equivalent circuit parameters and V_G/F , the machine performance can be evaluated as:

$$I_S = V_{G/F} / (R_S/F + j X_{LS} - j X_C/F^2) \quad (3.9)$$

$$V_T/F = V_{G/F} - I_S (R_S/F + j X_{LS})$$

$$I_C = I_S$$

$$CVAR = 3. |V_T| |I_C|$$

3.2.2 Case II

The steady state equivalent circuit of a capacitor self excited induction generator with resistance and inductance (R-L) series load has been shown in Fig. 3.1. The loop equation for stator current I_S can be written as:

$$Z_S I_S = 0 \quad (3.10)$$

$$\text{where } Z_S = (R_L/F + j X_L) \parallel (-j X_C/F^2) + (R_S/F + j X_{LS}) \\ + j X_m \parallel (R_R/(F - p) + j X_{LR})$$

Here assuming $X_{LS} = X_{LR} = X_1$

$$\begin{aligned} \text{Now } Z_S &= (R_L/F + j X_L) \parallel (-j X_C/F^2) + (R_S/F + j X_1) \\ &+ j X_m \parallel (R_R/(F - s) + j X_1) \end{aligned} \quad (3.11)$$

Under steady state self excitation, stator current (I_S) is having some considerable value so $I_S \neq 0$. Now from loop equation (3.10). It can be written:

$$Z_S = 0 \quad (3.12)$$

Or the impedance of the whole network is zero which implies that the real and imaginary parts would be separately zero. So from equation (3.11) and (3.12) two nonlinear simultaneous equations with X_m and F as unknown variables are given as:

$$\begin{aligned} f_2(X_m, F) &= F^3(C_1 X_m + C_2) + F^2(C_3 X_m + C_4) + F(C_5 X_m + C_6) \\ &+ (C_7 X_m + C_8) = 0 \end{aligned} \quad (3.13)$$

$$\begin{aligned} g_2(X_m, F) &= F^4(B_1 X_m + B_2) + F^3(B_3 X_m + B_4) + F^2(B_5 X_m + B_6) \\ &+ F(B_7 X_m + B_8) + (B_9 X_m + B_{10}) = 0 \end{aligned} \quad (3.14)$$

Where $C_1, C_2 \dots C_8$ and $B_1, B_2 \dots B_{10}$ are constants and are defined in Appendix A.2.

Equations (3.13) and (3.14) being nonlinear simultaneous equations are not easily solvable. So an appropriate numerical technique has to be adopted to calculate X_m and F for given values of machine parameters, at fixed capacitance, given speed and different loads. The 'Newton Raphson Method' has been found suitable to solve the equations (3.13) and (3.14) for the unknown parameters. The same method has been adopted for the solution of equations (3.4) and (3.5) for unknown variables X_m and F . So the Jacobian Cofactors and increments h and k will

be calculated from equation (3.13) and (3.14) in same way as in equation (3.6) and (3.8) by considering the functions $f_2(X_m, F)$ & $g_2(X_m, F)$. The initial guess of unknown variables X_m and F and iterative process will remain as such as it is done in case I.

After the determination of X_m and F , at fixed X_C and given speed corresponding V_G/F is calculated by using the V_G/F and X_m equation. The characteristic equation of V_G/F and X_m is given in Appendix B.4. Now knowing the value of V_G/F , X_m , F , X_C , ν , R_L and X_L and machine parameters, it is required to compute terminal voltage (V_T), load current (I_L), power output (POUT), in watts and VA both, power generated (PGEN), capacitive VAR (CVAR), stator current (I_S), rotor current (I_R) with the help of equivalent circuit in Fig. 3.1. Expressions for the various machine performance parameters are as follows:

$$\begin{aligned}
 I_S &= V_G/F / (R_S/F + j X_1 + (R_L/F + j X_L) \parallel (-j X_C/F^2)) \\
 V_T/F &= V_G/F - I_S (R_S/F + j X_1) \\
 I_L &= V_T/F / (R_L/F + j X_L) \\
 POUT &= 3 \cdot |I_L|^2 R_L \\
 VAOUT &= 3 \cdot |I_L| \cdot |V_T| \\
 I_C &= V_T/F / (-j X_C/F^2) \\
 CVAR &= 3 \cdot |V_T| \cdot |I_C| \\
 I_R &= -V_G/F / (R_R/(F-\nu) + j X_1) \\
 PGEN &= -3 \cdot |I_R|^2 \cdot R_R \cdot F / (F - \nu)
 \end{aligned} \tag{3.15}$$

3.2.3 Case III

Here it is required to compute capacitive reactance (X_C) and output frequency (F) at given speed and different loads to keep the terminal voltage constant. From equation (3.11) and (3.12), it yields two nonlinear simultaneous equations with X_C and F as unknown variables by putting real and imaginary parts equal to zero separately. So the two nonlinear equations can be written as:

$$f_3(X_C, F) = C_{11}F^3 + C_{12}F^2 + F(C_{13}X_C + C_{14}) + C_{15}X_C = 0 \quad (3.16)$$

$$g_3(X_C, F) = D_{11}F^4 + D_{12}F^3 + F^2(D_{13}X_C + D_{14}) + F(D_{15}X_C + D_{16}) + D_{17}X_C = 0 \quad (3.17)$$

Where C_{11} , C_{12} --- C_{15} and D_{11} , D_{12} --- D_{17} are defined in Appendix A.3.

The equation (3.16) and (3.17) being nonlinear simultaneous equations with unknown variables X_C and F are solved by using 'Newton Raphson Method'. Since the analytical technique is adopted in determining X_C and F at constant terminal voltage (V_T), a computer program has to be developed in which X_m is modified in steps with X_C and F to obtain the desired accuracy i.e. $|f_3(X_C, F)| \leq \epsilon$ and $|g_3(X_C, F)| \leq \epsilon$. In the proposed method the Jacobian matrix cofactors can be written as:

$$J_{11} = \partial f_3(X_C, F) / \partial X_C, \quad J_{12} = \partial f_3(X_C, F) / \partial F, \quad J_{21} = \partial g_3(X_C, F) / \partial X_C, \\ J_{22} = \partial g_3(X_C, F) / \partial F \quad (3.18)$$

The Newton Raphson Method' requires the initial guess of the unknown variables say X_{C0} and F_0 . Here X_{C0} is the max.

capacitive reactance (p.u.) necessary for self excitation and F_0 is equal to the p.u. speed. So $X_{CO} = X_C \text{ Max.}$ and $F_0 =$ (3.19)

It gives $f_3(X_{CO}, F_0) \neq 0$ and $g_3(X_{CO}, F_0) \neq 0$

After first iteration X_C and F will assume values as $X_{CO} + h$ and $F_0 + k$ respectively, in the process of satisfying equation (3.16) and (3.17). The increments h and k are given by

$$\begin{bmatrix} h \\ k \end{bmatrix} = [j]^{-1} \begin{bmatrix} -f_3(X_{CO}, F_0) \\ -g_3(X_{CO}, F_0) \end{bmatrix} \quad (3.20)$$

The iteration process will remain continue until the desired accuracy is achieved i.e. $|f_3(X_C, F)| \leq \epsilon$ and $|g_3(X_C, F)| \leq \epsilon$, where ϵ is the desired accuracy.

Now knowing the value of machine parameters, X_C , F at constant terminal voltage, given speed (ω) and load (R-L), the machine performance is evaluated by using equation (3.15).

3.2.4 Case IV

Here the analysis has been done on the basis of constant flux which leads to constant magnetising reactance (X_m). To keep V_G/F constant. both V_G and F are kept constant at particular values. For different loads (R and R-L), the value of X_C and ω are to be computed to keep the V_G/F ratio constant. From equation (3.11) and (3.12) two nonlinear simultaneous equations with unknown variables X_C and ω can be obtained by equating real and imaginary parts to zero separately. The equations are as follows:

$$f_4(X_C, \nu) = X_C(C_1\nu + C_2) + (C_3\nu + C_4) = 0 \quad (3.21)$$

$$g_4(X_C, \nu) = X_C(D_1\nu + D_2) + (D_3\nu + D_4) = 0 \quad (3.22)$$

Here C_1, C_2, \dots, C_4 and D_1, D_2, \dots, D_4 are constants and are defined in Appendix A.4.

Equations (3.21) and (3.22) can be solved for X_C and for each set of resistive and reactive (R-L) load by using 'Newton Raphson Method'. But to compute the constants in Appendix A.4 first of all X_m is to be found out which can be calculated by using the characteristic equation of V_G/F and X_m in Appendix B.4. The Jacobian matrix cofactors are given as follows:

$$\begin{aligned} J_{11} &= \partial f_4(X_C, \nu) / \partial X_C, & J_{12} &= \partial f_4(X_C, \nu) / \partial \nu, & J_{21} &= \partial g_4(X_C, \nu) / \partial X_C, \\ J_{22} &= \partial g_4(X_C, \nu) / \partial \nu \end{aligned} \quad (3.23)$$

The method requires the initial guess of unknown variables X_C & ν to start the iteration. Here the initial value of speed (p.u.) can be assumed as output frequency F (p.u.) and X_C can be taken as the max. capacitive reactance necessary for self excitation at that speed. Now

$$X_{CO} = X_C \text{ Max.} \quad \text{and} \quad \nu_0 = F \quad (3.24)$$

and $f_4(X_{CO}, \nu_0) \neq 0$ and $g_4(X_{CO}, \nu_0) \neq 0$

After first iteration X_C and ν will assume new values $X_{CO} + h$ and $\nu_0 + k$ respectively, in the process of satisfying equation (3.21) and (3.22). The increment h and k are given by:

$$\begin{bmatrix} h \\ k \end{bmatrix} = [J]^{-1} \begin{bmatrix} -f_4(X_{CO}, \nu_0) \\ -g_4(X_{CO}, \nu_0) \end{bmatrix} \quad (3.25)$$

The iteration and continued until the desired accuracy is reached i.e. $|f_4(X_C, \nu)| \leq \epsilon$ and $|g_4(X_C, \nu)| \leq \epsilon$ where ϵ is the desired accuracy. Now knowing the value of $X_C, \nu, X_m, V_G/F, F, RL, X_L$ and machine parameters, the machine performance can be evaluated by using equation (3.15).

3.3 Digital Simulation

As earlier shown in section 3.2 that the mathematical model of equivalent circuit results in two nonlinear simultaneous equations having two unknown variables. Newton Raphson Method has been adopted as suitable to solve these nonlinear equations. The calculations for the unknown variables are quite difficult so the computation for the unknown variables and machine performance has been done through computer program. The flow charts and computer programs are developed by using the proposed analytical technique for different cases as considered in section 3.2. The computer algorithm is developed for each case which is based on the adopted analytical technique. For case I the program reads the machine parameters, speed and X_{MC} where X_{MC} is the magnetising reactance of point C in Fig. B-1. First of all it takes the initial value of capacitance as C_{MIN} and the initial value of X_m and F as $X_{m \max}$ (unsaturated) and speed respectively. For the given capacitance corresponding X_C is computed to compute the constants of equations (3.4) and (3.5) with the available data. Now the Jacobian cofactors and

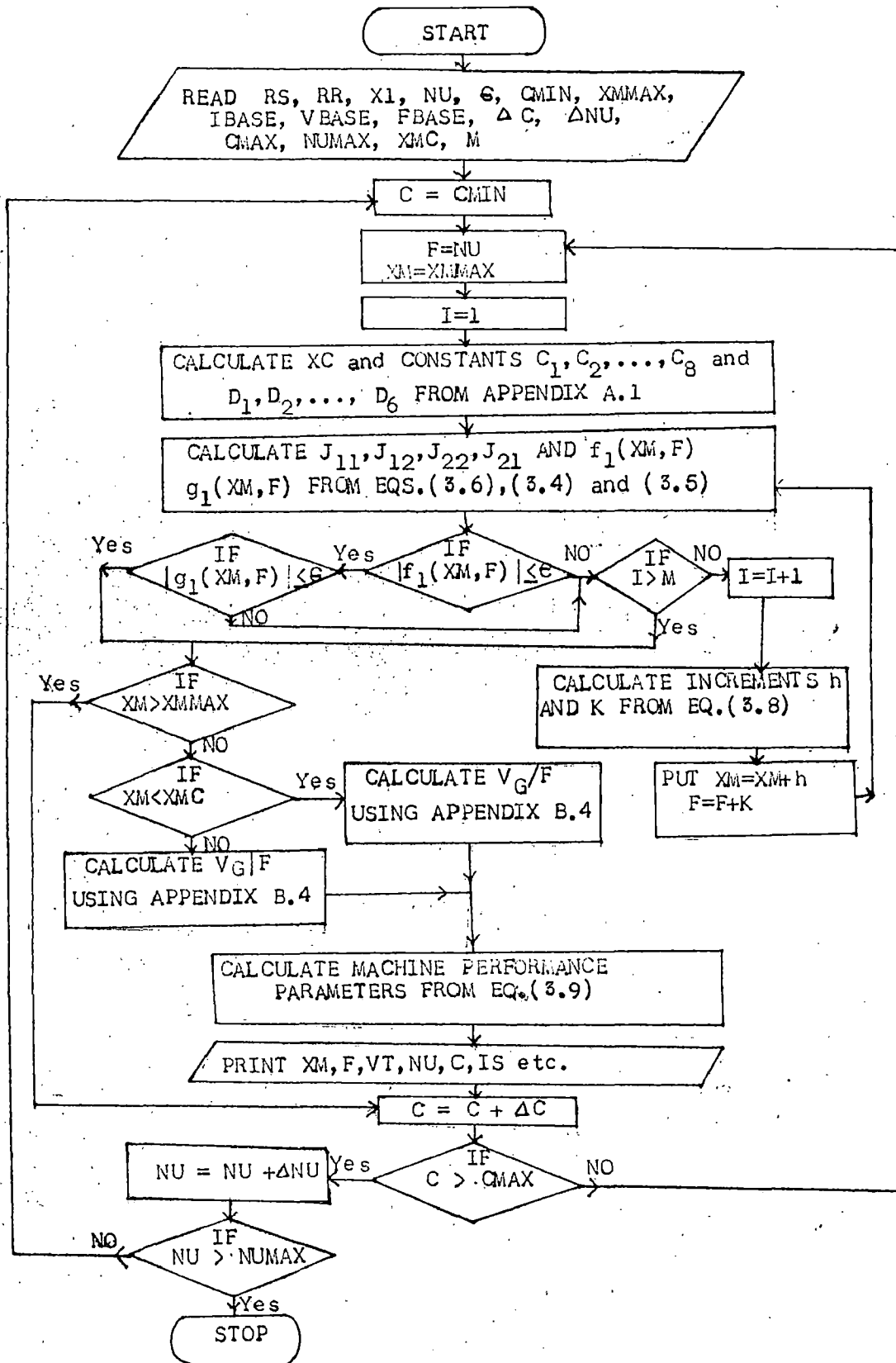


Fig.3.3 Flow chart for case I

functions $f_1(X_m, F)$ and $g_1(X_m, F)$ are computed by using equations (3.6), (3.4) and (3.5). The iterations are carried out until the magnitudes of $f_1(X_m, F)$ and $g_1(X_m, F)$ are less than or equal to the desired accuracy ϵ . So the increments h and k are computed from equation (3.8) to modify X_m and F to satisfy the above condition.

When X_m and F are computed by using the analytical technique, the corresponding air gap voltage to frequency ratio V_G/F is determined from Appendix B.4 and the using the machine parameters, X_m , F , V_G/F , X_L , ω the machine performance is evaluated from equation (3.9). Now take new value of $C = C + \Delta C$ to computer the new value of X_m and F for this capacitance and machine performance is also evaluated at this new set^{of} values. To check the value of capacitance C_{max} is fixed. After reaching capacitance C beyond this specified value the computation is made for new value of speed $\omega' = \omega + \Delta\omega$. The above process is repeated for new values of speed ω until ω_{max} is reached.

For case II the program reads the machine parameters, speed and X_{MC} as in case I. Taking capacitance C equal to C_{MIN} and initial values of X_m and F as in case I. Now consider a setting of load (R_L and X_L) and proceed similarly as in case I for the computation of X_m and F at this load value by considering functions $f_2(X_m, F)$ and $g_2(X_m, F)$ from equations (3.13) and (3.14

When X_m and F is computed by analytical method, the corresponding air gap to frequency ratio V_G/F can be determined from the characteristic equation in Appendix B.4. Now machine

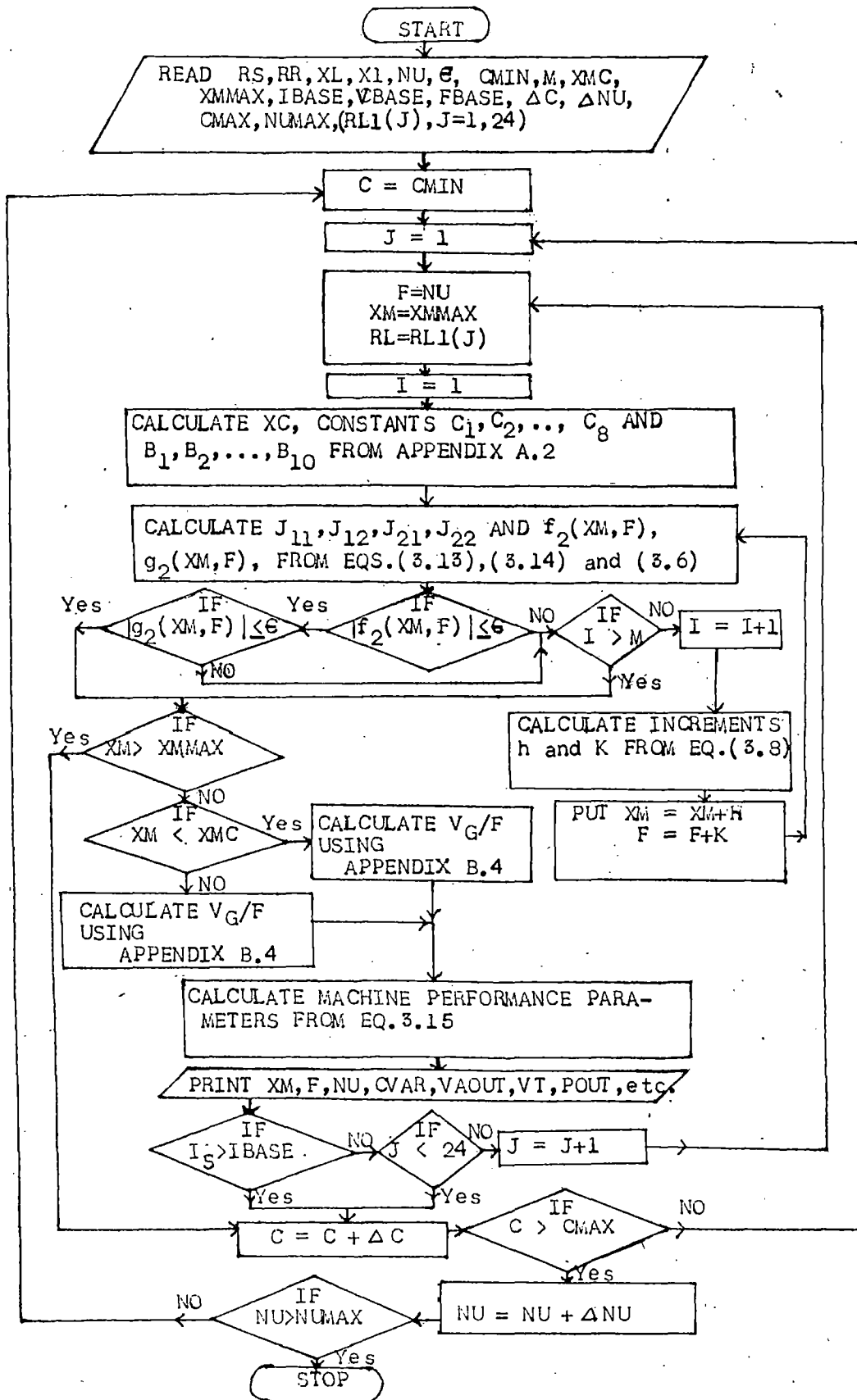


Fig. 3.4 Flow chart for case II

performance is evaluated from equation (3.15) by using the machine parameters, computed and given values. The above process is repeated for different load values when the computation is made for all loads, take, new value of capacitance $C = C + \Delta C$ and computer X_m , F and machine performance at all values of load for this new value of capacitance C . This process is repeated until C is reached equal to C_{Max} . Now take new value of speed $\omega = \omega + \Delta \omega$ and repeat the above process until ω is reached ω_{Max} . To use the same program for resistive load only the inductive part (X_L) of reactive load is assumed to be zero.

For case III the program reads the machine parameters, speed and V_G/F where V_G/F corresponds to the value of V_G/F at point C in Fig. B.1. Take the terminal voltage V_T equal to $V_{T min}$ and initial values of X_C and F as $X_{C max}$ and speed ω respectively. Take a setting of reactive load (R_L and X_L) and calculate V_G/F from equivalent circuit Fig. 3.1. Computer the value of X_m for this computed value of V_G/F from the characteristic equation of V_G/F and X_m in Appendix B.4. Now compute the constants of equations (3.16) and (3.17) with the current available parameters. Compute the Jacobian cofactors and functions $f_3(X_C, F)$ and $g_3(X_C, F)$ from equation (3.16) and (3.17) and (3.18). The iterations are carried to modify the value of X_C , F and then X_m to get the desired condition as $|f_3(X_C, F)| \ll \epsilon$ and $|g_3(X_C, F)| \ll \epsilon$ is the desired accuracy the increments h and k are computed by using equation (3.20) to modify the value of X_C and F to satisfy the above condition.

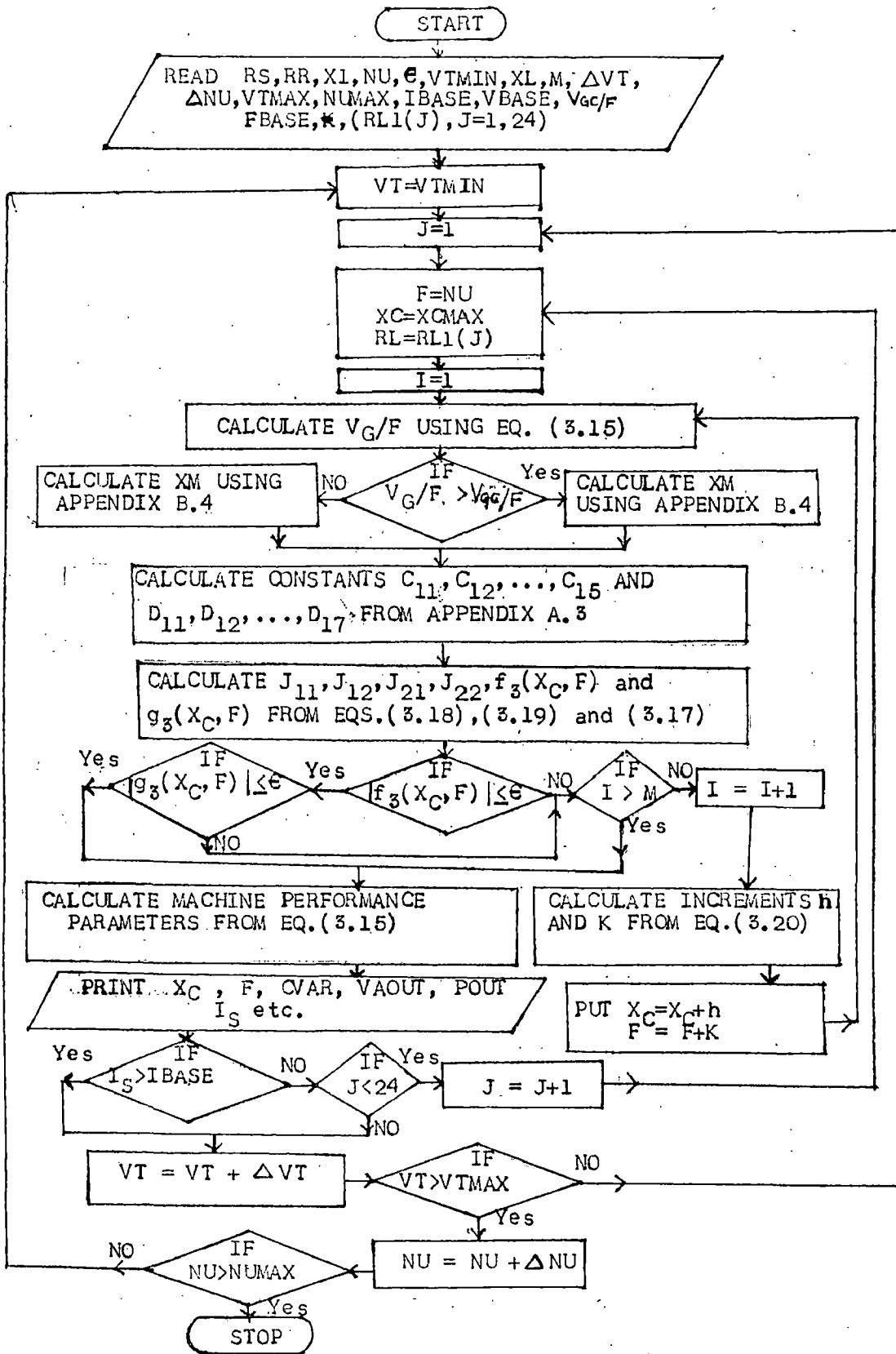


Fig.3.5 Flow chart for case III

When X_C and F are computed by using the analytical technique the machine performance is evaluated from equation (3.15). The above process is repeated for different load values to compute the corresponding X_C and F and machine performance. After the computation at all load value take new values of terminal voltage $V_T = V_T + \Delta V_T$ and repeat the above process for all load values at this new value of terminal voltage V_T until V_T is reached $V_T \text{ max}$. Now take new value of speed $\omega = \omega + \Delta \omega$ and repeat the above process for this new value of speed ω computation is made for different values of speed until ω is reached to ω_{max} . The same program can be used for the resistive load if only the inductive part (X_L) of reactive load is assumed to be zero.

For case IV the program reads the machine parameters, air gap voltage to output frequency ratio V_G/F , output frequency and V_{GC}/F as in case III. Take the value of output frequency F equal to F_{min} and X_m is determined from the characteristic equation between V_G/F and X_m in Appendix B-4. Take the initial values of X_C and ω as $X_C \text{ max}$ and F . Now consider a value of inductive load (R_L and X_L) and compute the constants of equation (3.21) and (3.22) with the available datas. Compute the Jacobian Matrix cofactors and functions $f_4(X_C, \omega)$ and $g_4(X_C, \omega)$ from equation (3.21), (3.22) and (3.23). The iterations are carried out until the magnitudes of the functions $f_4(X_C, \omega)$ and $g_4(X_C, \omega)$ are less than or equal to the desired accuracy ϵ . The increments h and k are computed from equation (3.25) to modify the value of X_C and ω to satisfy the above condition.

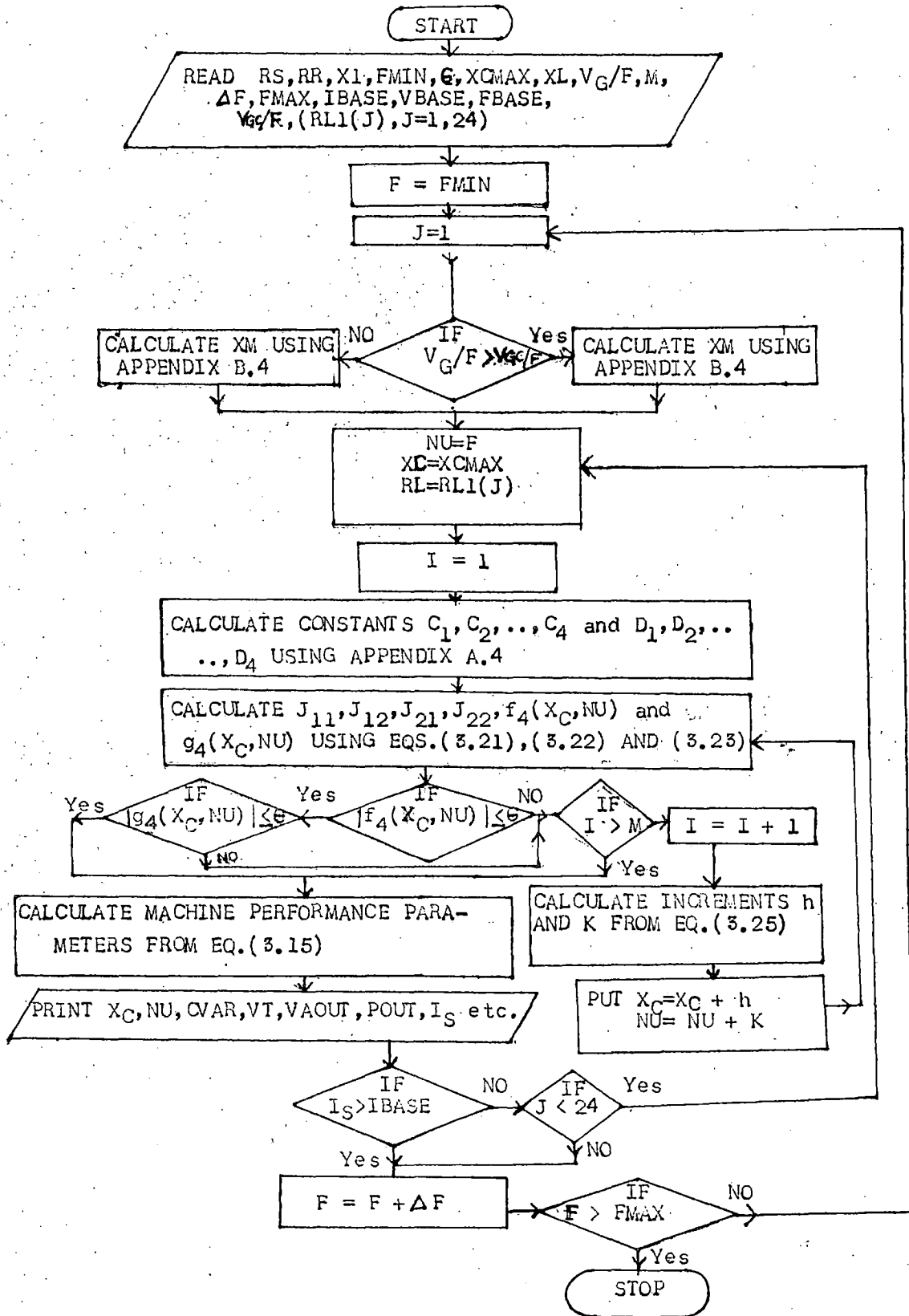


Fig. 3.6 Flow chart for case IV

When X_C and μ are computed by analytical technique, the machine performance can be evaluated from equation (3.15). The above process is repeated for all load values to obtain the corresponding X_C , μ and machine performance. Now take the new value of output frequency $F = F + \Delta F$ and repeat the above process to find out the X_C , μ and machine performance at all load values for this new value of F . Computation is made for different values of output frequency F until it is reached to F_{max} . The same program can be used for the resistive load if only the inductive part (X_L) of reactive load is assumed to be zero.

3.4 Experimental Set up and Machine Parameters:

To check the validity of theoretical results obtained from the different cases assumed in section 3.2, a number of experiments were conducted on a commercial three phase 5 h.p., 400 V, 4 pole, 50 Hz induction motor used as a self excited induction generator. The details of induction machine are given in Appendix B-1.

The above mentioned squirrel cage induction motor was coupled to a 5 h.p. synchronous motor to achieve constant speed at varying loads. The synchronous motor was fed from a 7.5 KVA alternator coupled to a variable speed 8 KW d.c. motor. The speed of d.c. motor was kept constant by adjusting its field resistance. To get the experimental results on the different speeds. The supply frequency from alternator was varied by changing the speed of D.C. motor. A three phase Δ - connected variable capacitor bank was connected to the terminals of the

induction machine to get the induction machine self excited and to obtain the terminal voltage constant of the self excited induction generator, a three phase star connected inductor was connected in parallel with capacitor bank. A variable three phase resistance bank was used to load the induction generator for pure resistive loading and for reactive load (R-L), the same was used in series with a three phase reactor.

All the theoretical computations have been carried out in per unit values and the base values of voltage, current, power etc. for the induction machine are given in Appendix B-2.

Here it is important to mention that the rated input KVA and rated output of induction machine would be equal to 3.0 and approximately 2.0 respectively. The machine parameters like stator resistance, leakage reactance and rotor resistance, leakage reactance were obtained by using standard methods and the values are given in Appendix B-3.

The synchronous speed test was carried out to get the necessary V_G/F and X_m characteristic for the steady state analysis of self excited induction generator. The test was conducted by feeding power supply to the synchronous motor at base frequency to drive the induction machine at synchronous speed and connecting the same power supply through an auto-transformer of appropriate rating to the terminals of induction motor. One thing is to be noted that the direction of rotation should be same for both induction motor and synchronous motor. The line current and electrical losses of induction machine

were measured at different voltage settings. The calculations for V_G/F and X_m are done by assuming rotor side open in the equivalent circuit of induction motor. The calculated results in per unit are plotted as shown in Fig. B.1. Here the variation of V_G/F and X_m is nonlinear due to magnetic saturation of the machine and is simplify the analysis. The variation of X_m with V_G/F in the saturated region may be linearised by using approximate curves as drawn in Fig. B.1. The relation between V_G/F and X_m is given in Appendix B-4 to use it for the analysis of self excited induction generator.

3.5 Results and Discussion :

The steady state performance of the 5 h.p. induction machine as self excited induction generator has been computed for different cases by using the machine parameters with their variations as mentioned in section 3.3. The computation has been done by using the analytical technique of which the flow charts are given in section 3.3. In order to verify the validity of the predicted computed results, tests have been connected on the induction machine under similar conditions to obtain the experimental results and these results are compared with the computed results.

No Load Characteristics : Fig. 3.7 shows the no load characteristic of the self excited induction generator. The computed results are given for the variation of terminal voltage with capacitance at three different constant speeds .9, 1.0 and 1.1 p.u. The experimental results for speed 1.0 p.u. are also

plotted in the same figure. A close agreement has been found between the experimental and computed results. The terminal voltage increases with the increasing capacitance. The computed results show that the self excitation occurs at higher capacitance value i.e. 9 μF at .9 p.u. speed. From the characteristic at 1.0 p.u. speed it has been observed that the increase in capacitance from 8 μF to 9 μF gives more boost to the terminal voltage than the rise in voltage for the change of capacitance from 1,3 μF to 14 μF . This all is due to the effect of saturation characteristic as the saturated magnetising reactance restricts the final voltage build up for a particular capacitance and speed. The computed results at three different speeds give the idea that at particular capacitance if speed is varied, the terminal voltage is also changed. Fig. 3.8 shows the variation of terminal voltage with speed at no load for the fixed values of capacitance (10 μF and 12 μF). At 10 μF the terminal voltage varies from .8525 p.u. to 1.335 p.u. for the speed variation from .9 p.u. to 1.1 p.u. Here the terminal voltage varies with speed almost linearly.

Load Characteristics at Fixed Capacitances:-

Fig. 3.9 shows the computed and experimental variation of terminal voltage with apparent power output VAOUT (p.u.) for fixed values of capacitances 13 μF , 14 μF and 15 μF at resistive load and constant speed (1.0 p.u.). For both computed and experimental results the trend of characteristics is similar as the terminal voltage drops with the increase of load and the maximum VAOUT increases with the increase

in terminal capacitance. All the three characteristics are almost parallel and the percentage drop in terminal voltage from no load to maximum loading at 15 μF is 24.42% which is a considerable amount and creates the need of voltage regulator to keep the terminal voltage constant. The frequency Vs. VAOUT characteristics both for computed and experimental results show that the variation is very much linear and small. The frequency variation from no load to maximum load for 15 μF at resistive load and 1.0 p.u. speed is 4%. The difference in the computed and experimental results is due to the assumptions made in the analysis. The analytical technique is quite accurate because the characteristics are similar for both results. Now the effect of speed can be seen for fixed capacitance case. The Fig. 3.10 shows the variation of terminal voltage with VAOUT at resistive load and different constant speeds (0.9, 1.0 and 1.1 p.u.) for fixed values of capacitance (13 μF , 14 μF and 15 μF). It shows that at particular speed the requirement of capacitance increases with the increasing load to keep the terminal voltage constant and as the speed is increased, the maximum VAOUT for a particular value of capacitance is also increased. At 1.1 p.u. speed, 13 μF capacitance is found sufficient to load the machine up to 3.0 p.u. and at 0.9 p.u. the machine can be loaded up to 1.213 p.u. The frequency variation with VAOUT at different speeds shows that it is linear for all speed and the variation of frequency at 15 μF from no load to maximum load is small i.e. nearly 3 - 4%.

The resistive load is very common for the domestic pur-

pose electric supply but for some small industrial purpose reactive (R-L) load is considered. Here the computation has been done for the series combination of fixed reactance and variable resistance. The Fig. 3.11 shows the experimental and computed variation of terminal voltage with VAOUT at reactive (R-L series) load for fixed values of capacitance and constant speed (1.0 p.u.). Here the X_L is assumed 3.0 p.u. at base frequency. For a particular value of capacitance the maximum VAOUT is less than the maximum VAOUT in the case of resistive load. It is due to the reason that the reactive power for lagging load is fed directly from the capacitor. The variation of terminal voltage with VAOUT is similar for experimental and computed results. The characteristics for all the capacitors are almost parallel as in Fig. 3.9. From the computed results, the maximum VAOUT at 13 μF is .6119 p.u. whereas the maximum VAOUT at the same capacitance with resistive load is 2.1336 p.u. The drop in the terminal voltage at 15 μF from no load to maximum VAOUT is 17.55%. The frequency variation with VAOUT at 15 μF from no load to maximum VAOUT is only 1%. The variation of terminal voltage with VAOUT at reactive (R-L series) load for fixed values of capacitance (13 μF , 14 μF and 15 μF) and different constant speeds (.9, 1.0 and 1.1 p.u.) has been shown in Fig. 3.12. The effect of speed on the performance of the machine for the reactive load is similar as discussed in Fig. 3.10.

Load Characteristics at Terminal Voltage Constant:-

When a self excited induction generator is used for

the electric supply, it is considered that the terminal voltage should remain constant irrespective of load. So the capacitance value will be varied according to the variation of load to maintain the terminal voltage constant. Fig. 3.13 shows the variation of capacitive VAR (CVAR) with VAOUT for constant speed 1.0 p.u. at resistive load to maintain different constant terminal voltages (.9, 1.0 and 1.1 p.u.). The capacitive VAR requirement increases with the increase of load at constant terminal voltage. All the three characteristics at .9, 1.0 and 1.1 p.u. are having rising nature with the increase of load. It shows that the CVAR requirement increases for the increase in operating terminal voltage. The nature of curves for experimental and theoretical results is more or less of the same type. The CVAR requirement for 1.0 p.u. terminal voltage at constant speed (1.0 p.u.) and 3.0 p.u. VAOUT is 1.479 p.u. at resistive load. The frequency variation at particular terminal voltage for different loads is small as well as linear and at terminal voltage 1.0 p.u. from no load to 3.0 p.u. VAOUT the frequency variation is 7.12%. The experimental and computed results show a difference in the values which appears due to the reason that the core losses are neglected in the computed results. Now to observe the effect of speed on CVAR at different constant speeds and constant terminal voltage for different load is really of great importance because the wind turbines are having sufficient speed variation to use with the self excited induction generators. Fig. 3.14 shows the variation of computed CVAR with VAOUT at resistive load and different constant speeds (.9, 1.0 and 1.1 p.u.) to keep the

terminal voltage constant at .9, 1.0 and 1.1 p.u. It gives the minimum & maximum limits of capacitive VAR to keep the terminal voltage constant at resistive load for the speed variation from .9 p.u. to 1.1 p.u. For particular terminal voltage the CVAR requirement decreases with the increase in speed and vice versa. The CVAR requirement at .9 p.u. speed for terminal voltage 1.0 p.u. and 3.0 p.u. VAOUT of pure resistive load is 1.912 p.u. and at no load it is .64 36 p.u. which will become a guideline for the design of voltage regulator at pure resistive load. The frequency of variation at different speeds and increased load is quite small as well as linear. All the characteristics for frequency variation with VAOUT are almost parallel. Fig. 3.15 shows the computed and experimental variation of stator current with VAOUT at resistive load and constant speed 1.0 p.u. for different constant terminal voltages. The stator current rises with the increase of load. For different terminal voltage and rated stator current the output power increases as the terminal voltage is varied from .9 to 1.1 p.u. and decreases as there is more increases in terminal voltage. This aspect has been more illustrated in Fig. 3.16 which provides the guideline for the selection of operating terminal voltage of system to make the optimum use of the machine. The maximum power 2.7926 p.u. at rated machine current and constant speed 1.0 p.u. is obtained at the terminal voltage 1.1 p.u. The experimental and computed results for resistive load has been already given. But when a.c. motors are used as load, it is essential to consider the ~~reactive~~ load.

Fig. 3.17 shows the experimental and computed variation of CVAR with VAOUT at reactive load (R-L) and constant speed 1.0 p.u. to keep different constant terminal voltages (.9, 1.0 and 1.1 p.u.). Here the reactive load consider the series combination of fixed X_L 3.0 p.u. at base frequency and variable resistance. The behaviour of CVAR variation with VAOUT is similar as in the Fig. 3.13. In the case of R-L load the CVAR requirement is more than the case of resistive load for the same VAOUT at particular terminal voltage and constant speed 1.0 p.u. It happens because the reactive power for lagging loads is directly fed from the capacitor. So the capacitor provides leading VAR for the excitation of induction generator and additional leading power corresponding to reactive power and active power of load to keep the terminal voltage constant. For 1.0 p.u. terminal voltage and 1.0 p.u. VAOUT the CVAR is 1.795 p.u. and .9262 p.u. for R-L load and resistive load respectively. The frequency variation with VAOUT is small and it varies according to variation of active power. The frequency falls down for more active power and rises as the active power becomes less. For terminal voltage 1.0 p.u. at speed 1.0 p.u., the frequency drops by .4% from VAOUT .289 to .602 p.u. and there is no significant change in frequency from .602 p.u. to .8 p.u. VAOUT. Again the frequency rises by .6% for VAOUT from .8 p.u. to .984 p.u.

Load Characteristics at Air Gap Voltage to Output Frequency Ratio (V_G/F) Constant :

For the proper use of magnetic material the machine

should be operated at rated air gap flux because at less flux value the magnetic material will not be utilised properly and at higher values of flux the magnetising reactance is less and gives rise to more machine losses. The air gap flux is held constant by keeping the air gap voltage and output frequency ratio (V_G/F) constant. Fig. 3.18 shows the variation of terminal voltage and stator current with VAOUT at resistive load by keeping V_G/F constant at 1.0 p.u. (air gap flux constant) for different constant frequencies (.9, 1.0 and 1.1 p.u.). The terminal voltage drops with the increase of load and it varies by 4.115% from the minimum load to the load corresponding to rated stator current. All the three characteristics at different frequencies are parallel and linear. The stator current variation with VAOUT shows the rising characteristic with increased resistive load. The VAOUT corresponding to rated stator current is 2.666 p.u. which is not much far from the maximum power drawn at constant terminal voltage 1.1 p.u. and speed 1.0 p.u. So the machine can be utilised economically at the constant flux because the terminal voltage variation is small with the different loads. Fig. 3.19 shows the variation of terminal voltage and stator current with VAOUT at reactive load (R-L) by keeping V_G/F constant at 1.0 p.u. (air gap flux constant) for different constant output frequencies (.9, 1.0 and 1.1 p.u.). The R-L load consists of the fixed reactance 3.0 p.u. and variable resistance. The variation of terminal voltage is according to the variation of active power. It falls down as the active power is increased and rises for the drop in active power.

The behaviour for all the three characteristics of terminal voltage V_s , VAOUT is similar. At frequency 1.0 p.u. and V_G/F 1.0 p.u. the terminal voltage remains slightly higher than 1.0 p.u. for full range of load. But in the case of resistive load under similar conditions the terminal voltage varies from slightly higher than 1.0 p.u. to lower than 1.0 p.u. At different frequencies the maximum stator current is almost equal and at higher loads for a fixed stator current the VAOUT increases with the increase in frequency as shown in Fig. 3.19.

3.6 Conclusion :

Steady state analysis of self excited induction generator has been done by using the equivalent circuit of capacitor self excited induction generator and analytical technique makes use of 'Newton Raphson Method' to compute the steady state results for different cases. The nonlinear simultaneous equations appearing in the analysis are solved with this analytical technique to determine the unknown parameters like saturated magnetising reactance and output frequency in case I and II. Four cases are considered to predict the steady state behaviour of capacitor self excited induction generator and the computer programs are developed for all four cases separately. The flow charts for these computer programs have been discussed in detail. The analytical technique is found suitable for the analysis as it is fast converging. It computes the unknown parameters within 3 or 4 iterations. The comparison between computed results and experimental results

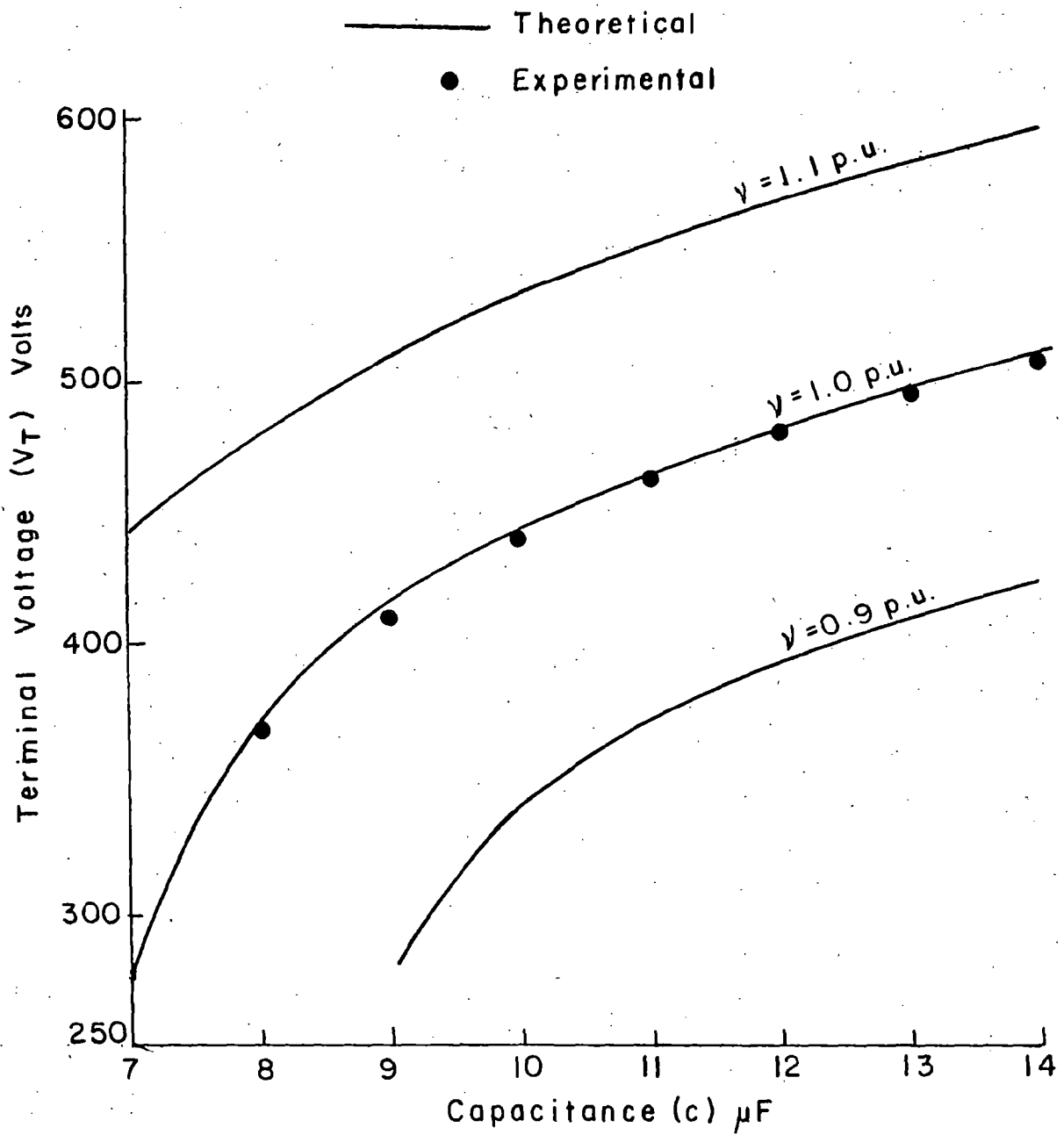


Fig. 3.7 No load characteristics

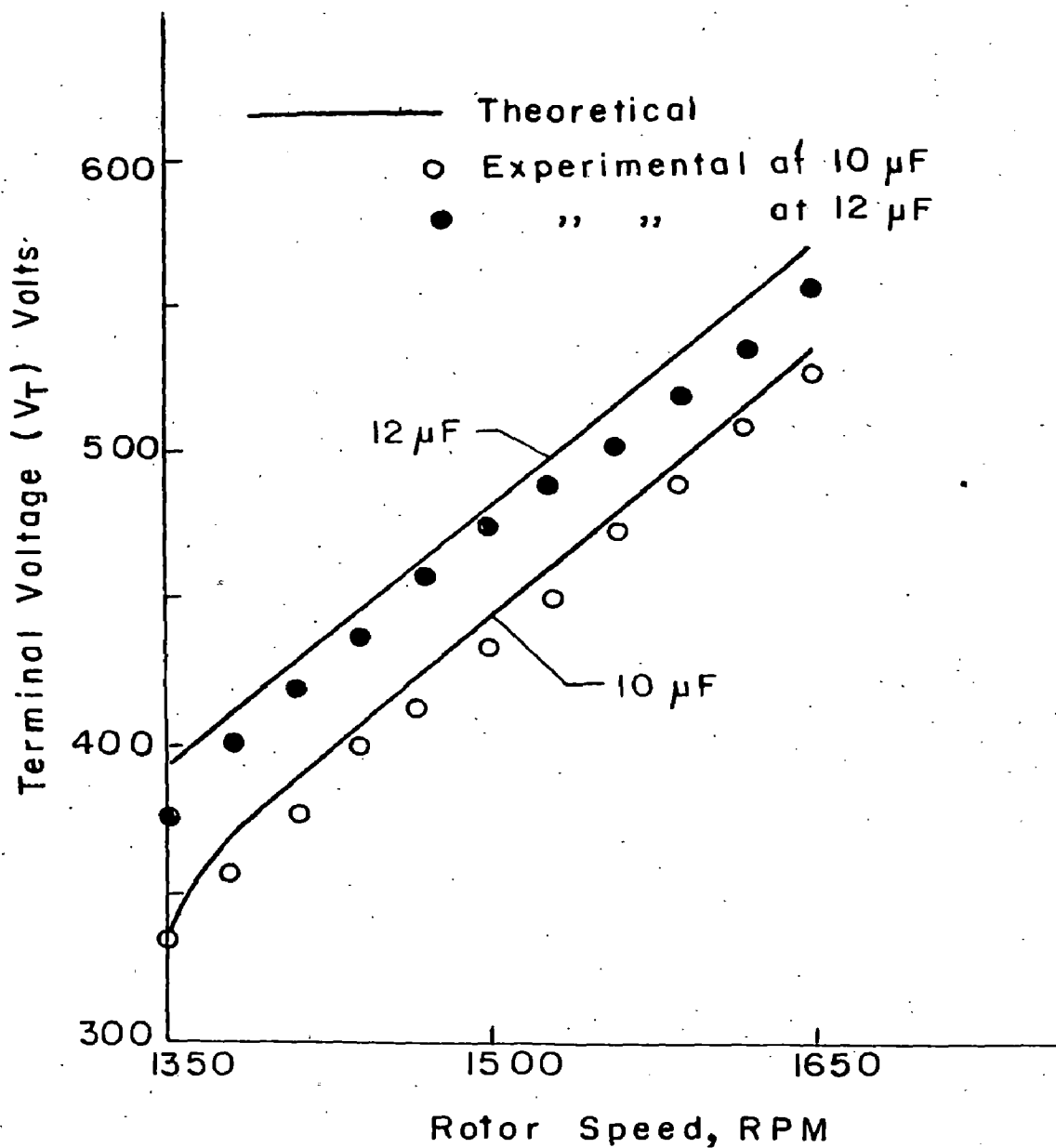


Fig. 3.8 Variation of terminal voltage with speed at no load.

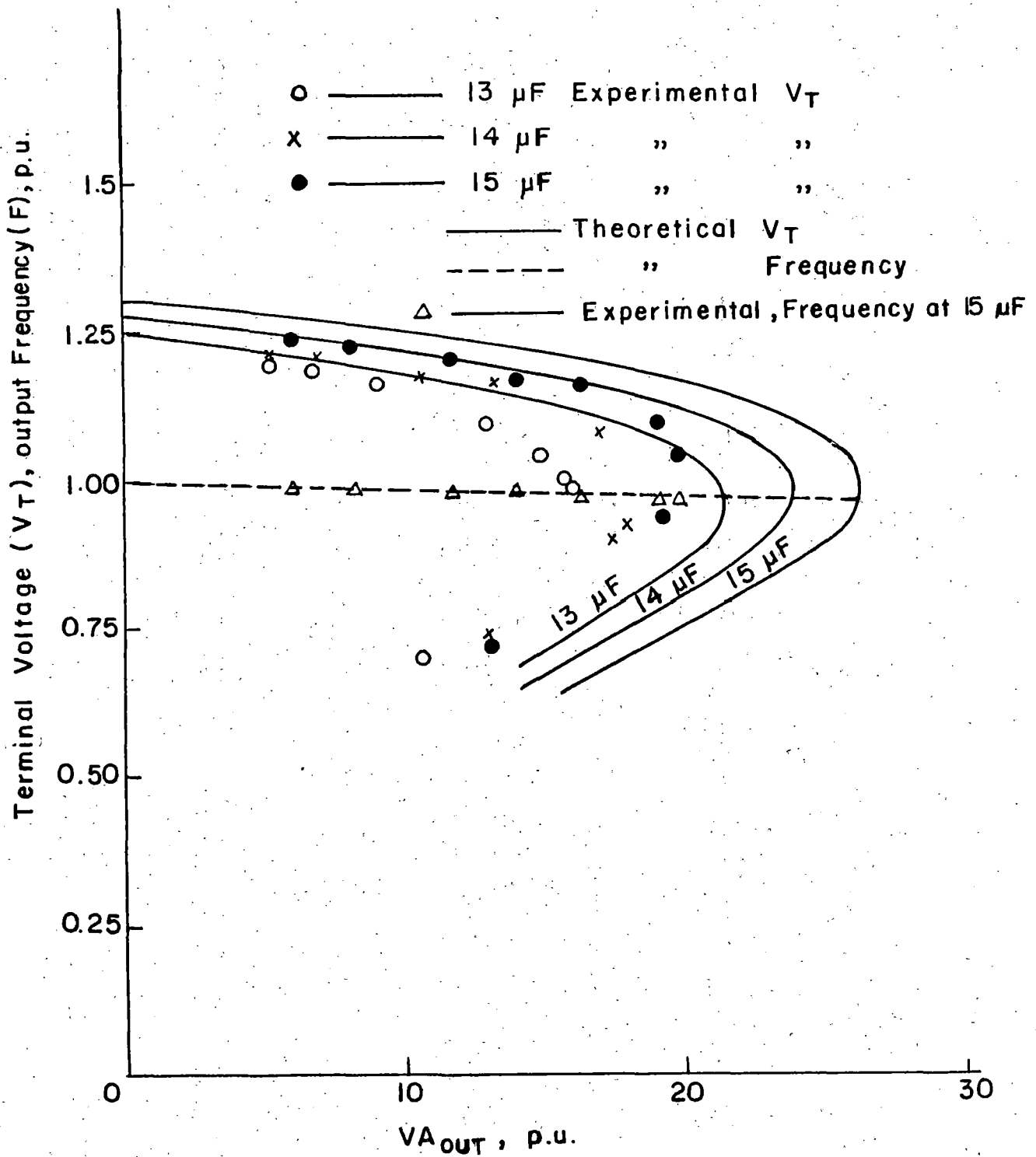


Fig. 39 Variation of terminal voltage and output frequency with resistive load at fixed capacitance

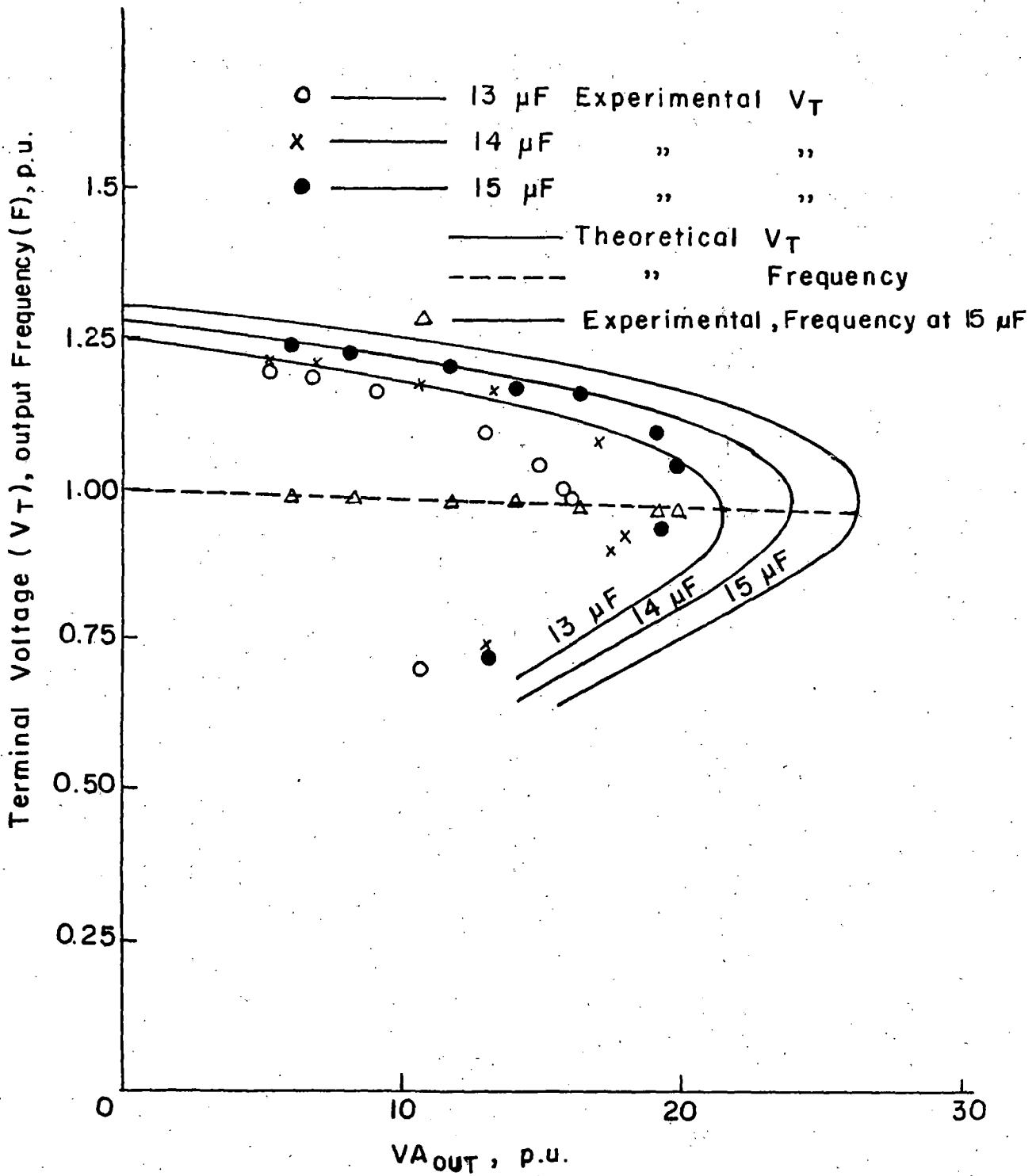


Fig. 39 Variation of terminal voltage and output frequency with resistive load at fixed capacitance

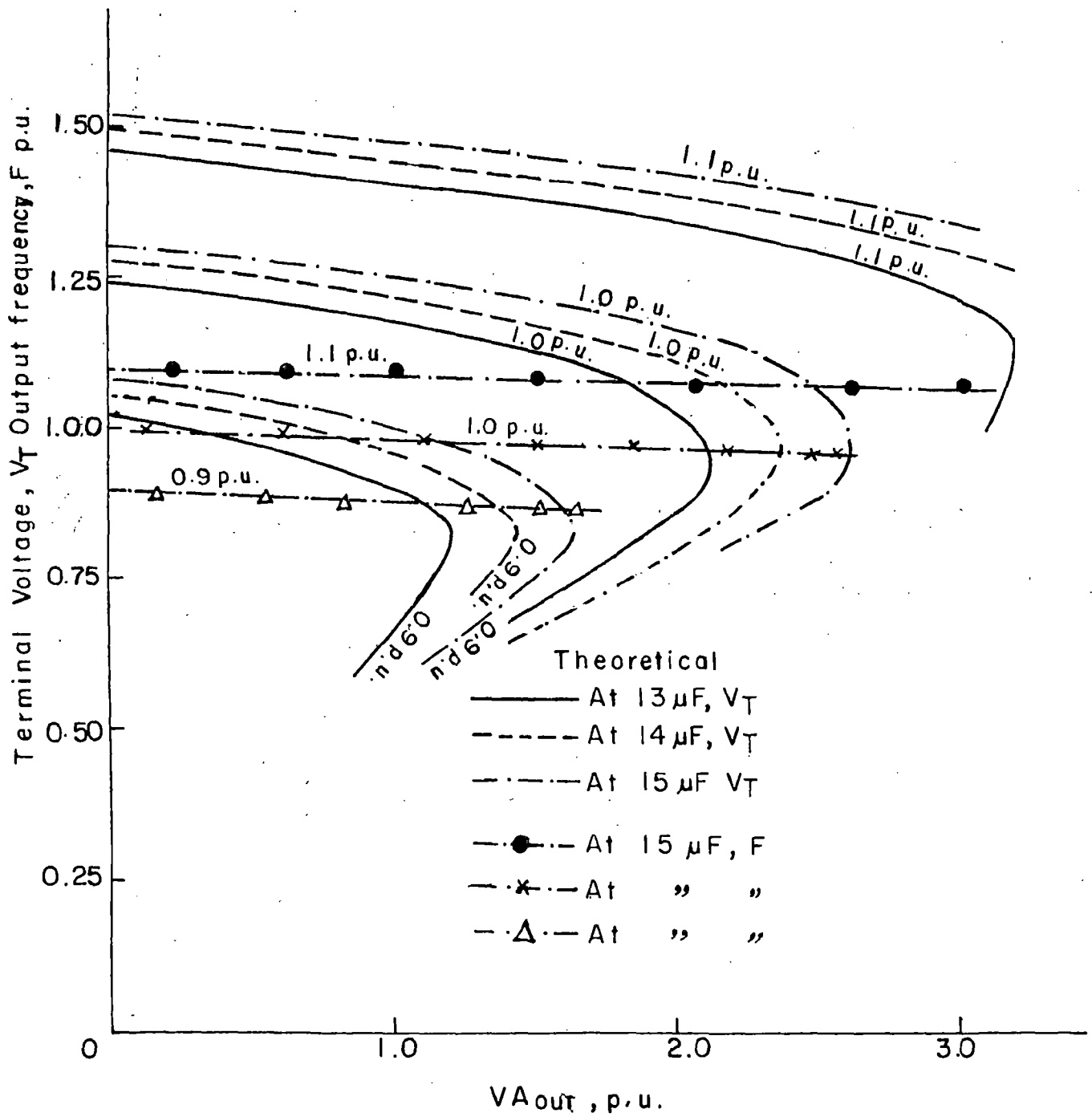


Fig. 3.10 The effect of speed on load resistive characteristics at fixed capacitances.

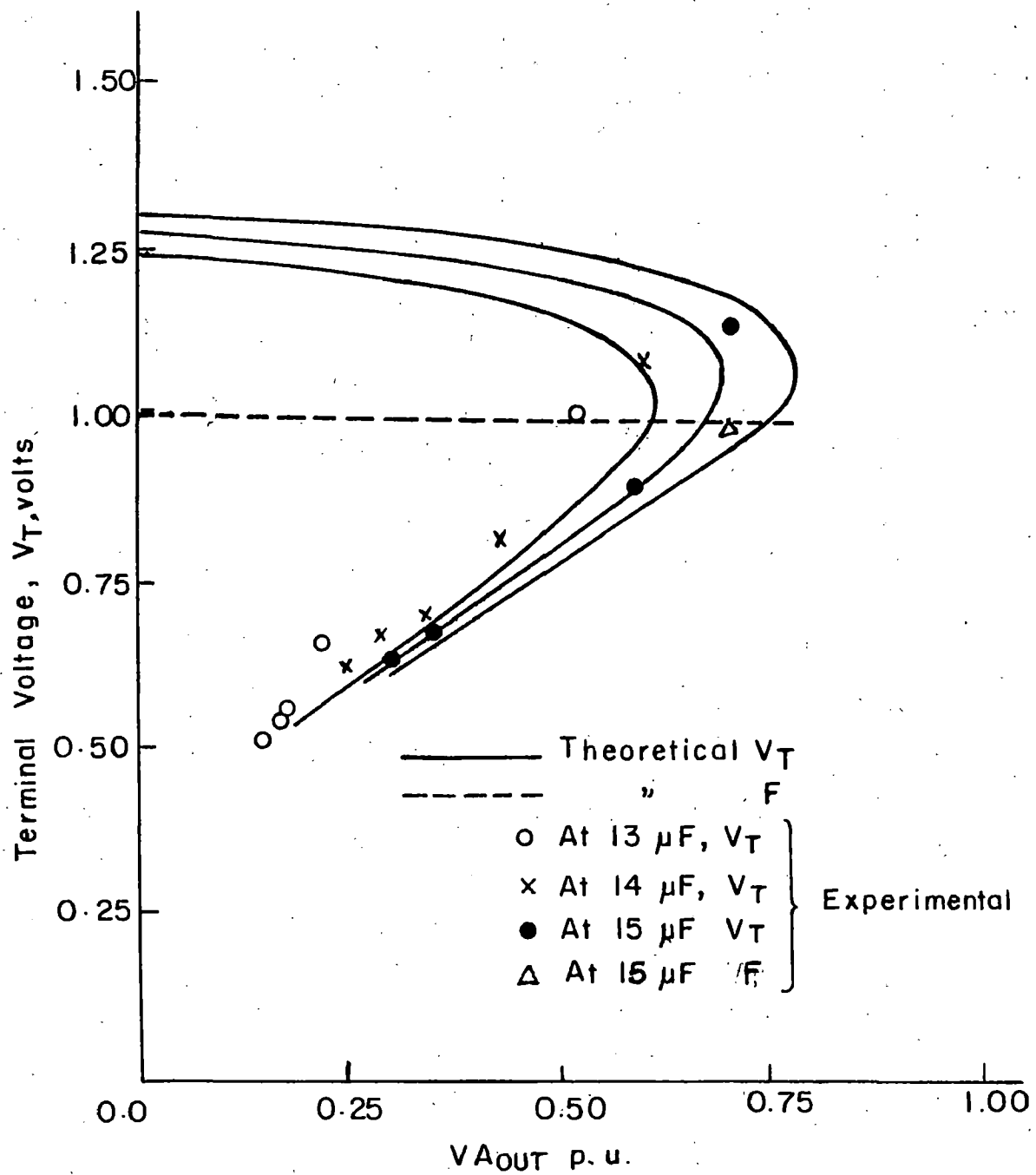


Fig. 3.11 Variation of terminal voltage and output frequency with R-L load at fixed capacitances

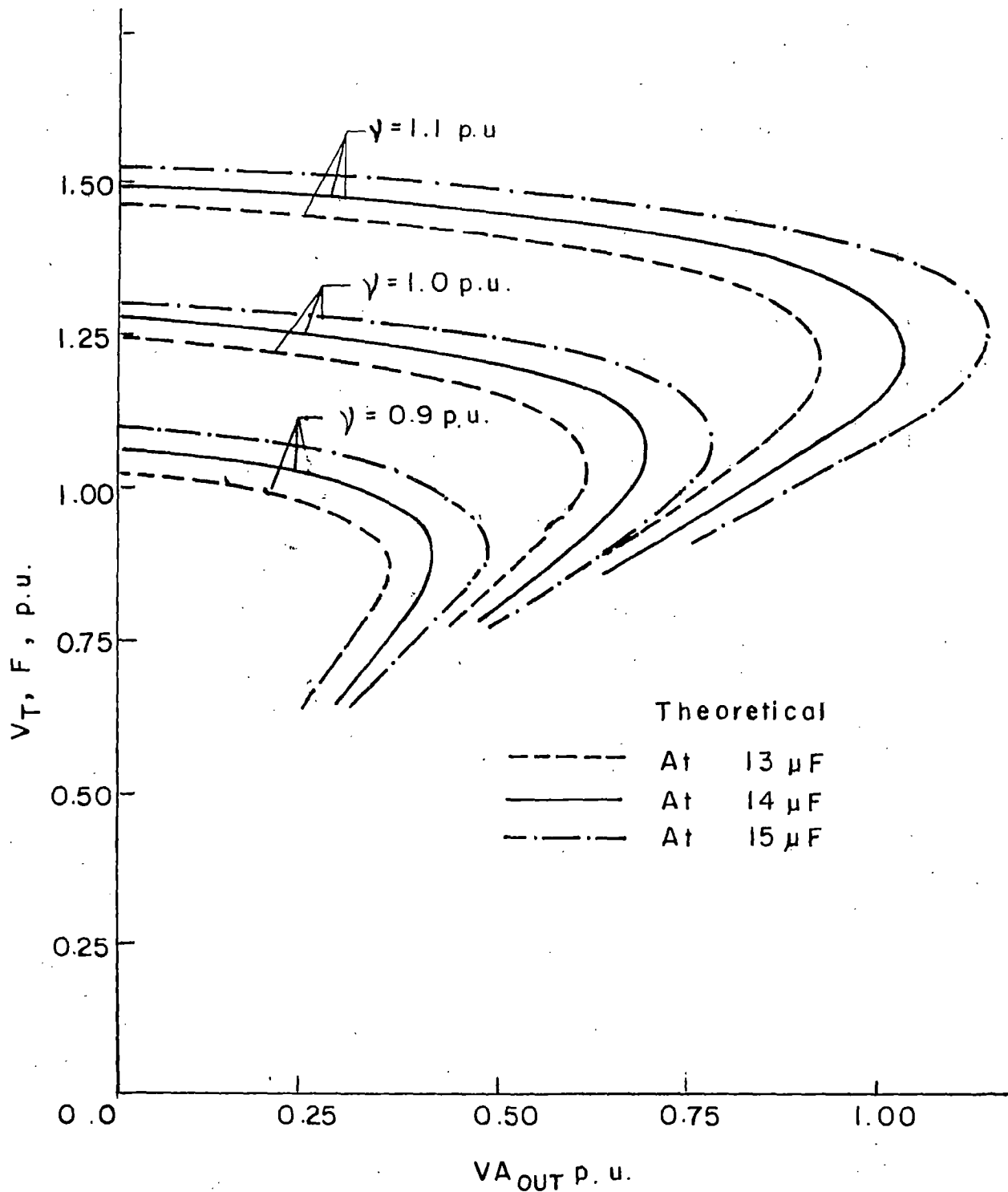


Fig.3.12 The effect of speed on load (R-L) characteristics at fixed capacitances

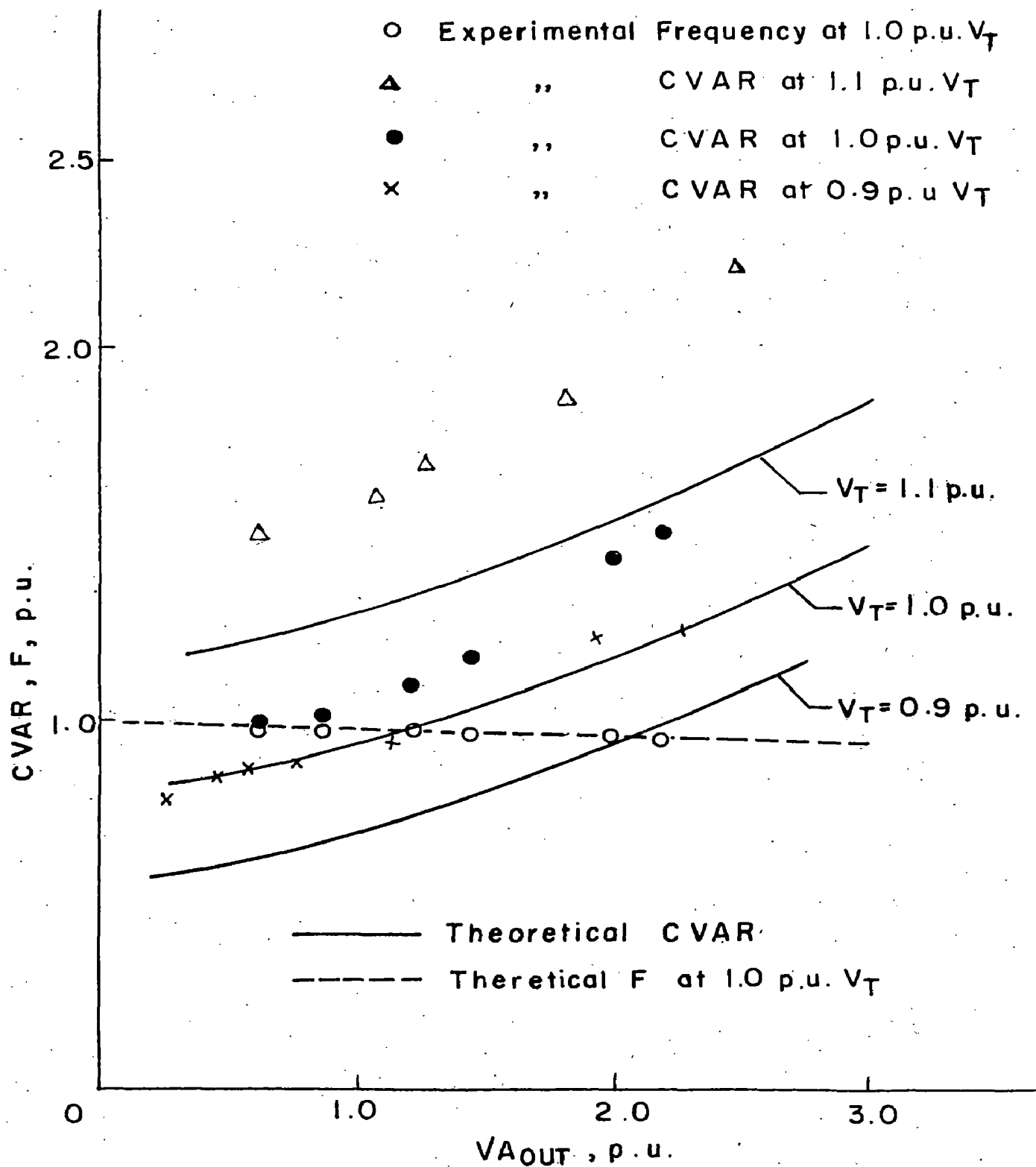


Fig.3.13 Variation of VAR with VA_{OUT} to keep terminal vol constant for resistive load

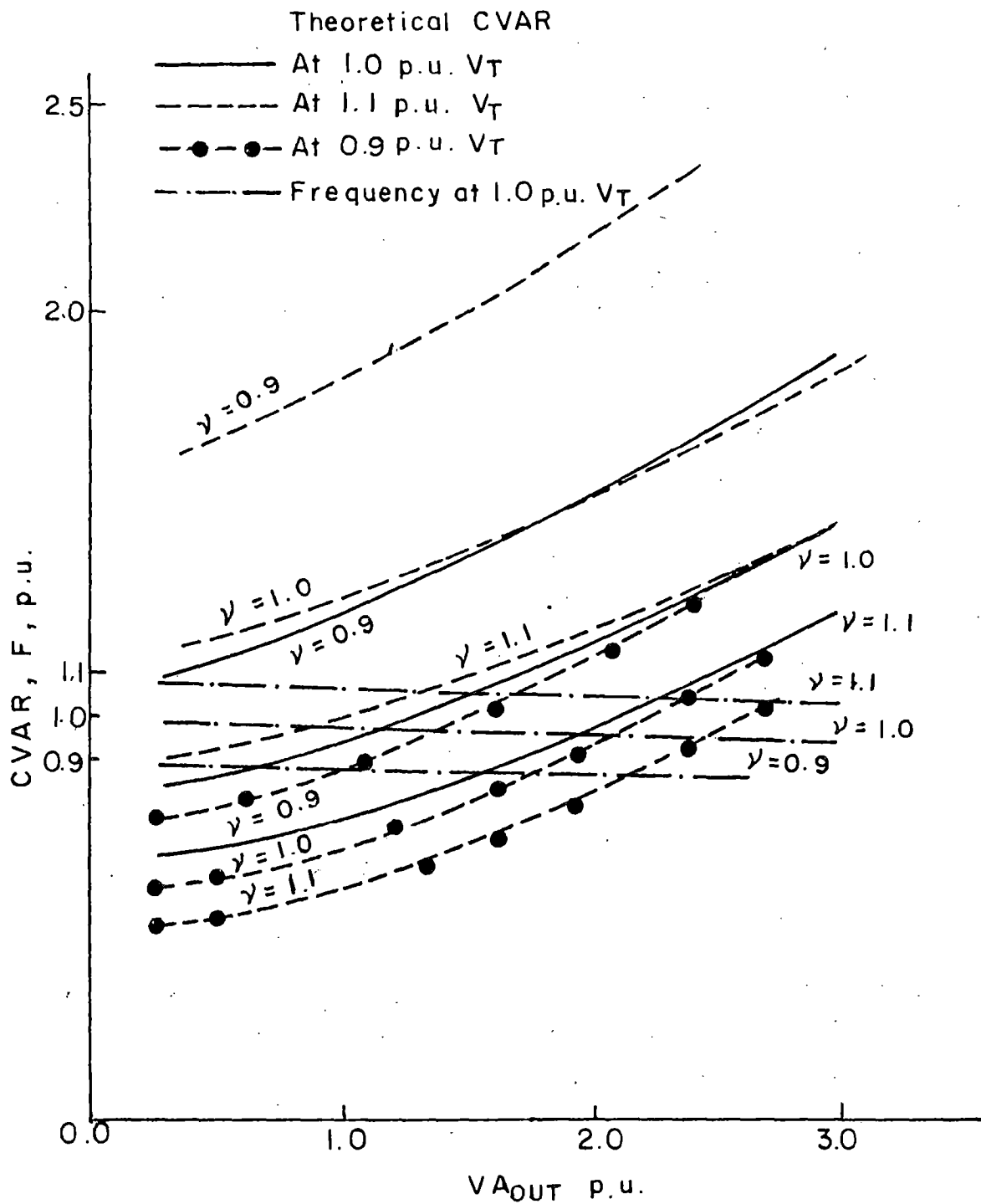


Fig.3.14 The effect of speed on required CVAR and output frequency to keep V_T constant at resistive load.

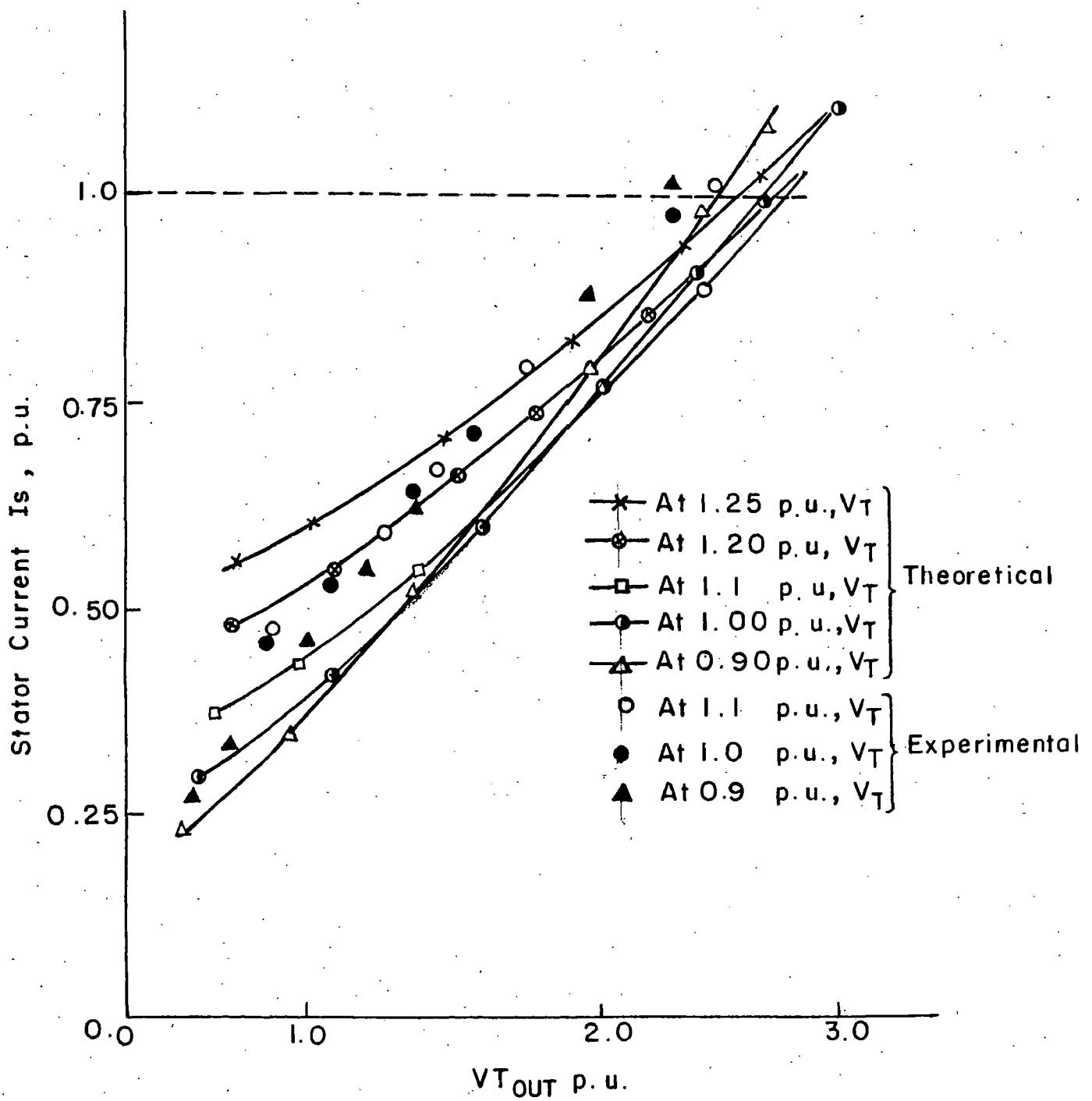


Fig. 3.15 The variation of stator current with V_{AOUT} to keep V_T constant at resistive load.

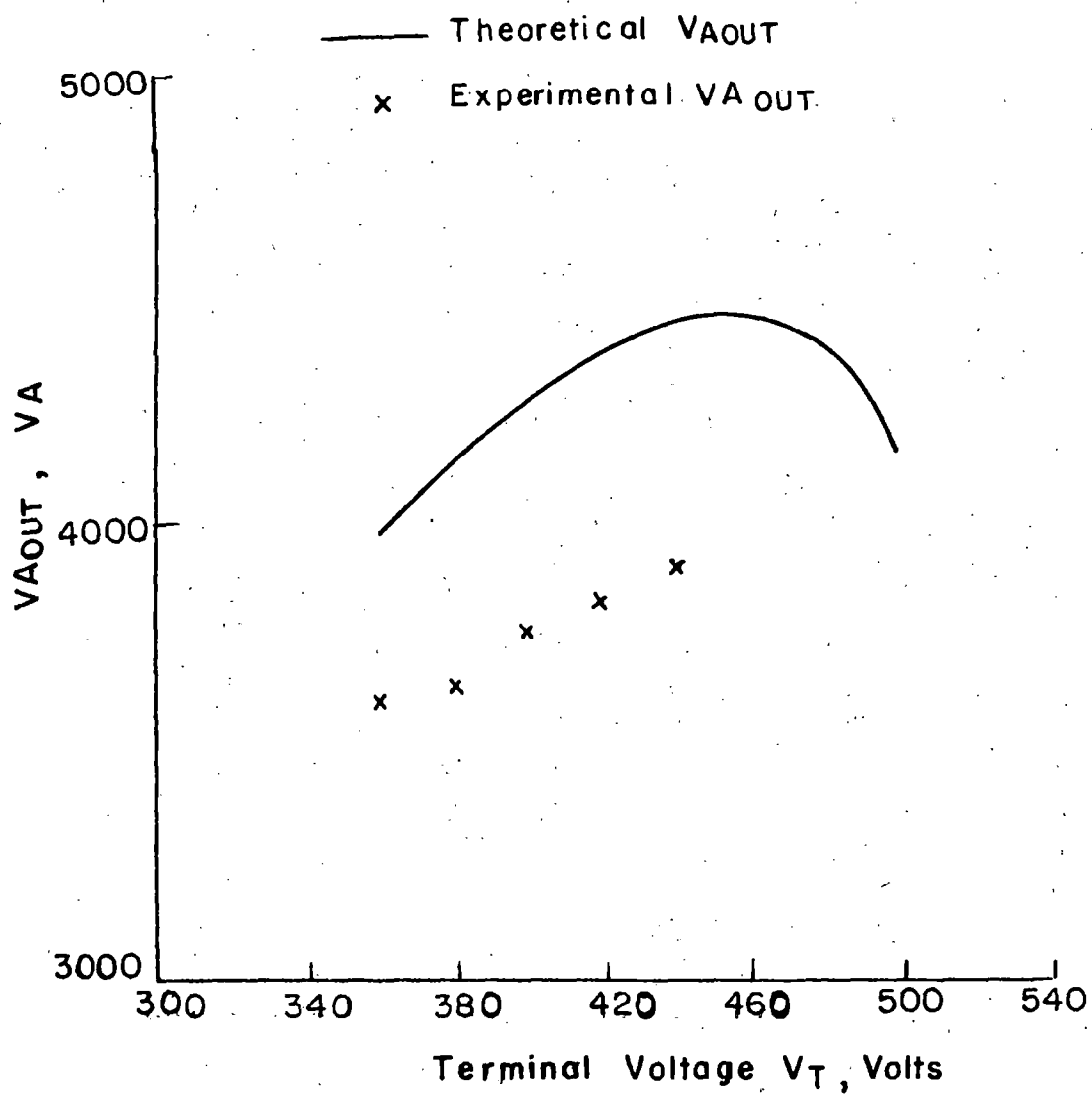


Fig.3.16 The variation of maximum output power with terminal voltage at rated stator current.

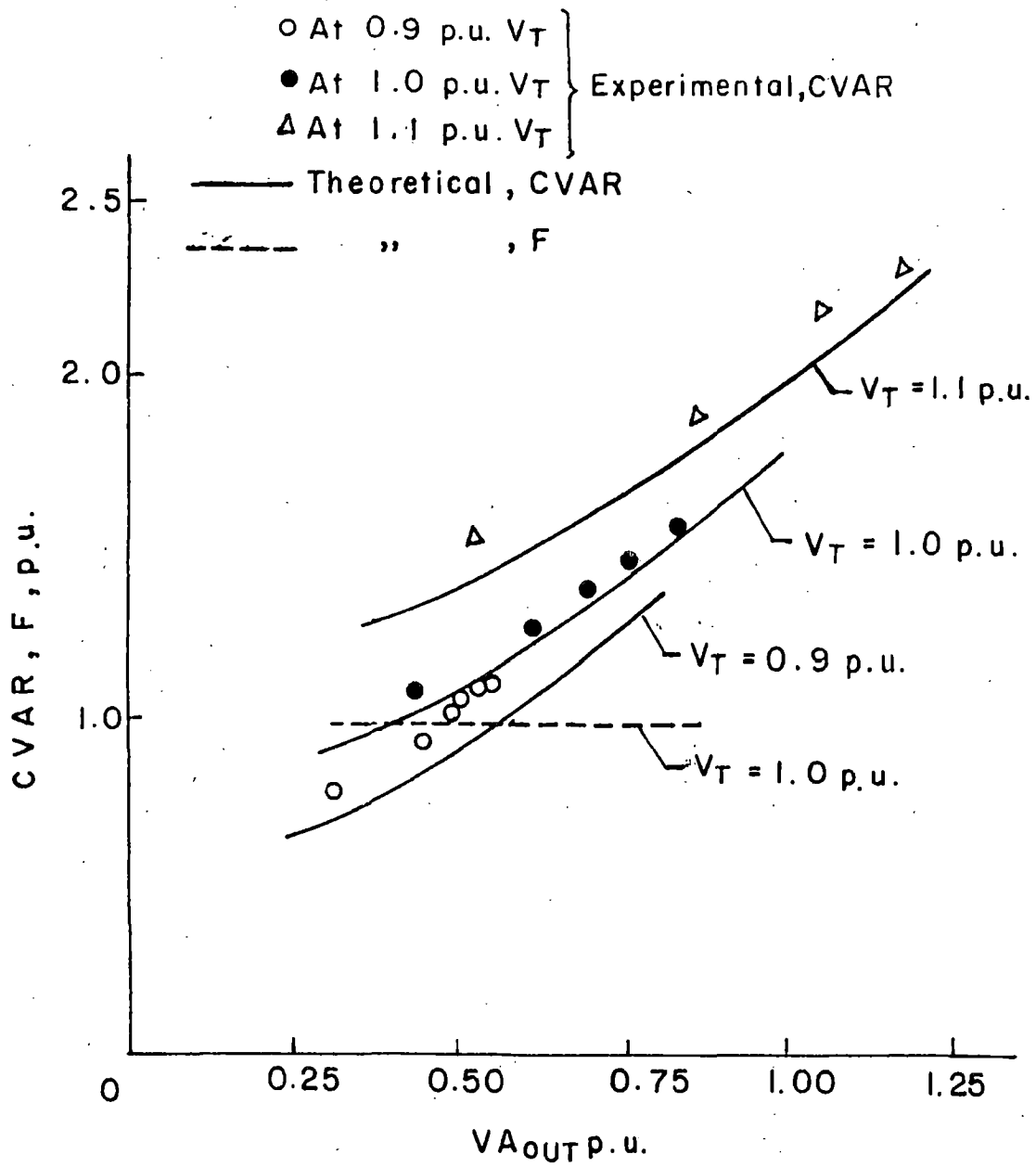


Fig.3.17 Variation of CVAR & F with V_{AOUT} to keep terminal voltage constant for R-L load.

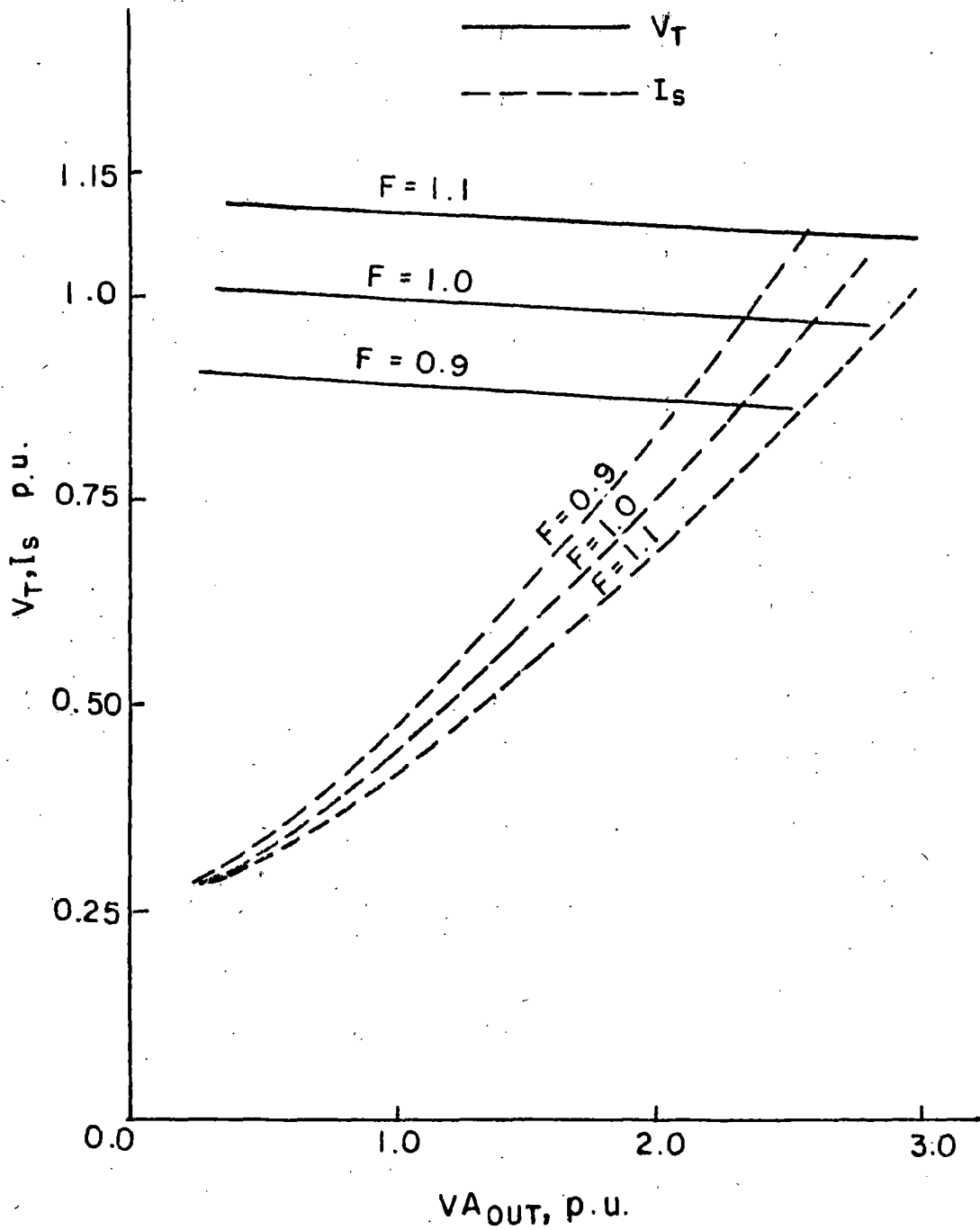


Fig. 3.18 Variation of V_T and I_s with VA_{OUT} to keep air gap flux (VG/F) constant for resistive load

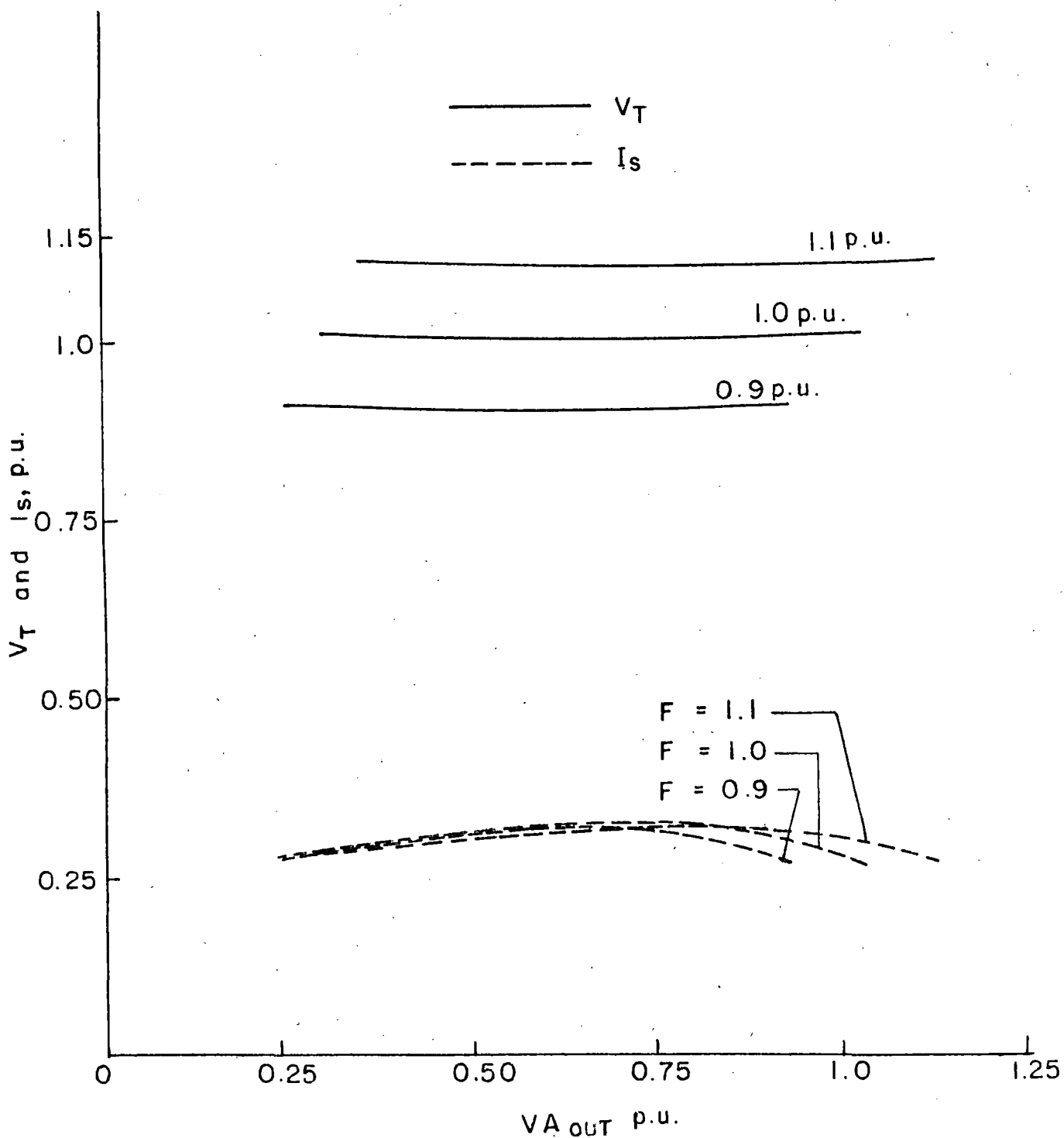


Fig. 3.19 Variation of V_T and I_s with VA_{OUT} to keep air gap flux (V_G / F) constant for R-L load

shows close similarity and due to which represents the validity of adopted analytical technique.

The results are presented for all four cases at resistive (R) and reactive (R-L) load for constant/different speeds. There is a good correlation between the computed and experimental results. Speed, VAOUT and terminal voltage are the important parameters and the effect of load on the terminal voltage and CVAR is studied for the different cases. The effect of these parameters is directly on the CVAR requirement for the induction generator. The results are presented for the variation of CVAR with VAOUT to maintain the constant terminal voltage at constant/different speed for resistive/reactive load. A minimum and maximum limit of CVAR is obtained to design a suitable voltage regulator for the self excited induction generator.

A suitable terminal voltage is to draw the maximum output at the rated stator current. For the economic use of the machine magnetic material steady state results are presented for the constant air gap flux and different loads. The study has been used for the design of components for the voltage regulating system of a 5 h.p. induction machine which is being used as a self excited induction generator.

CHAPTER - 4

DESIGN AND FABRICATION OF VOLTAGE REGULATOR

Summary :

This chapter includes the detailed description of a practical solid state voltage regulator. The closed loop scheme is having firing circuit, power circuit and controller. Complete design of voltage regulator including firing circuit, feedback circuit with proportional (P) and preportional integral (PI) controllers has been done. The over current and d_v/d_t protections are provided for the safe operation of thyristors.

4.1 Introduction :

When a suitable capacitor bank is connected across the terminals of an induction machine which is driven by a suitable prime mover at a particular speed, it gets excited to build up the voltage which is restricted by the magnetic saturation of the machine. If the induction machine is self excited with a particular value of capacitor and is loaded with resistive or reactive load, the terminal voltage drops by a considerable amount. However, in most of the applications, constant terminal voltage is needed at different loads. To achieve this simple and economical static VAR generator has been adopted which keeps the terminal voltage constant with varying load. The basic block diagram of the system is given in Fig. 4.1.

To realise the closed loop scheme it is essential to design the various elements of this closed loop system. The design of static VAR generator would be done to get the continuously varying VAR for the induction generator at varying loads. The static VAR generator comprises of a firing circuit which provides the variation of firing angle to change the firing instant of thyristors to control the effective inductor current and for the continuous variation of net VAR's at the generator terminals, controllers are also designed on the basis of practical observations. Two type of controllers (P and PI) have been implemented for the closed loop control of system.

4.2 Description of Closed Loop Control System :

The schematic diagram of the closed loop scheme has been shown in Fig. 4.2. In which an induction machine is coupled to a synchronous motor (as primer mover). A suitable valued capacitor bank is connected across terminals of the induction machine and to control the VAR's a static VAR generator has been developed. This static VAR generator includes a delta connected reactor with back to back thyristors in each arm to control the reactive current. These thyristor are getting firing pulses from the firing circuit. The instant of firing pulses is controlled by a feedback circuit and controller. The sensing of terminal voltage is done by a centre tapped step down transformer for the desired operation of voltage regulator. The a.c. voltage signal from feedback circuit is compared with the d.c. reference and the error signal voltage is amplified by the controller. The out-

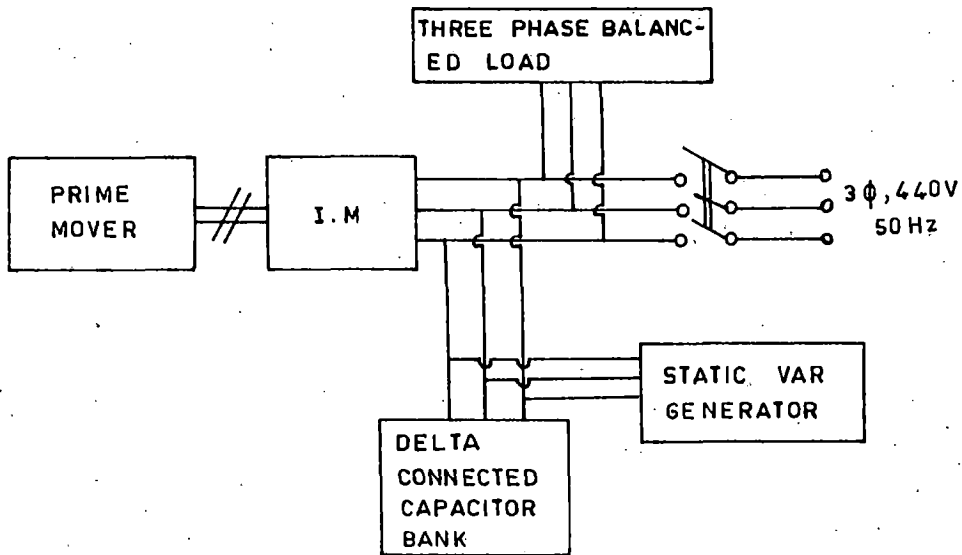


Fig.4.1 Basic block diagram of self excited I.G. with voltage regulator.

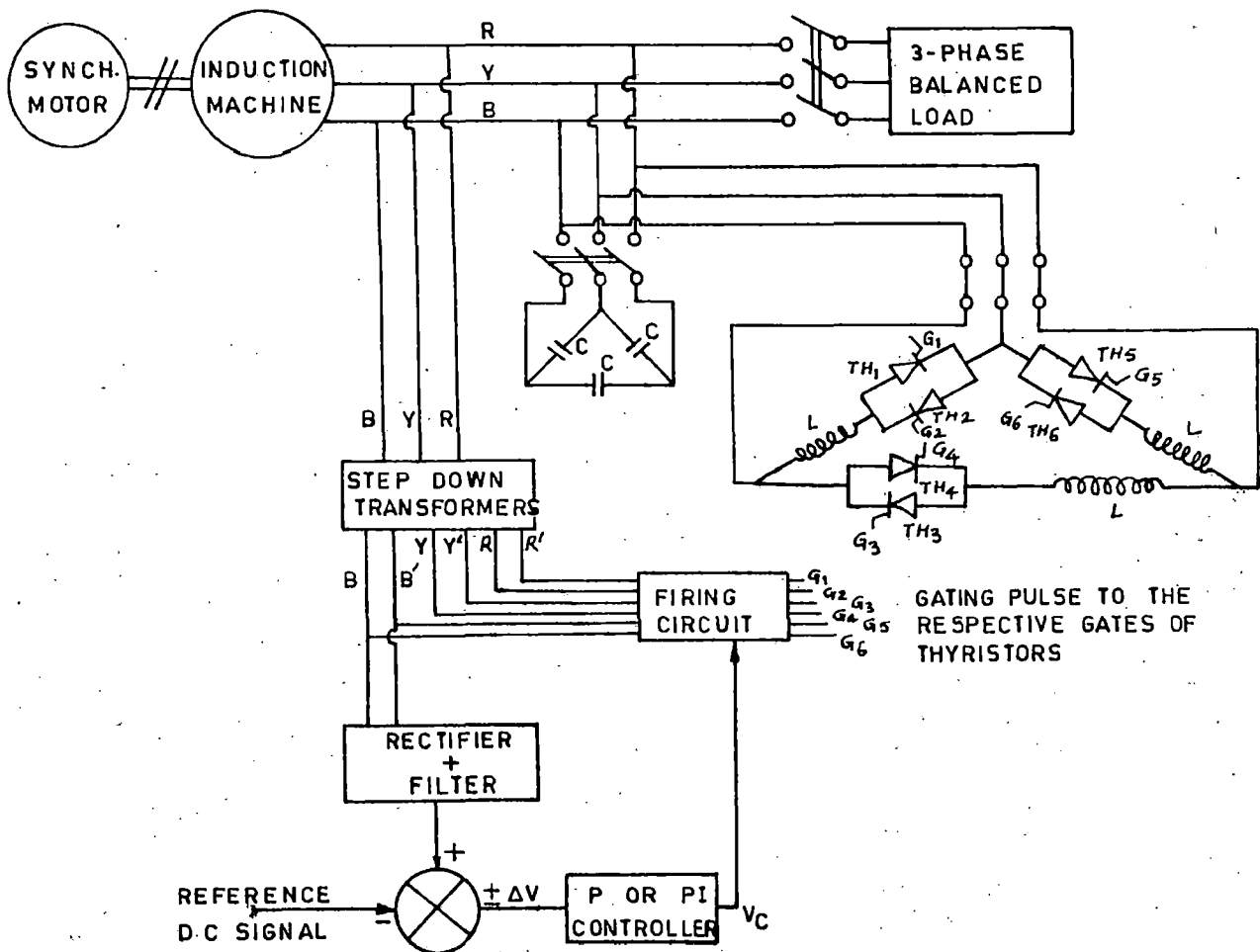


Fig.4.2 Schematic diagram of closed loop system

put of controller is used as the comparing signal of the comparator to vary the firing angle (α).

4.3 Principle of Operation :

When a large valued capacitor bank is connected across the terminals of a self excited induction generator, it can be loaded up to some considerable value but the terminal voltage will not remain constant as it is having drooping characteristic as shown in Fig. 3.9. The Fig. 3.9 shows that if the load is increased the voltage falls down considerably and at light loads there will be noticeable rise in the terminal voltage. To maintain the terminal voltage constant, it is required to connect a variable leading VAR source at the terminals of induction machine. This variable VAR source can be obtained with a discrete capacitors bank where the capacitors are changed in steps to fulfil the requirement of capacitive VAR to maintain the terminal voltage constant at different loads. But due to the step change in the capacitance terminal voltage can not be maintained exactly constant at different loads and the control will not be simple and in this type of control it needs more man power and constant attention to be paid to change the value of capacitance as per the load condition.

Another alternative for variable VAR source is to connect a variable inductor in parallel with a large valued capacitor bank. Here static VAR's generator is used to provide continuous variation of VAR's loads. This static VAR compen-

sator operates on the principle that a variable inductor is connected in parallel with a capacitor as shown in Fig. 4.3. This variable inductor compensates the extra capacitance available at light loads and as the load is increased the inductor current is reduced to increase the effective capacitance at the terminals of the induction generator. The static VAR compensators have been shown in Fig. 4.4. Here delta connected controlled inductor has been adopted in parallel with a delta connected capacitor bank which is quite simple and economical to use due to natural commutation and minimum number of thyristors.

Here a pure inductor is connected in series with a back to back connected thyristors, so the conduction angle of thyristor will be 180° for the variation of firing angle from 0° to 90° and the conduction angle reduces from 180° to 0° as the firing angle is varied from 90° to 180° as shown in Fig. 4.5(a). So for maximum leading VAR the thyristors are open or not conducted and for minimum leading VAR demand the thyristors are supposed to be closed or fully conduct. This static lagging VAR generator in parallel with a capacitor bank may be called as a static excitor for the self excited induction generator. Here, the delta connected thyristor controlled inductor has been selected which can be used effectively for balanced as well as unbalanced loads because each arm of this delta connection can be controlled separately.

The basic function of this static VAR generator is to vary the leading VAR to the induction generator as per the load

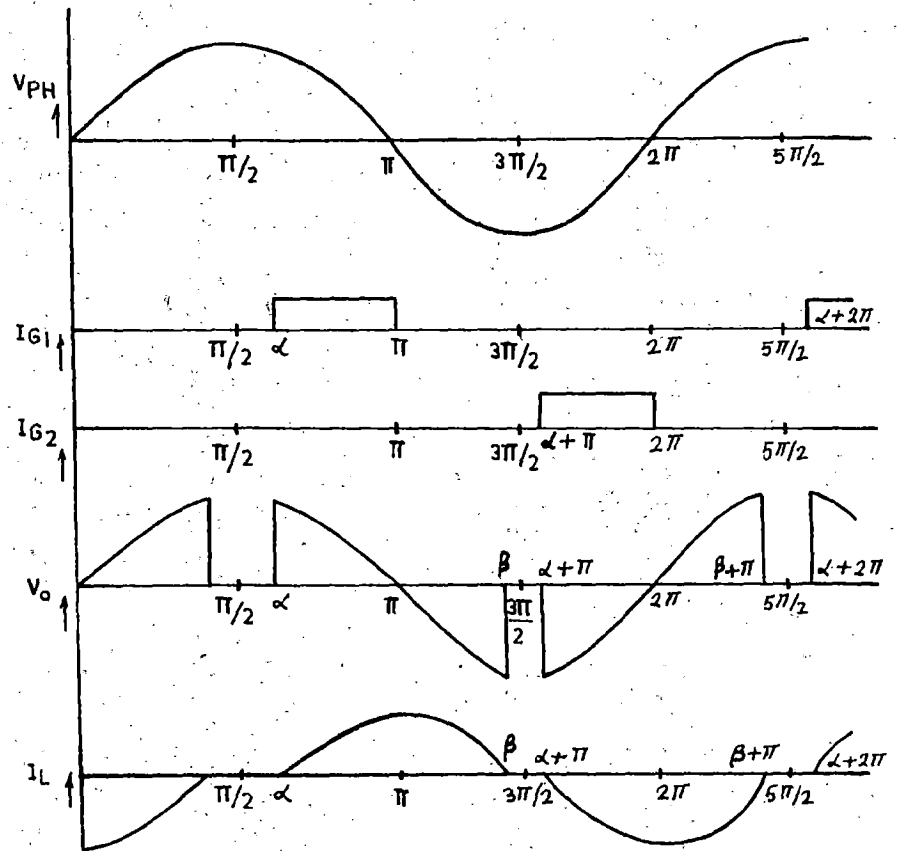
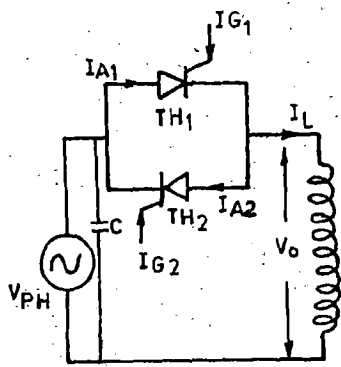


Fig.4.3 Single phase fullwave controller

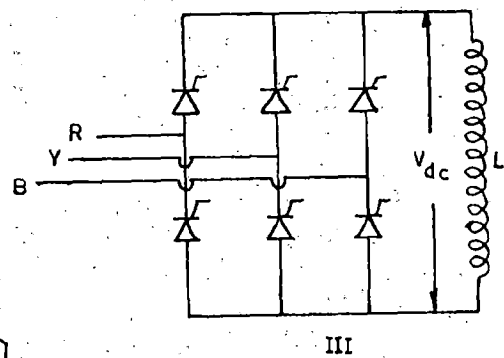
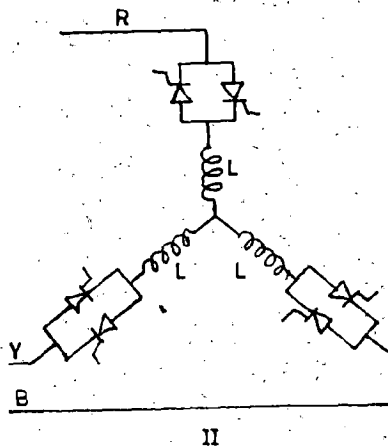
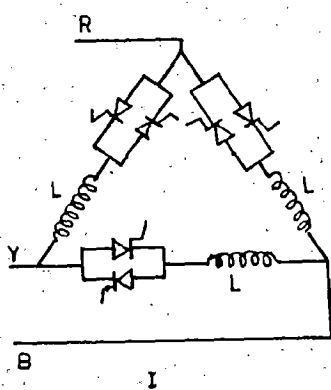


Fig.4.4 Naturally commutated lagging var generator

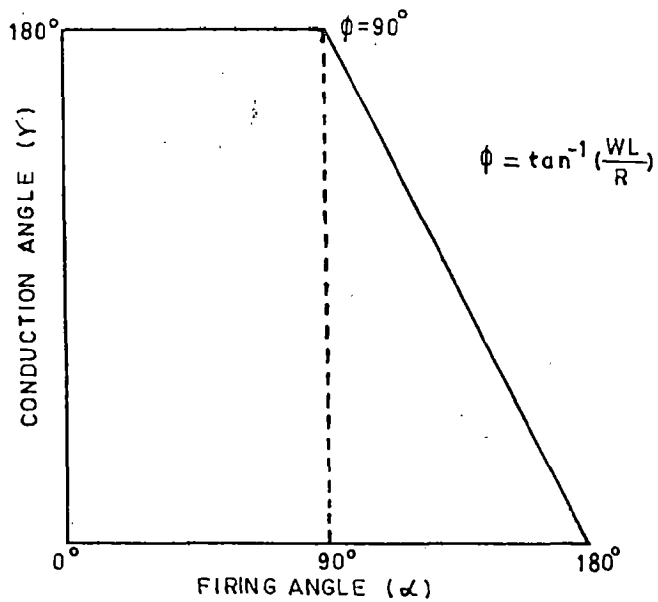


Fig.4.5(a) Relation between firing angle (α) and conduction angle (γ) for pure inductive load

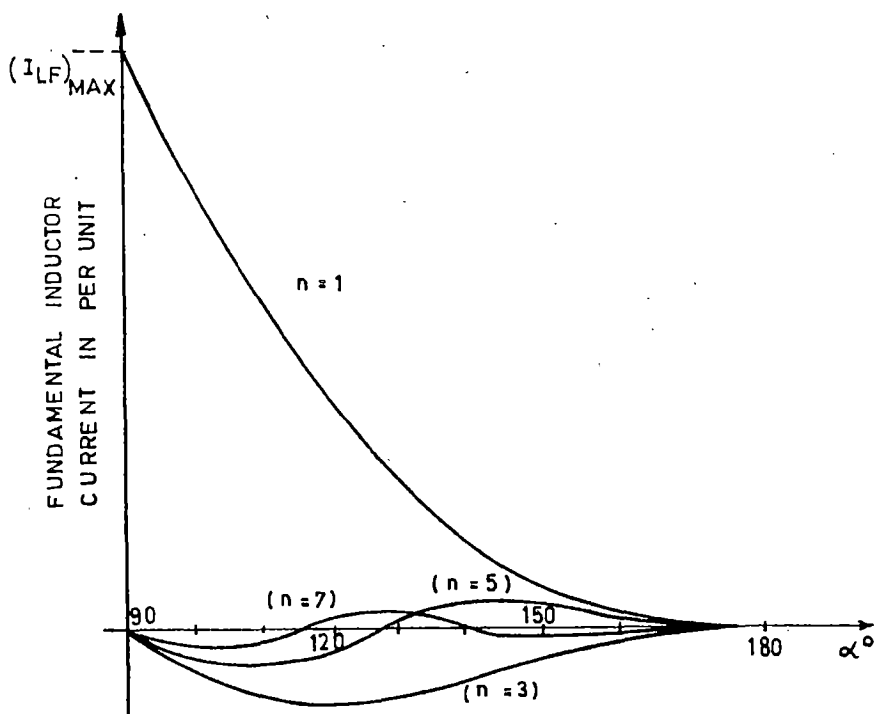


Fig.4.5(b) Fundamental of inductor current ($n=1$) versus firing angle

and for this purpose it has to determine the corresponding firing angle (α) to control the inductor current I_{IND} . To control the firing angle for the conduction of the thyristors P and PI controllers are implemented. For this controller voltage reference signal V_{REF} & voltage feedback signal V_F are compared and error is fed to the controller to modify the firing angle to make the error minimum. The time taken to modify the firing angle for a new value of load is depending upon the time constant of feedback path, controller firing circuit and induction generator. The time constant of feedback path is taken less because the terminal voltage should be sensed ^{fast} to compare with the reference signal. If it delays in the sensing of terminal voltage, there may be some large oscillations in the voltage and current of the machine with the sudden change of load. This type of controller is capable to operate at variable speeds also. Because the terminal voltage varies with the change of speed and again the leading VAR is controlled to keep the terminal voltage constant.

4.4 Selection of Thyristors Voltage Rating :

The operating voltage of the system is considered 400 volts and the thyristorised controlled inductor is connected in delta. So the line to line voltage will be impressed on each arm of delta. Under off condition the thyristor should be capable to withstand at the peak inverse voltage (PIV). When 400 volts (line to line) is used, the peak inverse voltage will be 1131.37 volts so the thyristor is selected for 1200 PIV.

Current Rating :- The maximum allowable current in inductor is 7.74 Amp. and with 25% over loading the current reaches up to 9.67 Amp. So the thyristors should be selected for 9.67 Amp. The specifications of thyristors are given below:

Type SS 1012, 16 Amp., 1200 PIV (convertor grade)

The thyristor are mounted on heat sinks to increase the surface area for the adequate dissipation of heat to the surrounding atmosphere. This production of heat is mainly at the cathode junction with the use of heat sinks the temperature of cathode junction does not exceed from an allowable limit for the safe operation of thyristors.

For over current protection a fuse has been employed in each arm. The d_v/d_t protection to the thyristor has been provided by using a suitable snubber circuit with 10 ohm, 5 watt resistance in series with .1 uF, 1200 volt capacitor.

4.5 Selection of Inductor and Capacitor :

To maintain the generator terminal voltage constant with varying loads of different power factor, a fixed leading current equal to magnetising current and a variable leading current equal to lagging load current plus rotor reactive current component are required with their consideration the self excited induction generator should be equipped with a fixed valued capacitor bank. In the earlier chapter for resistive load the capacitive reactance is found 1.57 p.u. to maintain the generator voltage at 1.0 p.u. at the speed .9.

p.u. for full load. For the design of capacitance value which should be suitable for the maximum lagging load, the reactive load ($X_{L \text{ Rated}}$) of 1.0 p.u. is considered at the terminals of induction machine. In the same way for the design of inductor capacitive load ($X_C \text{ Rated}$) of 1.0 p.u. is considered which is capable to compensate the capacitive effect of load and the extra capacitance connected under no load conditions at the induction generator terminals for capacitance calculation.

$$X_{C \text{ MIN}} = \frac{X_{C \text{ Max}} \cdot X_{L \text{ Rated}}}{X_{C \text{ Max}} + X_{L \text{ Rated}}}$$

$X_{L \text{ Rated}}$ = Rated pure inductive load in p.u.

For inductance calculation

$$X_{L \text{ MIN}} = \frac{X_{C \text{ MIN}} \cdot X_C \text{ Rated} \cdot X_{C \text{ Max}}}{X_{C \text{ Max}} (X_{C \text{ MIN}} + X_C \text{ Rated}) \cdot X_{C \text{ MIN}} \cdot X_C \text{ Rated}}$$

$X_C \text{ Rated}$ = Rated pure capacitive load in p.u.

From the results presented in third chapter of the value of $X_C \text{ Max}$ is found 3.708 p.u. at 1.0 p.u. speed to generate the terminal voltage at 1.0 p.u. Now assuming $X_{L \text{ Rated}}$ as 1.0 p.u. the value of $X_{C \text{ MIN}}$ is .7876 p.u. and if this $X_{C \text{ MIN}}$ is considered on the base frequency the value of capacitance is calculated as 39.75 μF .

In the same the reactor value is calculated, assuming $X_C \text{ Rated}$ equal to 1.0 p.u. and the value of $X_C \text{ Max}$ and $X_{C \text{ MIN}}$ are taken from the design of capacitor value formulation, as .504 p.u. which gives the value of inductance (L) at base

frequency as 161 mHz. For the present voltage regulator 16 μ F capacitor bank is connected at the terminals of the induction machine and a 1.0 p.u. reactor (Delta connected) has been used.

4.6 Design of Firing Circuit :

The design of firing circuit incorporates input step down transformer, attenuator circuit, zero crossing detector, constant current ramp generator, comparator, AND gate, high frequency oscillator and pulse amplifier. The block diagram and corresponding waveforms are shown in Fig. 4.6. The practical firing circuit for one phase has been shown in Fig. 4.7. The static VAR generator is comprising six thyristors in three phase. So three symmetrical circuits are used to produce six gating pulses in synchronism with the input terminal voltage but the single feedback and controller circuit will be used to change the firing instant of all the phases.

4.6.1 Design of Input Transformers :

The operating voltage for the self excited induction generator is around 400 volts. The induction generator stator is delta connected and a delta connected capacitor bank in parallel with a delta connected controlled inductor is also connected at the terminals of the induction machine. To take the input as voltage for the firing circuit, step down transformers are used which are free from the saturation at the higher voltages. The system consists of three 600/15-0-15 volts

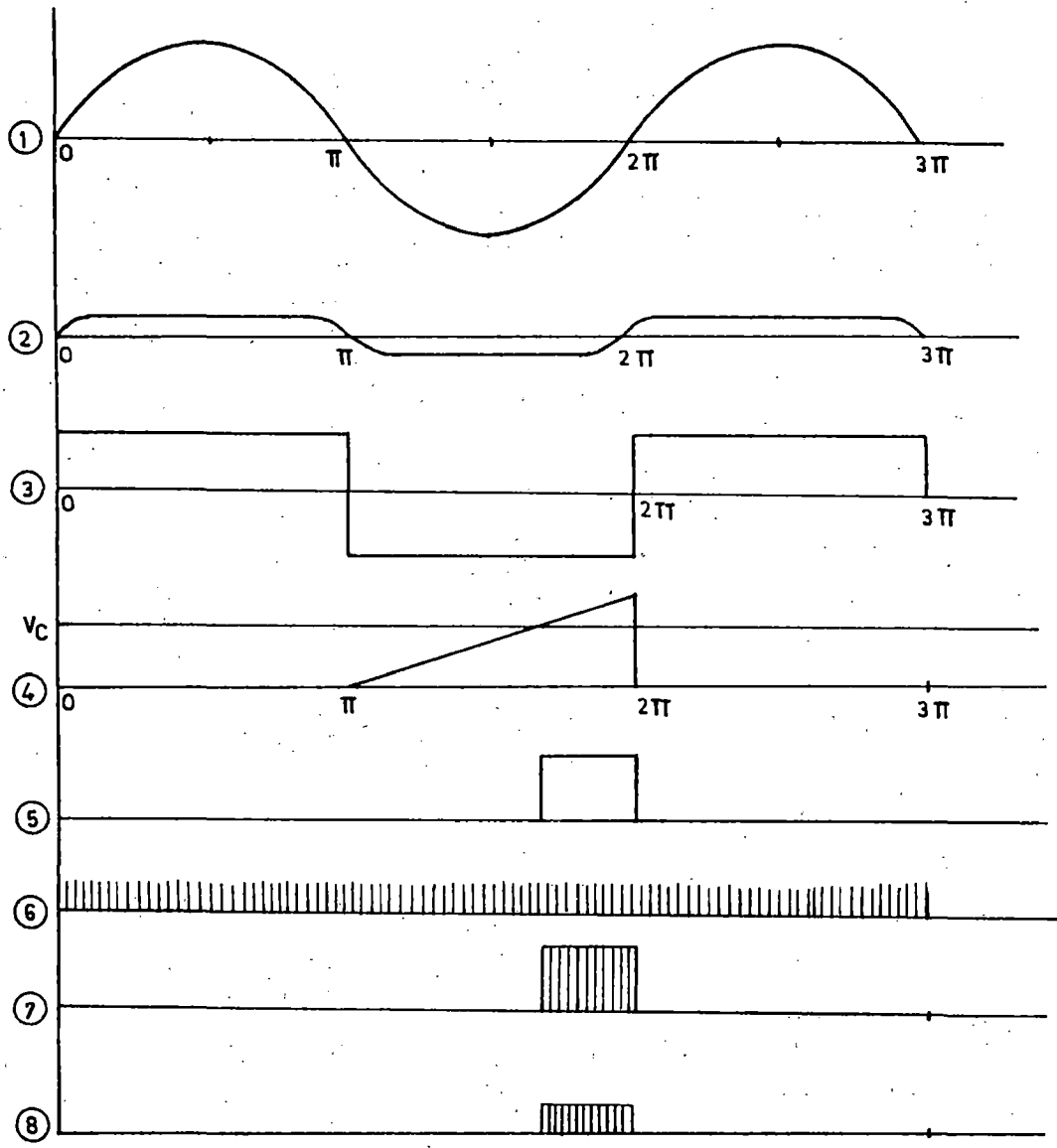
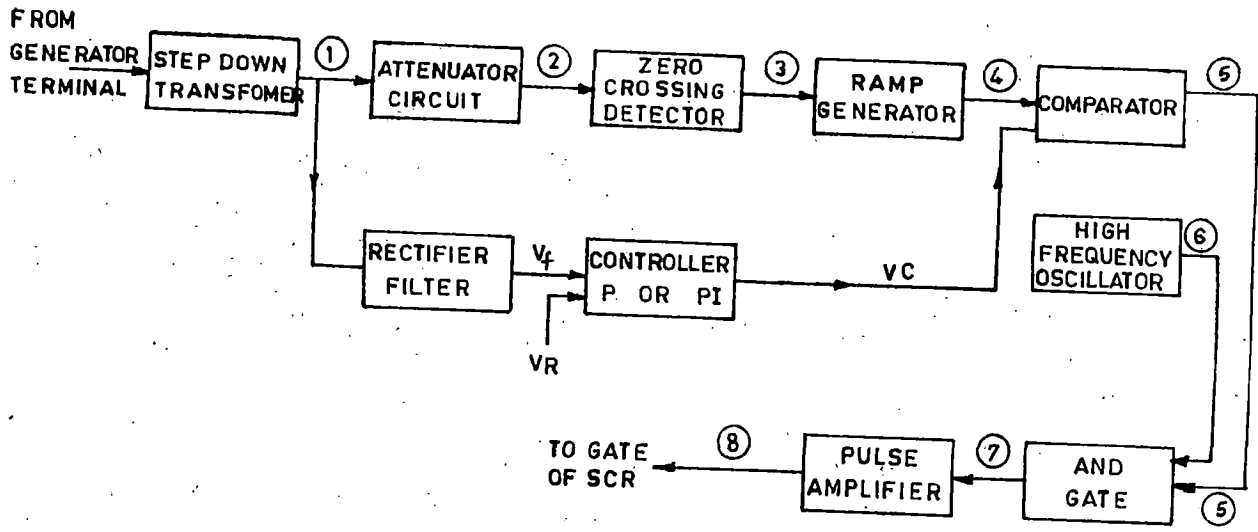


Fig.4.6 Block diagram of firing circuit and corresponding waveforms

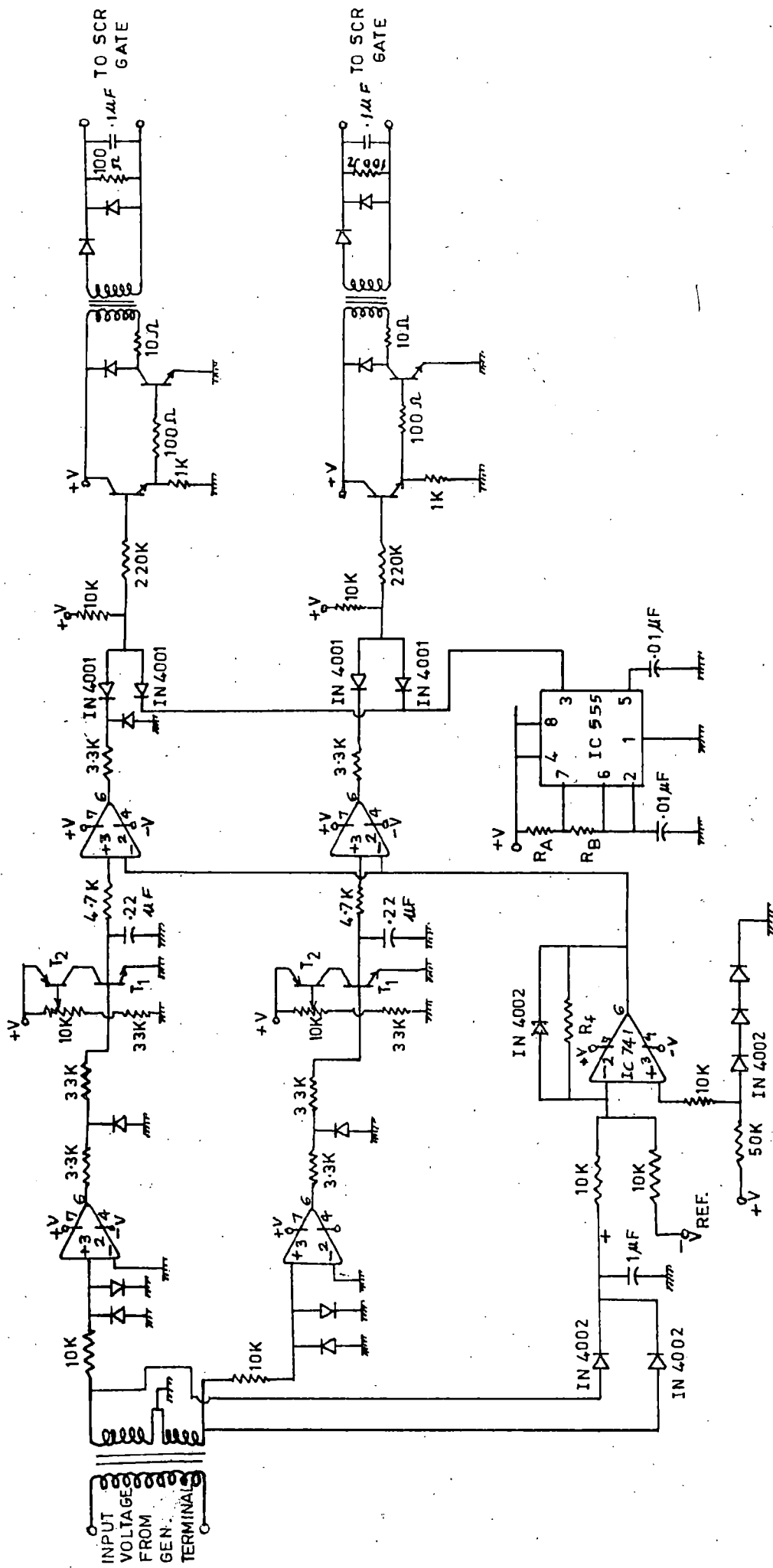


Fig.4-7 Practical firing circuit for single phase of three phase controlled inductor

transformers as input transformers for the firing circuit and the feedback signal is also taken from the secondary of the input transformers.

4.6.2 Attenuator Circuit :

The secondary of input transformer is centre tapped. The centre point is grounded to obtain to input a.c. voltages with 180° phase difference. The secondary is connected to a antiparallel connected diodes (IN 4002) through a 10 K resistance as in Fig. 4.8.1. The input a.c. voltage to the firing circuit is attenuated because one diode conducts in positive half of sine wave and other in negative half. The output of this circuit which is in synchronism with the input sine wave, is nonlinear attenuated wave as shown in Fig. 4.9.1.

4.6.3 Zero Crossing Detector :

The output of nonlinear attenuator is fed to the zero crossing detector. Here op amp IC 741 is used with PIN No. 2 grounded and input at PIN No. 3. The circuit configuration is shown in Fig. 4.8.2. If the reference voltage at the inverting input is set equal to zero and the input to op amp is the attenuated wave the output is square wave. The output of square wave generator is shown in Fig. 4.9.2.

4.6.4 Constant Current Ramp Generator :

The principle of constant current source has been used to get the slope of the ramp linear. The circuit

configuration is shown in Fig. 4.8.3. Here two transistors P-N-P(BC 157) and N-P-N (HCHL 1008) are used with R_1 , R_2 , R_3 and C. The capacitor C is charged linearly through a constant current source consisting R_1 , R_2 , R_3 and T_2 and isolates from the timing circuit through emitter follower buffer stage T_1 . The output of the zero crossing detector is applied at the gate of transistor T_1 (NPN) through resistance R_1 . The transistor T_1 turns on when positive pulses are appeared at the gate of T_1 . So the transistor remains on for the period of positive pulse and capacitor discharges as soon as the transistor T_1 turns ON. The capacitor C starts charging through constant current source from the instant the transistor T_1 turns OFF. Thus a ramp is obtained across the capacitor C. Here the ramp height was +15 volts. The output of ramp generator is shown in Fig. 4.9.3.

4.6.5 Comparator :

The circuit configuration of comparator is shown in Fig. 4.8.4. The op amp IC 741 is used as comparator where the output of ramp generator is connected to PIN No. 3 (non inverting input) through a 4.7 K resistance and the comparing signal is applied at PIN No. 2 (inverting input). Here as the comparator signal is varied from 0 to +15 volts the firing angle can be varied from 0° to 180° . The output waveform of the comparator is shown in Fig. 4.9.4.

4.6.6 AND Gate :

The circuit configuration for this is given in Fig. 4.8.5. The diode used is IN 4001. The output of

comparator is connected to the cathode of diode through 3.3 K resistance and other diode is connected to the output of oscillator. This AND gating results in high frequency pulses during comparator output pulse as shown in Fig. 4.9.5. The high frequency of gating pulse reduce the gate losses sufficiently and the size of pulse transformer is also reduced.

4.6.7 High Frequency Oscillator :

The timer IC 555 is used as high frequency oscillator. The circuit configuration for the as table multivibrator is shown in Fig. 4.8.6. The timer IC 555 trigger itself and runs freely as multivibrator. The external capacitor C_T charges through R_A and R_B but discharges through R_B only. The charging and discharging time is in dependent of supply voltage. The charging time is given by

$$T_1 = .693 (R_A + R_B) \cdot C_T$$

Discharging time

$$T_2 = .693 R_B C_T$$

Time period of one cycle

$$T = T_1 + T_2 = .693 (R_A + 2R_B) C_T$$

Now the frequency of oscillator

$$f = \frac{1}{T} = \frac{1.44}{(R_A + 2R_B) C_T}$$

Here 4.76 KHz oscillator is used to perform AND gating with comparating signal.

4.6.8 Pulse Amplifier :

The amplitude of output from AND gate may not be sufficient to turn ON the thyristor. To obtain an amplified pulse to turn ON the thyristor, the output of AND gate is amplified through a two stage transistor amplified as the circuit configuration is shown in Fig. 4.8.7.

The NPN transistor (HC HL 100 B) is used for the first stage amplification, which serves the purpose of current amplification. To enhance the power level of signal emitter follower configuration is used. The output of the emitter follower is applied to the base of second stage amplifier. The NPN transistor (SL 100) is used as common emitter configuration for the voltage amplification. To achieve the desired amplification the output of AND gate connected to the base of emitter follower through a 2,20 K resistance the output of emitter is taken from 2K resistance connected between emitter and ground. Now this output is fed to the base transistor of voltage amplifier through a 100 ohm resistance. The V_{CC} applied is +22 volts.

These amplifiers pulses are applied to the primary winding of pulse transformer through a 10 ohm resistance. The main purpose of pulse transformer is to isolate the control circuit from the power circuit.

To avoid saturation of the pulse transformer core, a diode IN 4001 is connected across load resistance and primary winding of pulse transformer. For the over-voltage

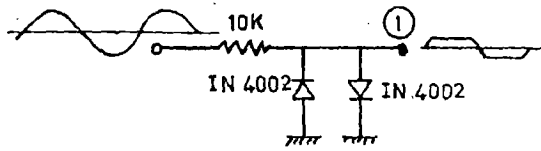


Fig.4.8.1 Attenuator circuit

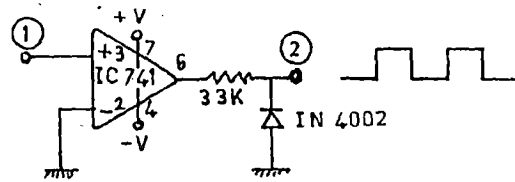


Fig.4.8.2 Zero crossing detector circuit

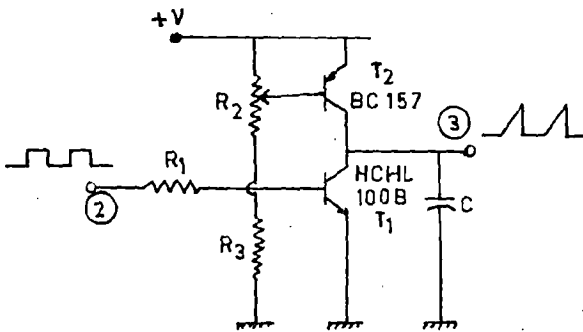


Fig.4.8.3 Constant current ramp generator circuit

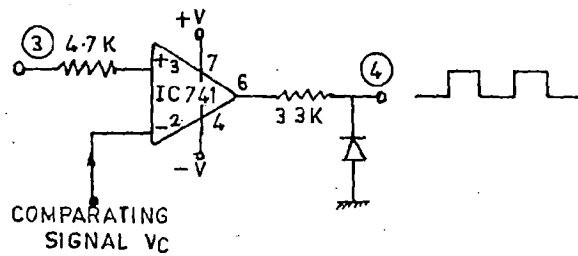


Fig.4.8.4 Comparator circuit

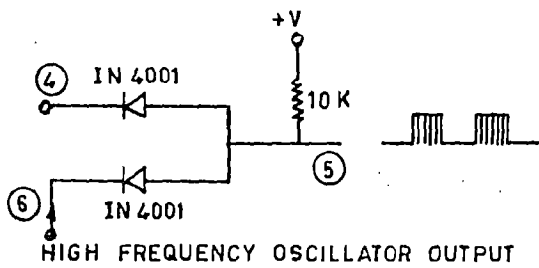


Fig.4.8.5 And gate circuit

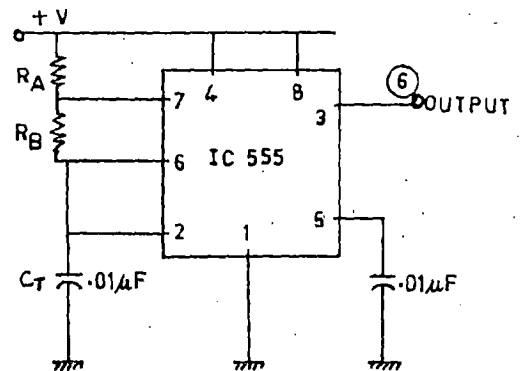


Fig.4.8.6 High frequency oscillator circuit

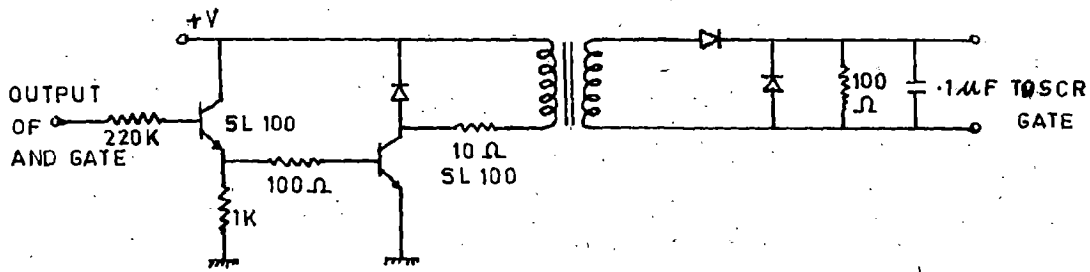


Fig. 4-8-7 Configuration of pulse amplifier circuit

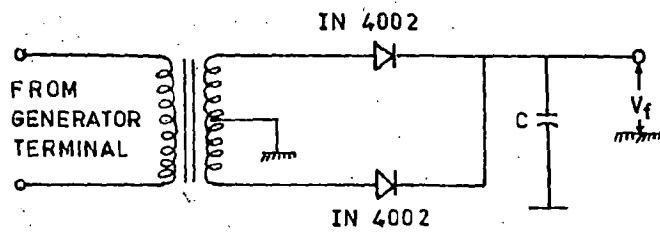


Fig. 4-10 Configuration of rectifier and filter circuit

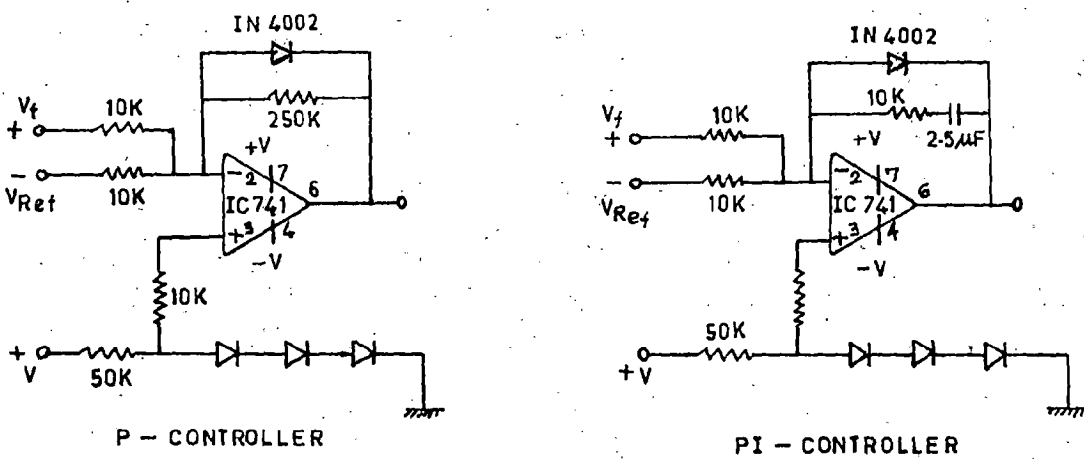


Fig. 4-11 Configuration of proportional (P) and proportion plus integral (PI) controllers

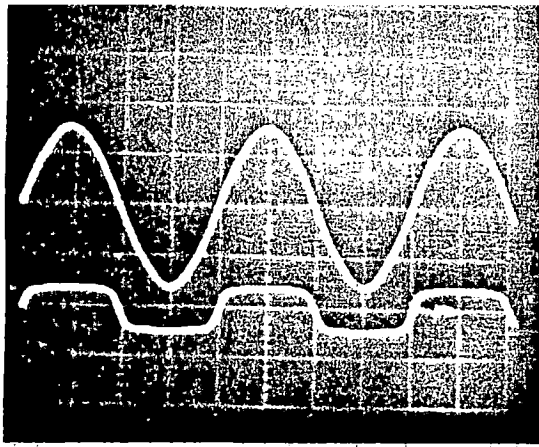


Fig. 4.9.1 Waveforms of input voltage and attenuator output of firing circuit

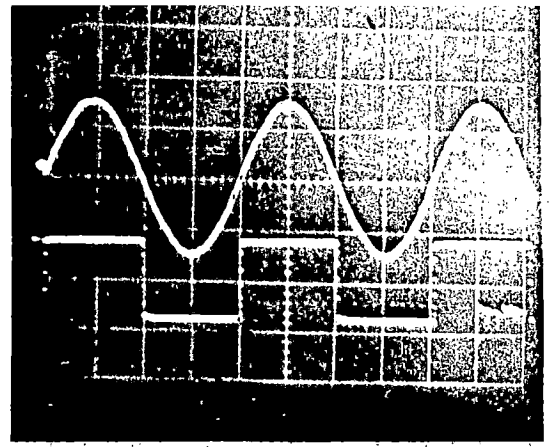


Fig. 4.9.2 Waveforms of zero crossing detector and input voltage of firing circuit

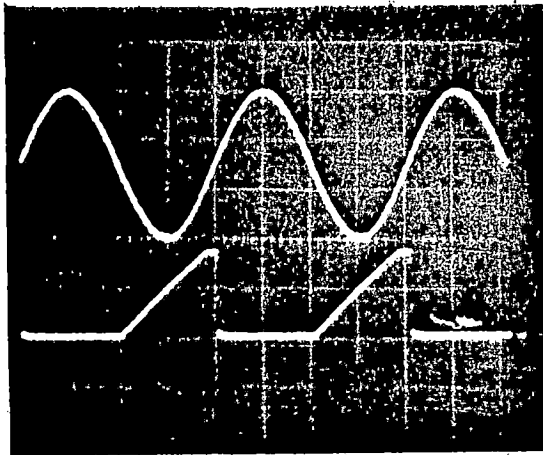


Fig. 4.9.3 Waveforms of input voltage and constant current ramp generator output of firing circuit

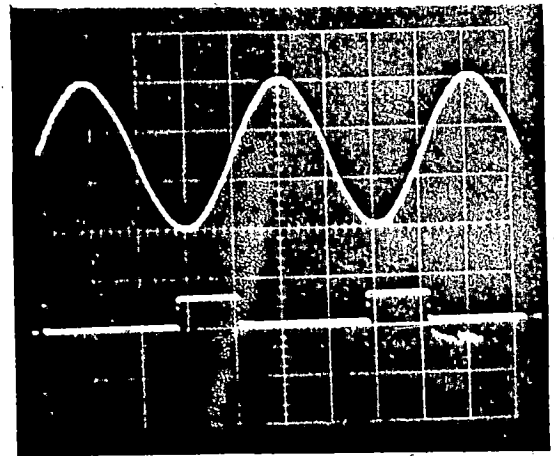


Fig. 4.9.4 Waveforms of input voltage and comparator output of firing circuit

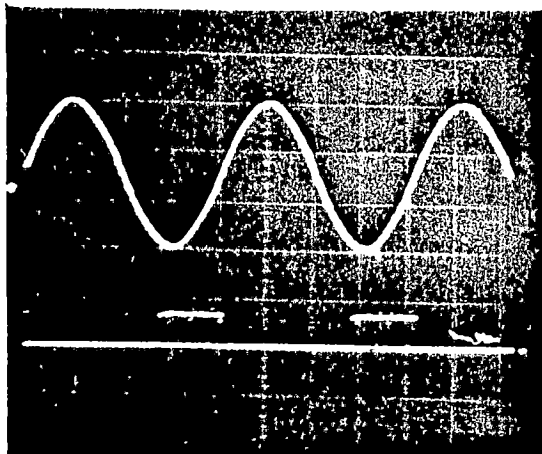


Fig. 4.9.5 Waveforms of input voltage and AND GATE output of firing circuit

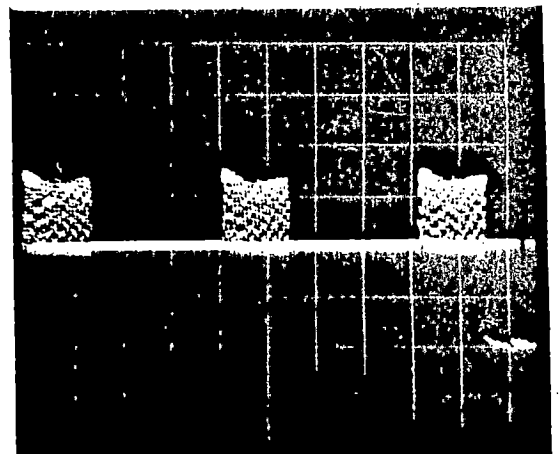


Fig. 4.9.6 Waveforms of pulse amplifier output of firing circuit

protection of gate of thyristor, a diode IN 4001 is connected between gate and cathode as shown in Fig. 4.8.7. A diode IN 4001 is connected in series with the secondary of pulse transformer to block negative spikes. Trigger pulses may be induced at the gates due to turn ON and turn OFF of a neighbouring thyristor or transients in the power circuit which may cause spurious firing of the thyristor. To avoid this problem a capacitor of 0.1 μF and resistance of 100 ohm are connected to by pass noise pulses. The output of this pulse amplifier as gating pulse is shown in Fig. 4.9.6.

4.7 Design of Voltage Feedback Circuit :

The line voltage is impressed on the input transformer (step down transformer) to give the input a.c. voltage to the firing circuit. This a.c. voltage on the secondary of the input transformer can be used for the feedback. So this voltage is rectified with a full wave rectifier using only two diodes (IN 4002) as shown in Fig. 4.10. But there are ripples in d.c. output of this rectifier which are eliminated to some extent by using a 0.1 μF capacitor at the output of this rectifier.

4.8 Design of Controller :

From steady state analysis of self excited induction generator it has been noticed that the CVAR demand increases with the increase of load to maintain the terminal voltage constant either resistive or reactive (R-L) load

is applied at the induction generator. In stable region the variation of CVAR with VAOUT is monotonic in Fig. 3.13 and Fig. 3.17. Therefore since feedback sign inversion does not occur in the control region of interest, it is possible to control the exciter based on the integrated voltage error. This also means that the firing angled versus fundamental inductor current characteristic Fig. 4.5(b) will be contained in the closed voltage feedback loop. [1]

Controllers are usually of proportional (P) and proportional plus integral (PI) type. In general terms proportional control influences the transient response and the integral component gives good steady state accuracy. Here the controllers utilise the principle of negative feedback which provides good stability for the system. The proportional control is having the relationship between output of the controller and actuating error signal i.e. transfer function.

$$G_P(S) = K_P$$

K_P is the gain of proportional controller, so the proportional controller is essentially an amplifier with adjustable gain.

For proportional plus integral controller the transfer function is

$$G_{PI}(S) = K_P \left(1 + \frac{1}{T_I S} \right)$$

K_P represents the proportional gain and T is the

integral time, both K_p and T are adjustable.

The circuit configurations of P and PI controllers are shown in Fig. 4.11. The gain of proportional controller is adjusted at 25 and for portional plus integral control the proportional gain 1 and the integral time constant is 25×10^{-3} sec. The limiters are also used to the limit the output of controllers at 1.4 volt to the lowest level and 15 volt at the maximum. This can be achieved by applying 2.1 volts at the Non inverting input (PIN No. 3) of op amp IC 741 and connecting a diode IN 4002 with anode on PIN No. 2 and cathode on PIN No. 6. The limiter connection remains similar for both P and PI controller.

Conclusion :

The design and development of the voltage regulator for a capacitor self excited induction generator is carried out. The principle of operation of the closed loop scheme is described. A power circuit, with adequately protected thyristor is designed for the induction generator voltage regulating system. The phase controlled inductor used for the continucusly varying VAR to the self excited induction generator and a firing circuit is designed to control the inductor current for the compensation of large capacitor connected at the terminal of generator. The elements of voltage controller are designed on the basis of experimental study.

CHAPTER - 5

PERFORMANCE OF VOLTAGE REGULATION SYSTEM

Summary :

The chapter includes the experimental investigation on the performance of the voltage regulating system. The performance of the system has been observed for the steady state and transient response for the parameters like terminal voltage, load current and stator current. The oscillograms of these various waveforms are recorded for steady state and transient response of the induction generator with proportional (P) and proportional plus integral (PI) controller by using a storage cathode ray oscilloscope.

5.1 Introduction :

In the previous chapter various components of the voltage regulating system for the self excited induction generator have been designed and on that basis a practical solid state voltage regulator has been fabricated. The performance of induction generator is observed with the developed voltage regulator at different loads. The tests are conducted for steady state performance to study the effect of load on the terminal voltage. The effect of reference voltage on the terminal voltage is also observed under steady state as well as transient state. The oscillogram of terminal voltage, load current and stator current are recorded under steady and transient state by using a storage C.R.O. These

results provide the information regarding the terminal voltage and current waveforms under steady state and response of the voltage regulating system. Proportional (P) and proportional plus integral (PI) controllers have been used to observe the performance of voltage regulator at constant speed and different loads.

5.2 Experimentation :

The schematic diagram of voltage regulating system for self excited induction generator has been shown earlier in Fig. 4.2. The experimental setup with the voltage regulator has been arranged according to this schematic diagram. The synchronous motor is connected ^{to} the supply at line frequency to run it at some constant speed. So the rotor of induction machine is also driven at the speed corresponding to the line frequency as the shaft of induction machine is coupled to the rotor shaft of synchronous motor. Now ^{at} no load the capacitor switch is closed. The voltage starts building up due to the large valued capacitor at the armature terminals of induction machine final value of voltage build up is controlled by the value of reference voltage. A three phase resistive load has been used to study the performance of self excited induction generator with the voltage controller at different loads.

5.3 Results and Discussion :

The voltage regulator is tested at constant speed and balanced resistive load. The terminal voltage (V_T)

variation with the reference voltage (V_{REF}) at no load with P-controller has been shown in Fig. 5.1. Here the terminal voltage increases almost linearly with increase of reference voltage. The terminal voltage Vs. reference voltage characteristic at no load for PI controller has been given in Fig. 5.2. The curve plotted in Fig. 5.2 depicts that there is a linear rise in terminal voltage with the rise in reference voltage.

The machine is loaded with the resistive load to study the performance of voltage regulator under loaded conditions. These results with P and PI-controllers have ^{been} plotted in Fig. 5.3. The terminal voltage drops with the increasing load for both P and PI controllers. The drop in terminal voltage with $V_{A_{OUT}}$ is very much linear for both the controllers as it is clear from the Fig. 5.3. The drop in terminal voltage for particular load is more for P controller than PI controller.

The steady state results have been taken in the form of oscillograms of terminal voltage (V_T), load current (I_L), and stator current (I_S) at different resistive loads. These oscillograms have been recorded by using a storage C.R.O. The waveforms for load current (I_L) and terminal voltage (V_T) at two different loads with P-controller have been shown in Fig. 5.4(a) and (b). The waveforms of load current and terminal voltages are almost sinusoidal. The load current is slightly distorted which is due to the non sinusoidal inductor current which affects the line current and

so the terminal voltage is also affected. The waveforms of stator current (I_S) and terminal voltage (V_T) at no load and balanced resistive load have been shown in Fig. 5.4(c) & (d). The percentage of harmonic in stator current at no load is observed more and as the load is increased the percentage of harmonics decreases, as the stator current waveform becomes very near to sinusoidal ^{under} / the loaded condition. The oscillograms for steady state terminal voltage stator current and load current have been recorded with a PI-controller. The waveforms of terminal voltage and load current at different loads have been presented in Fig. 5.5(a) and (b). The results show that the waveform for the load current and terminal voltage is near to sinusoidal and it improves with increasing load. The stator current and terminal voltage waveforms have been shown in Fig. 5.5(c) and (d). The behaviour of wave forms for terminal voltage, load current and stator current with PI-controller is similar to P-controller. The load current and stator current are slightly distorted due to the effect of induction current and saturation of magnetic circuit of induction ^{machine which} / causes harmonics. The transient performance of the voltage regulator with sudden application/removal of balanced resistive load for P and PI controller has been recorded by using a storage C.R.O. The transient response for sudden reference voltage variation and the voltage building up for a particular reference voltage has also been recorded to study the transient performance of the induction generator with the voltage regulating system. First of all the study has been done with P-controller. The voltage building up at

$V_{REF} = 12.8$ V at no load has been shown in Fig. 5.6(a). The voltage starts building up from 0 to the steady state value (372 Volts). The system is quite fast as it takes around .9 sec to achieve steady state. The Fig. 5.6(b) consists of the response at no load for sudden reference change from 12.8 V to 10.8 V. The terminal voltage drops from 372 Volts to 320 Volts for this reference change and the steady state is achieved within 2 or 3 cycles which gives rise to the idea that the system is stable and considerably fast. The sudden variation of load (application/removal) has been given in Fig. 5.6(c) and (d) which consist of the terminal voltage and load current waveforms. The sudden application of load affects the terminal voltage. The terminal voltage drops momentarily and rises again to reach the steady state value as shown in Fig. 5.6(a). In the same way when the load is removed terminal voltage gets a boost and finally reaches to steady state value. There is a difference in the frequencies of the generated voltage at different loads but it cannot be predicted exactly from the Fig. The Fig. 5.6(e) gives the variation of terminal voltage for the sudden application of load. Initially the system was running at no load and it is suddenly loaded. The effect on the terminal voltage will be same as in the case of load current. The variation of terminal voltage and stator current at sudden removal of load has been recorded as given in Fig. 5.6(f). The stator current drops and reaches to a steady state value within 2 or 3 cycles.

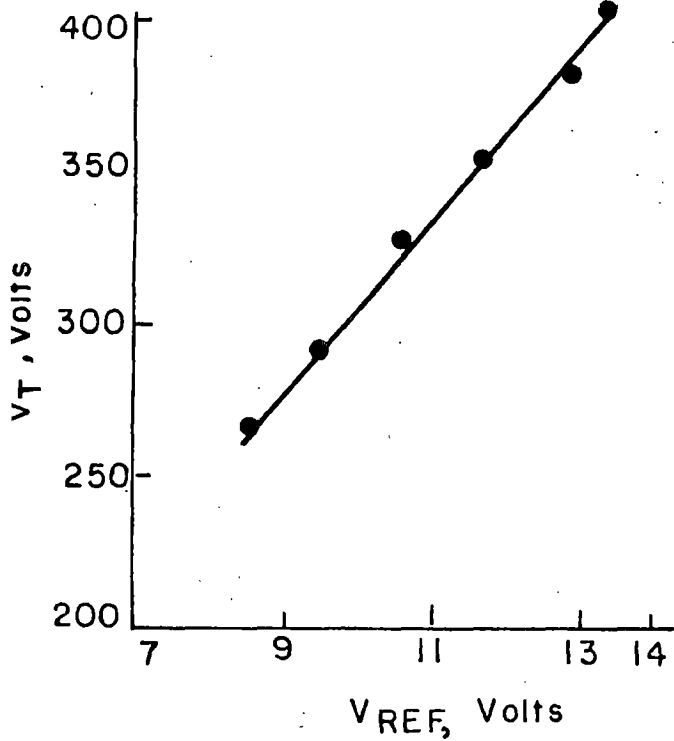


Fig.5.2 Variation of terminal voltage with reference voltage using PI controller.

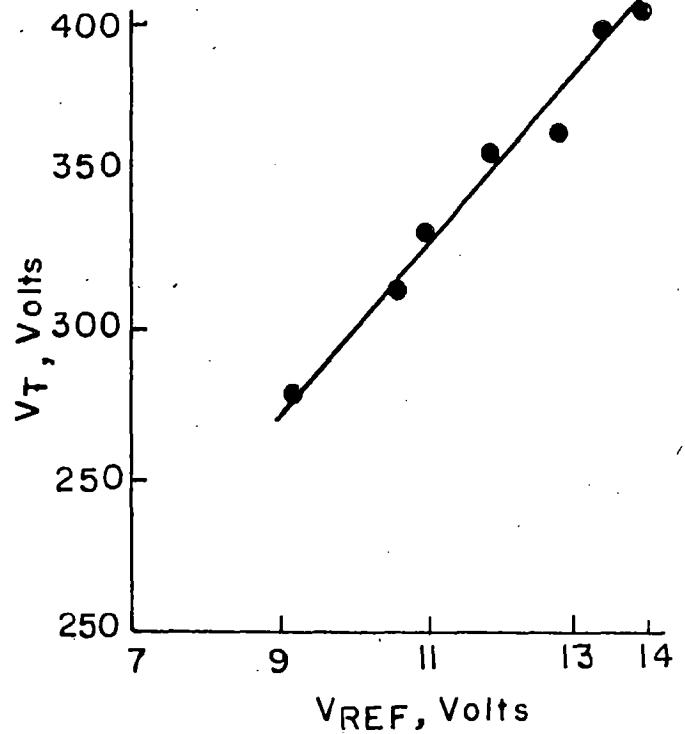


Fig.5.1 Variation of terminal voltage with reference voltage using P controller.

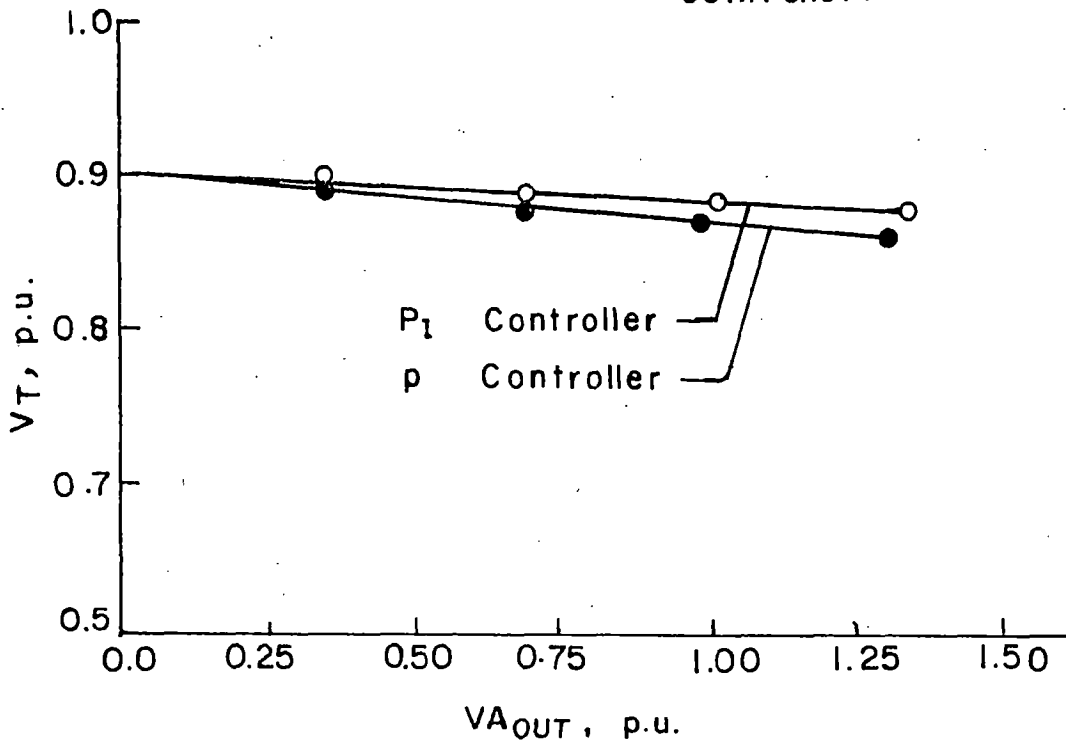


Fig.5.3 Variation of terminal with $V_{A_{OUT}}$

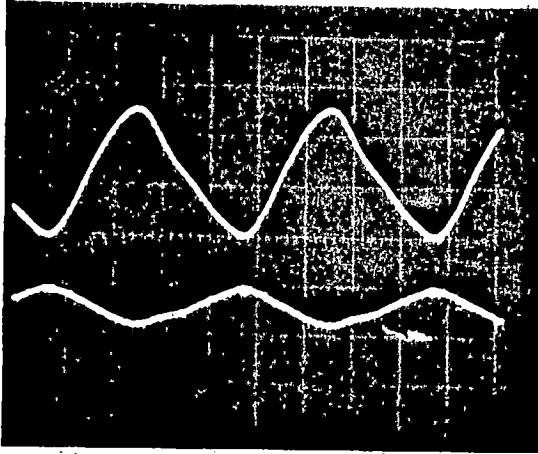


Fig. 5.4(a) Steady state waveforms of terminal voltage and load current ($I_L = 1.4$ Amp) with P-controller

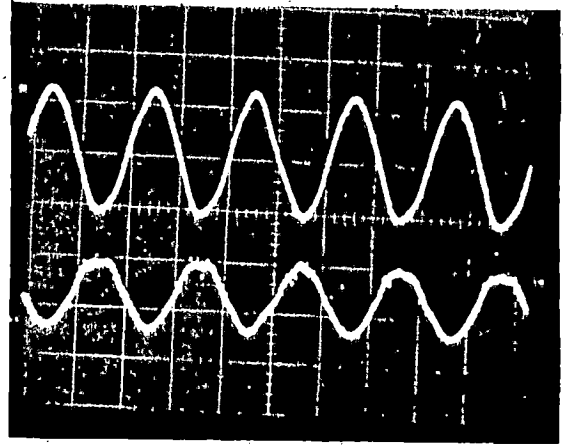


Fig. 5.4(b) Steady state waveforms of terminal voltage and load current ($I_L = 3.4$ Amp) with P-controller

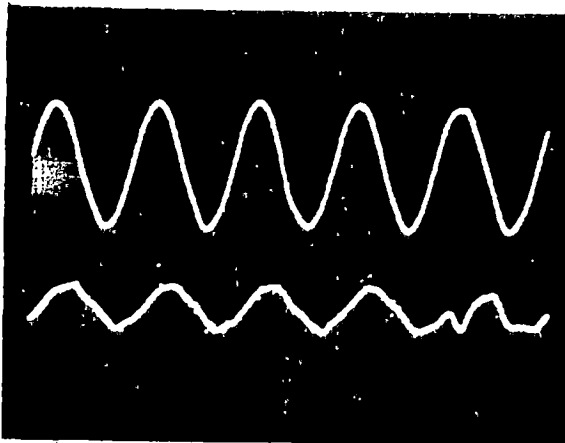


Fig. 5.4(c) Steady state waveforms of terminal voltage and stator current at no load with P-controller

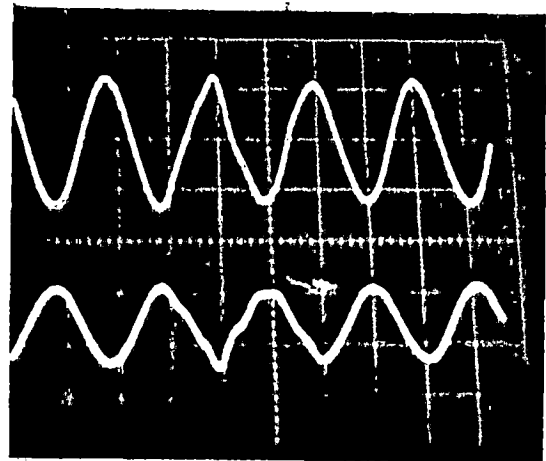


Fig. 5.4(d) Steady state waveforms of terminal voltage and stator current under loaded condition with P-controller

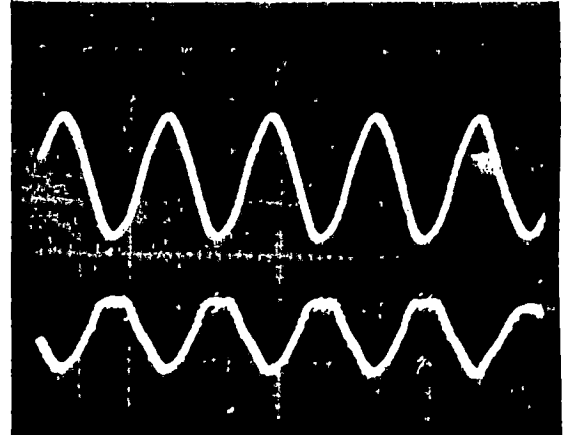
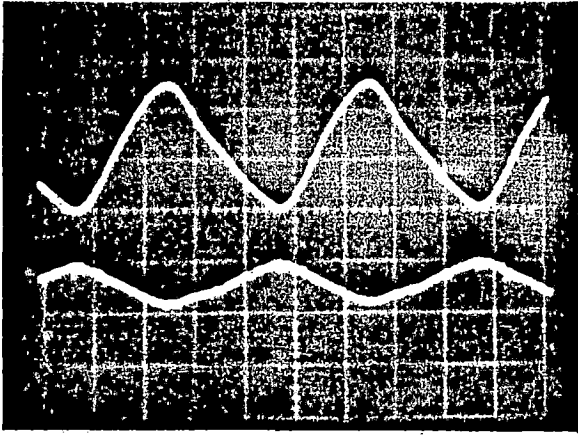


Fig. 5.5(a) Steady state waveforms of terminal voltage and load current ($I_L = 1.4$ Amp) with PI-controller

Fig. 5.5(b) Steady state waveforms of terminal voltage and load current ($I_L = 3.5$ Amp) with PI-controller

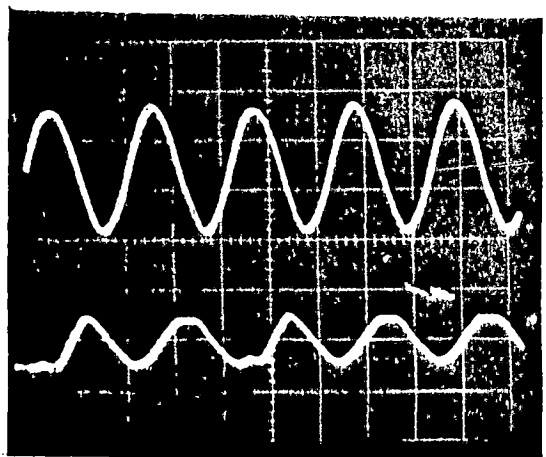
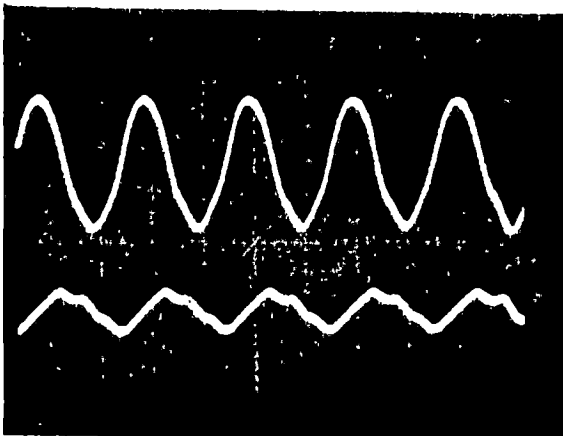


Fig. 5.5(c) Steady state waveforms of terminal voltage and stator current at no load with PI-controller

Fig. 5.5(d) Steady state waveforms of terminal voltage and stator current under loaded condition with PI-controller

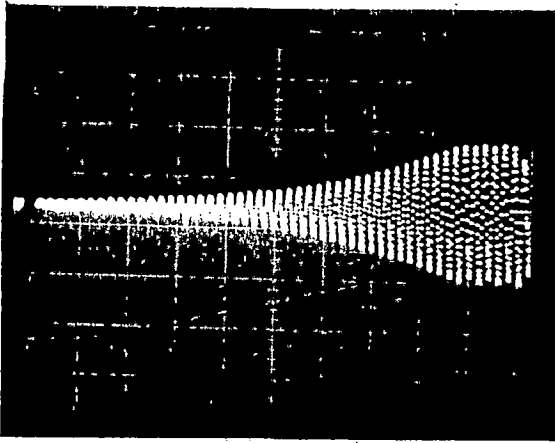


Fig. 5.6(a) Transient waveforms of terminal voltage building up from zero to a steady state value ($V_T = 372$ volts) with P-controller

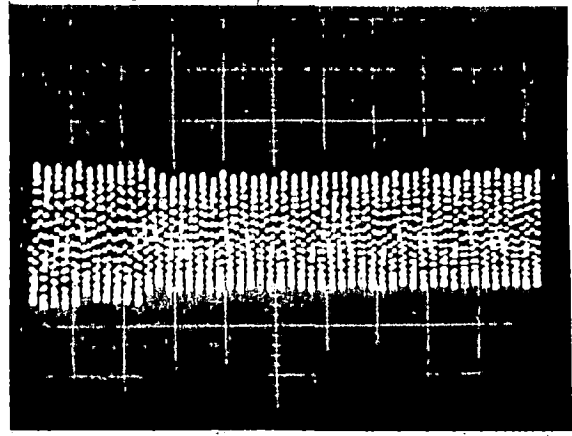


Fig. 5.6(b) Transient waveform of terminal voltage of sudden variation of reference voltage (V_r varies from 372 to 320 volts) with P-controller

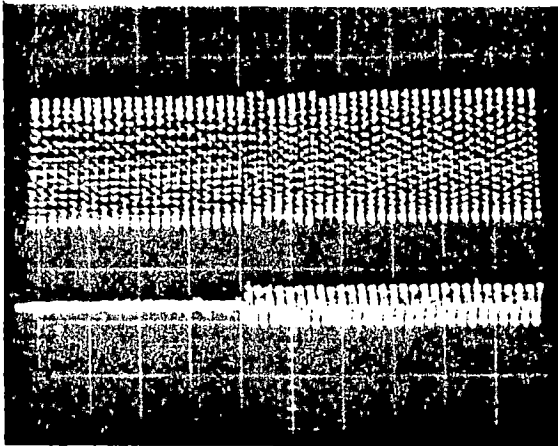


Fig. 5.6(c) Transient waveforms of terminal voltage and load current for the sudden application of load with P-controller

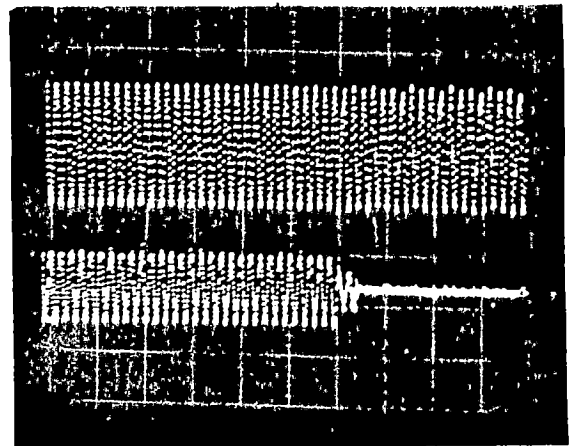


Fig. 5.6(d) Transient waveforms of terminal voltage and load current for the sudden removal of load with P-controller

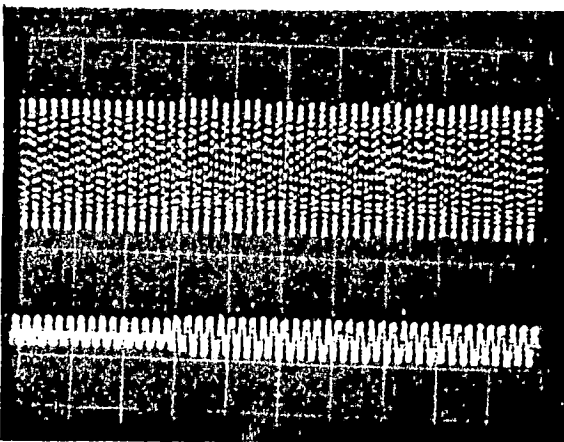


Fig. 5.6(e) Transient waveforms of terminal voltage and stator current for sudden application with P-controller

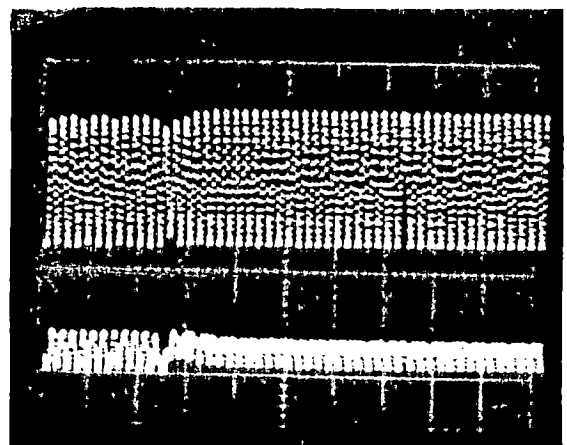


Fig. 5.6(f) Transient waveforms of terminal voltage and stator current for sudden removal of load with P-controller

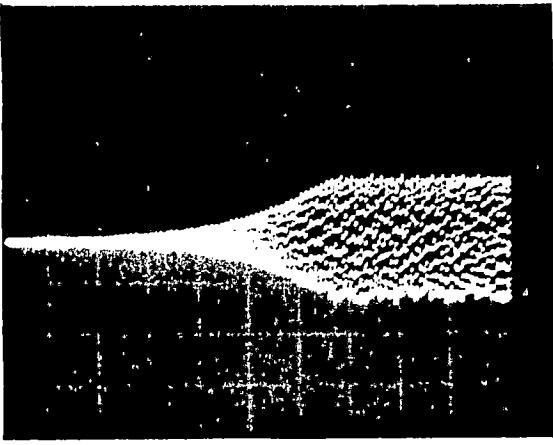


Fig. 5.7(a) Transient waveform of terminal voltage building up from zero to a steady-state value ($V_T = 330$ Volt) with PI-controller

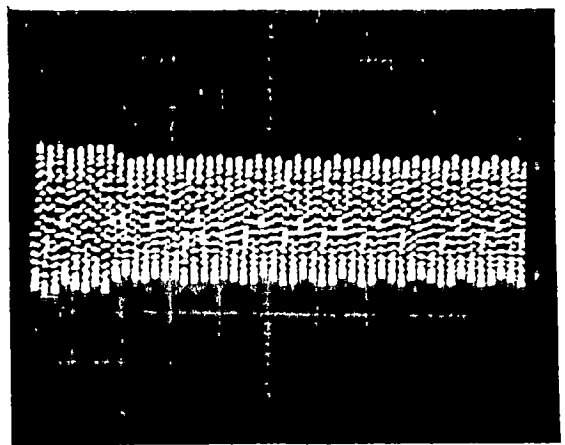


Fig. 5.7(b) Transient waveform of terminal voltage for sudden variation of V_{REF} (V_T varies from 370 to 340 volt) with PI-controller

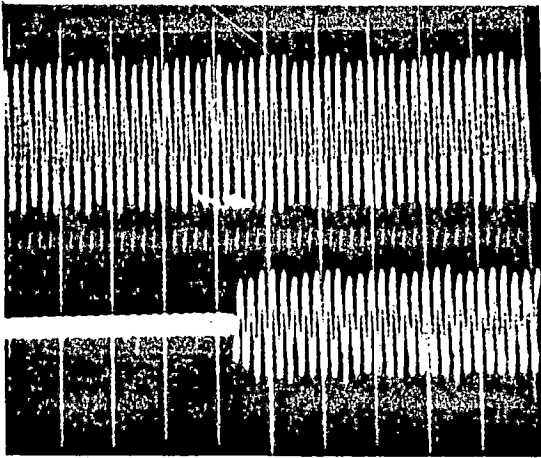


Fig. 5.7(c) Transient waveforms of terminal voltage and load current for the sudden application of load with PI-controller

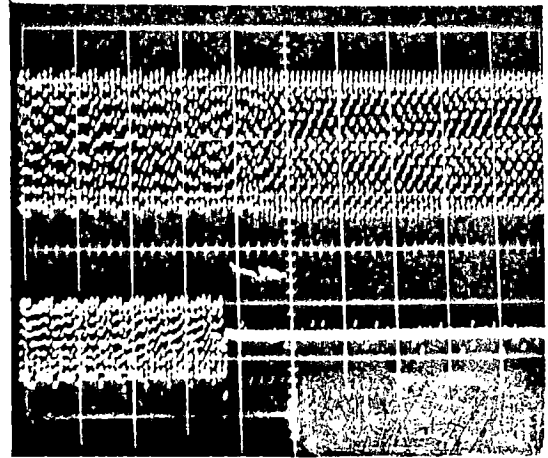


Fig. 5.7(d) Transient waveforms of terminal voltage and load current for the sudden removal of load with PI-controller

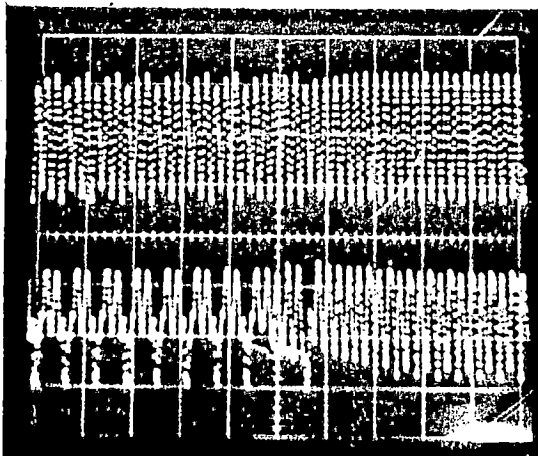


Fig. 5.7(e) Transient waveforms of terminal voltage and stator current for the sudden application of load with PI-controller

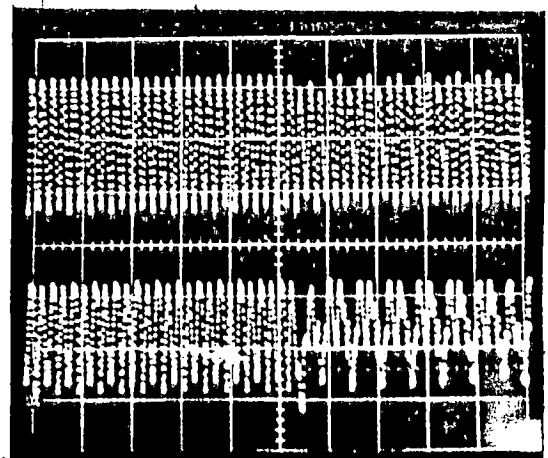


Fig. 5.7(f) Transient waveforms of terminal voltage and stator current for the sudden removal of load with PI-controller

Secondly, the PI-controller has been used to observe the transient performance of voltage regulating system for the sudden variation of load and reference voltage. The transient response of the voltage regulator with PI-controller for voltage build up from 0 Volt has been shown in Fig. 5.7(a). The terminal voltage builds up to 330 Volts in only 1.2 sec. So, with the comparison of P and PI-controller, it is found that P-controller^{response} is faster than the PI-controller. The variation of terminal voltage with sudden change of reference voltage has been given in Fig. 5.7(b). Which shows that the terminal voltage is affected directly with the change of reference voltage. The effect of sudden load variation on the terminal voltage and load current has been shown in Fig. 5.7(c) and (d). For both sudden application and removal of load, the system stabilizes within few cycles and the effect of load variation on the terminal voltage is similar as in the case of P-controller. Fig. 5.7(e) and (f), show the variation of terminal voltage and stator current with sudden application/removal of the load. The stator current reaches steady state value without losing stability. The stability improves with the increase in load as is clear from the Fig. 5.7(e) and (f).

Conclusion :

The steady state and transient performance of the developed voltage regulator for self excited induction generator have been studied. The steady state waveforms of

terminal voltage, stator current and load current for P and PI-controller show that these almost sinusoidal except slight distortion in stator current and load current. The waveforms improves at higher load as it becomes more sinusoidal. The steady state error for P-controller is observed more than the PI-controller. The machine is able to be loaded up to 1.3 p.u. for P-controller and 1.35 p.u. for PI-controller (when the terminal voltage is set at .9 p.u.). The transient performance under sudden reference and load perturbation shows satisfactory results. The system is sufficiently stable and response is quite fast. The voltage regulation is sought satisfactorily good at different loads and the machine does lose excitation at higher loads.

CHAPTER - 6

CONCLUSION AND SCOPE FOR FURTHER WORK

Summary :

A practical voltage regulator with P and PI controllers has been designed and fabricated for a capacitor self excited induction generator. The performance of induction generator with voltage regulating system is studied at different loads.

6.1 Main Conclusion :

An analytical technique has been developed for the analysis of capacitor self excited induction generator. The steady state performance characteristics have been obtained under the following cases:

- (i) No load
- (ii) At fixed capacitance at the generator terminals
- (iii) Keeping terminal voltage constant at all loads
- (iv) Keeping V_G/F (Air gap flux) constant at all loads.

Newton Raphson Method has been used to solve the non linear simultaneous equations which appear during the steady state analysis of the self excited induction generator. The computer programs have been developed to compute the performance of induction generator under considered cases. The computational technique has been found efficient, suitable and fast converging to do the computation for the performance

of the machine. The solution is obtained within three or four iterations for the computation of unknown parameter of the non linear simultaneous equations.

The computed and experimental results are presented for different resistive and reactive (R-L) loads for all four cases. A close agreement has been observed between the test and computed results. The characteristics for both the results have been found quite similar, thus demonstrating the validity of analytical technique.

The capacitive VAR requirement at resistive as well as reactive (R-L) loads to keep the terminal voltage constant at constant/different speeds is studied to select the suitable capacitor value for the stable operation of self excited induction generator. The power output variation with terminal voltage for rated stator current provides the guideline to select the most appropriate terminal voltage at which the induction generator can produce maximum power for the rated stator current. For all four cases the output frequency variation is well within limits.

The three phase naturally commutated (~~Δ~~- connected) VAR generator is designed and fabricated to regulate the terminal voltage at varying loads. A suitable firing circuit has been designed and fabricated to trigger the thyristors of phase controlled inductor. The voltage regulating system is comprising ^{of} feedback circuit and controllers (P or PI). The gains of proportional (P) and proportional plus Integral (PI)

controller are selected on the basis of experimental study for the stability and response of the voltage regulating system.

The steady state performance of voltage regulating system is studied at different resistive balanced loads for P and PI controllers separately. The steady state error with PI controllers is considerably less than the P-controller. Consequently there is more drop in the terminal voltage with the use of P controller in the voltage regulating system than a system having PI controller. The variation of terminal voltage with reference voltage is nearly linear for both P and PI controllers which shows the suitability of controllers. The wave forms of the terminal voltage, load current, and stator current are very close to sine wave and system has been found satisfactorily stable for both type of controllers. The transient responses of current and voltage with the sudden of application/removal of load are recorded by using a storage C.R.O. The oscillograms of transient response depict the nature of response for the sudden variation of load. The system approaches to steady state within few cycles. The oscillograms of voltage building up show that the time taken in achieving the steady state value with P-controller is less than the PI-controller. From the steady state and transient performance of voltage regulating system it is found that the system is quite competent to regulate the terminal voltage for the desired range of load. The residual magnetism in the rotor of induction machine is enough to build up the

voltage when it is rotated near to the synchronous speed by a prime mover. So it is able to build up the voltage without any external power supply to the induction machine and which confirms its suitability to use in the isolated areas where grid supply is not available.

6.2 Scope for Further Work :

The present work includes the testing of the voltage regulator at balanced resistive loads. So the testing of voltage regulator may be extended for unbalanced load as well as dynamic load, like a.c. motors with some possible modification in the design of controller. An analytical model could be developed for the dynamic study of the closed loop system at different loads which may be capable to give the transient response of the voltage regulating system. The study regarding the stability of system may be done to select the controller elements for a stable system. The testing of self excited induction generator may be performed for higher ratings with the similar type of voltage regulator as used in the present work, to provide some more useful informations about its commercial use. The controller may be modified to have V/F ratio constant for the case of variable speed prime mover to feed a.c. motors. A comparison would be made of the performances for self excited induction generators by implementing different type of VAR generators like saturable core reactor etc.

REFERENCES

1. Brennen Michael B. and Abbondanti Alberts, "Static Excitors For Induction Generators", IEEE Trans. IA Vol. IA-113, No. 5, Sept./Oct. 1977, pp 422 - 428.
2. Bolton, H.R. and Nicodemou, V.C., "Operation of Self Excited Generators For Wind Mill Application", Proceedings IEE, Vol. 126, No. 9, September 1979, pp 815 - 820.
3. Berchten, S., "Steady State Analysis of Capacitor Self Excited Induction Generators", Proceedings ICEM Lausanne, Switzerland, 18-21, Part 3, Sept. 1984, pp 1129 - 1132.
4. Elder, J.M., Boys, J.T. and Prof. Woodward, J.L., "The Process of Self Excitation in Induction Generators", IEE Proceedings, Part-B, Vol. 130, No. 2, March 1983 pp 103 - 108.
5. Elder J.M., Boys, J.T. and Prof. Woodward, J.L., "Self Excited Induction Machine as Low Cost Generator", IEE Proceedings, Part-C, Vol. , No. , March 1984, pp 33-41.
6. Gyugi Laszlo, "Reactive Power Generation and Control by Thyristor Circuits", IEEE Trans. IA, Vol. IA-15, No. 5, Sept./Oct. 1979, pp 521 - 532.
7. John R. Parsons, J.R. "Cogeneration Application of Induction Generator", IEEE Trans. IA, Vol. IA-20, No. 3, May/June 1984, pp 497 - 503.

8. Kontos George and Lytsikar Anatomy, "Steady State Operation of A Three Phase Induction Generator With A Three Phase Voltage Fed Autonomous Inverter", Proceeding ICEM Lansane, Switzerland, 18 - 21, Part-2, Sept. 1984, pp 818 - 821.
9. Kron, Gabriel, "Equivalent Circuits of Electric Machinery", John Wiley & Sons, Inc., Newyork Chapman & Hall Ltd., London, 1951.
10. Murthy, S.S., Malik, O.P. and Tandon, A.K., "Analysis of Self Excited Induction Generators", IEE Proceeding, Part-C, Vol. 123, No. 6, Nov. 1982, pp 260 - 265.
11. Melkebeek, J.A.A., "Magnetising Field Saturation and Dynamic Behaviour of Induction Machines Part-2: Stability Limits of A Voltage Fed Induction Motor and of A Self Excited Induction Generator", IEE Proceeding, Part-B, Vol. 130, No. 1, January 1983, pp 10 - 17.
12. Melkebeck, J.A.A. and Novotony, D.W., "Small Signal Dynamic Analysis of Regeneration and Self Excitation in Induction Machines", Electric Machines and Power System, Vol. 8, No. 4-5, July - Oct. 1983, pp 259 - 275.
13. Malik, O.P., Divan, D., Murthy, S.S., Grant, T. and Walsh, P., "A Solid State Voltage Regulator For Self Excited Induction Generators", IEEE 1983, Industrial and Commercial Power Systems Conference, Milwaukee, May 1983.

14. Murthy, S.S., Malik, O.P. and Walsh, P., "Capacitive Requirements of Self Excited Induction Generator to Achieve Desired Voltage Regulation", IEEE Industrial and Commercial Power Systems Conference, Milwaukee, 1983.
15. Murthy, S.S., Satyanarayan, K.V.V., Singh, B.P. and Nagmani, C., "Suitability of Using Normally Designed Induction Motors AS Capacitor Self Excited Induction Generators", Proceeding ICEM Lausanne, Switzerland, 18-21, Part-3, Sept. 1984, pp 1173 - 1176.
16. Novotny, D.W., Gritter, D.J. and Studtmann, G.H., "Self Excitation in Inverter Driven Induction Machines", IEEE Trans. PAS, Vol. PAS-96, No. 4, July/August 1977, pp 1117 - 1125.
17. Nagrial, M.H. and Shamsi, A.M., "Operation of Induction Generators for Wind Mill Applications", Proceedings ICEM Lausanne, Switzerland, 18-21, Part-1, Sept. 1984, pp 213 - 215.
18. Ouazene Laheene and Mepheron George, Jr., "Analysis of the Isolated Induction Generators", IEEE Trans. PAS, Vol. PAS-102, No. 8, July/August 1983, pp 2793 - 2798.
19. Prof. Arrillaga, J. and Watson, D.B., "Static Power Conversion from Self Excited Induction Generator", Proceedings IEE Vol. 125, No. 8, August 1978, pp 743-746.

20. Patel, H.K. and Dubey, G.K., "Harmonic Reduction in the Static VAR Compensator by Sequence Control of Transformer Taps", IEE Proceedings, Part-C, Vol. , No. , Nov. 1983, pp 300 - 305.
21. Say, M.G., "The Performance and Design of Alternating Current Machines", John Wiley, Third Edition, 1983.
22. Tandon, A.K., Murthy, S.S. and Jha, C.S., "New Method of Computing Steady State Response of Capacitor Self Excited Induction Generator", Journal of Institution of Engineers (India) Vol. 65, Part-EL6, June 1985, pp 196 - 201.
23. Vanderwag Peter and Inculet, I.I., "A.C. Power Generation with a Small Self Excited Poly-phase Induction Motor", Proceedings ICEM Lausanne, Switzerland, 18-21, Part-3, Sept. 1984, pp 1200 - 1202.
24. Watson, D.B., Arrillaga, J. and Densem, T., "Controllable D.C. Power Supply From Wind Driven Self Excited Induction Machines", Proceedings IEE, Vol. 126, No. 12, Dec. 1979, pp 1245 - 1248.
25. Watson, D.B. and Milner, I.P., "Autonomous and Parallel Operation of Self Excited Induction Generator", IJEE, Vol. 22, 1985, pp 365 - 374.

APPENDIX - A

THE CONSTANTS APPEARING IN NONLINEAR SIMULTANEOUS EQUATIONS

A.1 The constants appearing in the nonlinear simultaneous equations (3.4) and (3.5) are defined as follows:

$$C_1 = -2.X_1, \quad C_2 = -X_1^2, \quad C_3 = 2\gamma X_1, \quad C_4 = \gamma X_1^2$$

$$C_5 = X_C, \quad C_6 = X_1 C_C + R_S \cdot R_R, \quad C_7 = -\gamma \cdot X_C$$

$$C_8 = -\gamma \cdot X_1 \cdot X_C$$

and $D_1 = R_S + R_R, \quad D_2 = X_1 \cdot (R_S + R_R), \quad D_3 = -\gamma \cdot R_S$

$$D_4 = -\gamma \cdot X_1 \cdot R_S, \quad D_5 = 0.0, \quad D_6 = -R_R \cdot X_C$$

A.2 The constants appearing in non linear simultaneous equations (3.13) and (3.14) are defined as follows:

$$C_1 = -R_R X_L - 2.X_1 \cdot R_L - X_L R_S$$

$$C_2 = -X_L X_1 R_S - R_R X_L X_1 - X_1^2 \cdot R_L$$

$$C_3 = \gamma R_S X_L + 2\gamma X_1 R_L$$

$$C_4 = \gamma R_S X_L X_1 + \gamma X_1^2 R_L$$

$$C_5 = R_L X_C + X_C (R_S + R_R)$$

$$C_6 = R_R X_L X_C + R_L X_C X_1 + R_L R_S R_R + X_C X_1 R_S + R_R X_C X_1$$

$$C_7 = -\gamma R_L X_C - \gamma X_C R_S$$

$$C_8 = -\gamma R_L X_C X_1 - \gamma X_C X_1 R_S$$

AND $B_1 = 2.X_1 \cdot X_L, \quad B_2 = -X_1^2 X_L, \quad B_3 = 2\gamma X_1 X_L,$

$$B_4 = \gamma X_1^2 X_L, \quad B_5 = X_C (X_L + 2X_1) + R_S \cdot R_L + R_R R_L$$

$$B_6 = X_L X_C X_1 + R_L R_R X_1 + X_1^2 X_C + R_S R_R X_L + R_S R_L X_1$$

$$B_7 = -\gamma X_L X_C - 2\gamma X_1 X_C - \gamma R_S R_L$$

$$B_8 = -\gamma X_L X_C X_1 - \gamma X_1^2 X_C - \gamma R_S R_L X_1$$

$$B_9 = 0.0, \quad B_{10} = -R_L X_C R_R - X_C R_R R_S$$

A.3 Here $C_1, C_2, C_3 \dots C_8$ and $B_1, B_2 \dots B_{10}$ are taken from A.2 to use in the constants appearing in equations (3.16) and (3.17). These constants are defined as follows:

$$C_{11} = C_1 X_m + C_2, \quad C_{12} = C_3 X_m + C_4,$$

$$C_{13} = (C_5 X_m + C_6 - R_L R_R R_S) / X_C, \quad C_{14} = R_L R_S R_R$$

$$C_{15} = (C_7 X_m + C_8) / X_C$$

and $D_{11} = B_1 X_m + B_2, \quad D_{12} = B_3 X_m + B_4$

$$D_{13} = X_L (X_m + X_1) + X_1 (X_m + X_1) + X_m X_1$$

$$D_{14} = R_L R_R X_1 + R_R R_S X_L + R_S R_L (X_m + X_1) + R_L R_R X_m$$

$$D_{15} = (B_7 X_m + B_8 + \nu R_S R_L (X_m + X_1)) / X_C$$

$$D_{16} = -\nu R_S R_L (X_m + X_1), \quad D_{17} = (B_9 X_m + B_{10}) / X_C$$

A.4 The constants appearing in equation (3.21) and (3.22) are defined as follows:

$$C_1 = -R_L (X_m + X_1) - R_S (X_m + X_1)$$

$$C_2 = R_R X_L F + F \cdot R_L (X_m + X_1) + R_S \cdot F (X_m + X_1) + R_R F X_1 + X_m R_R F$$

$$C_3 = F^2 R_S X_L (X_m + X_1) + F^2 X_1 R_L (X_m + X_1) + F^2 X_m X_1 R_L$$

$$C_4 = -F^3 X_L R_S (X_m + X_1) + R_L \cdot R_S \cdot R_R \cdot F - F^3 R_R X_L X_1 - F^3 X_1 R_L (X_m + X_1) - F^3 X_m R_R X_L - F^3 X_m X_1 R_L$$

And $D_1 = -F X_L (X_m + X_1) - F \cdot X_1 (X_m + X_1) - X_m X_1 F$

$$D_2 = -R_L R_R F^2 X_L (X_m + X_1) + F^2 X_1 (X_m + X_1) - R_R R_S F^2 X_m X_1$$

$$D_3 = F^3 X_1 X_L (X_m + X_1) - R_S R_L F (X_m + X_1) + F^3 X_L R_S R_R$$

$$D_4 = F^2 R_L R_R X_1 - F^4 X_1 X_L (X_m + X_1) + F^2 X_L R_R R_S + R_S R_L F^2 (X_m + X_1) + R_R R_L F^2 X_m - F^4 X_L X_m X_1.$$

APPENDIX - B

DETAILS OF EXPERIMENTAL SETUP AND MACHINE PARAMETERS

B.1 Details of Induction Machine and Synchronous Motor

Induction Machine - 5 H.P., 400 Volts, 6.9 Amp., 1430 RPM
 3ϕ , 50 Hz, Δ - connected stator and squirrel cage rotor

Synchronous Motor - 3ϕ , 400 Volts, 6.75 Amp, 1500 RPM,
 50 Hz with attached exciter

B.2 Base values for theoretical computation

Base current I_{Base} = Rated phase current = 3.984 Amp

Base Voltage V_{Base} = Rated phase voltage = 400 Volts

Base Power P_{Base} = Base current x base voltage = 1593.486 VA

Base Impedance Z_{Base} = V_{Base}/I_{Base} = 100.4 ohm

Base Admittance Y_{Base} = 9.959×10^{-3} Mho

Base Frequency F_{Base} = 50 Hz

Base Speed ω_{Base} = 1500 RPM

B.3 Induction Machine Equivalent Circuit Parameters in per unit and Referred to stator

$$R_S = .0548, \quad R_R = .0581, \quad X_{LS} = X_{LR} = X_1 = .06$$

B.4 From V_G/F vs. X_m characteristic as shown in Fig. B.1.

The relations between V_G/F and X_m are as follows:

From C to D $V_G/F = 1.63 - .1733 \cdot X_m$ (X_m 3.75)

From B to C $V_G/F = 2.48 - .4 \cdot X_m$ (3.75 X_m 4.45)

and $X_m \text{ Max} = 4.45$ p.u.

From C to D $X_m = (1.63 - V_G/F)/.1733$ (V_G/F .976)

to B to C $X_m = (2.48 - V_G/F)/.4$ (.976 V_G/F .698)

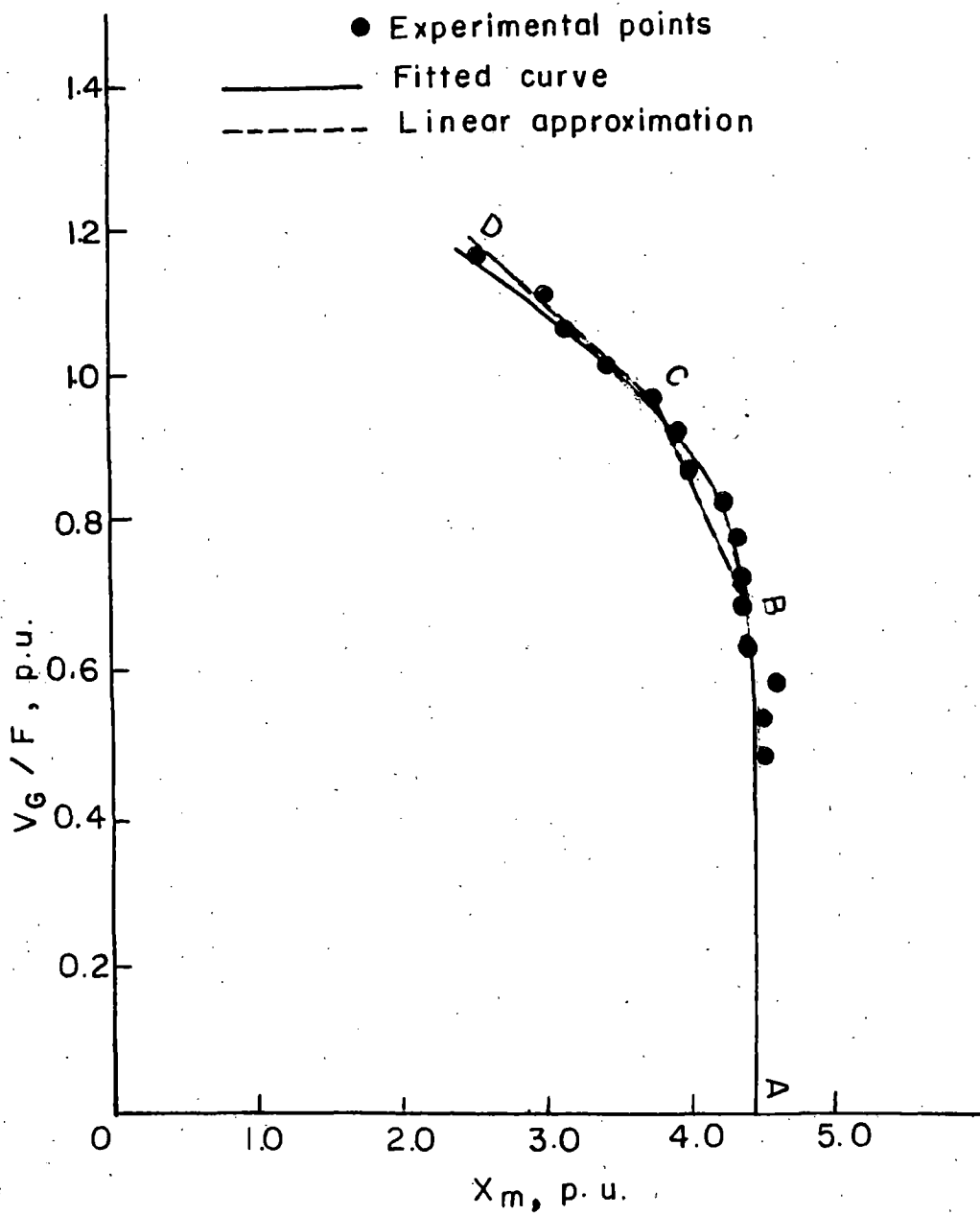


Fig. B.1 Variation of V_G / F with X from synchronous speed test

```

C      STEADY STATE ANALYSIS OF SELF EXCITED IND. GEN.
C**   PROGRAM FOR CASE (1) NO LOAD CHARACTERISTICS
C      ****
C      RS,RR=STATOR,ROTOR RESISTANCE(P,U)
C      X1=STATOR/ROTOR REACTANCE(P,U)
C      XC=CAPACITIVE REACTANCE(P,U)
C      XM=SATURATED MAGNETISING REACTANCE P.U)
C      VG, VT=AIR GAP, TERMINAL VOLTAGES
C      AIS=STATOR CURRENT
C      CVAL=CAPACITIVE VAR
C      F=FREQUENCY(P,U)
C      NU=ROTOR SPEED(P,U)
C      ****
C      COMPLEX ZS,ZLS,AIS,VTF
C      REAL J11,J12,J22,J21,NU,K,NUMAX,IBASE
C      OPEN(UNIT=2,DEVICE='DSK',FILE='MAG.DAT')
C      PRINT 150
150  FORMAT(4X,'MAGN.FDR')
C      READ(2,*)RS,RR,X1,NU,EPS,CMIN,XMAX
C      READ(2,*)CT,CMAX,DNU,HUMAX,JBASE,FBASE,VBASE
C      PRINT61,RS,RR,X1,NU,EPS,CMIN,XMAX
61  FORMAT(4X,'RS=',F6.4,4X,'RR=',F6.4,4X,'X1=',F6.4,4X,'NU=',F6.2,4
1X,'EPS=',E10.3,4X,'CMIN=',E12.5,4X,'XMAX=',F6.4)
25  C=CRID
23  XM=XMFAA
C      F=NU
C      PRINT62,C,NU
62  FORMAT(4X,'C=',E13.6,4X,'NU=',F8.6)
C      ****
C      NEWTON RAPHSON METHOD
C      I=1
C      XC=1/(2.*3.14*50.*C*1000.4)
C      C1=-2.*X1
C      C2=-X1**2
C      C3=-NU*C1
C      C4=-C2
C      C5=XC

```



```

C6=X1*XC+RS*RR
C7=-RU*XC
C8=-RU*XC*X1
D1=RS+RR
D2=X1*(RS+RR)
D3=-RU*RS
D4=-RU*X1*RS
D5=1.0
D6=-RF*XC
30 J11=C1*F**3+C3*F**2+C5*F+C7
J12=3.*(F**2)*(C1*XH+C2)+2.*F*(C3*XH+C4)+(C5*XH+C6)
J21=D1*(F**2)+D3*F+D5
J22=2.*F*(D1*XH+D2)+(D3*XH+D4)
FXHF=(F**3)*(C1*XH+C2)+(F**2)*(C3*XH+C4)+F*(C5*XH+C6)+(C7*XH+C8)
GXMF=(F**2)*(D1*XH+D2)+F*(D3*XH+D4)+(D5*XH+D6)
FXH=ABS(FXHF)
GXH=ABS(GXMF)
DELTA=J11*(J22-J12*J21)
IF(FXH.LE.EPS)GOTO20
GOTO10
20 IF(GXH.LE.EPS)GOTO40
GO TO 10
10 I=I+1
H=(-FXHF*J22+GXMF*J12)/DELTA
K=(-GXMF*J11+FXHF*J21)/DELTA
XM=XH+H
F=F+K
IF(I.GT.200)GOTO40
GOTO30
40 PRINT63,XH,F,FXH,GXH,F
63 FORMAT(4X,'XH=',F7.4,4X,'F=',F6.4,4X,'FXH=',E10.3,4X,'GXH=',
E10.3,4X,'I=',I3)
C *****
C PERFORMANCE OF MACHINE
RSP=RS/F
IF(XH.GT.4.45)GO TO 22
IF(XH.LE.3.75) GO TO 50

```

```
GO TO 60
57 VGF=1.63-.1733*XM
GO TO 51
6 VGF=2.48-.4*XM
51 Z1S=CMPLX(RSF,X1)
X2=(X)-XC/(F1*2)
ZS=CMPLX(RSF,X2)
AIS=VGF/ZS
AISM=CABS(AIS)
AISP=AISM*IBASE
AISL=AISP*1.732
VTF=VGF-Z1S*AIS
VTFM=CABS(VTF)
VT=VTF**F
VT1=VT*VBASE
CVAR=3.*AISP*VT1
F1=FBASE*F
PRINT64,XC,VT,CVAR,AISM,VGF,F1,VT1,AISP
64 FWRITE(4X,'XC=',F6.4,4X,'VT=',F6.4,4X,'CVAR=',
1F10.4,4X,'AISM=',F6.4,4X,
2'VGF=',F6.4,14X,'F1=',F7.4,4X,'VT1=',F9.4
3,4X,'AISP=',F7.4)
22 C=C+CT
IF(C.GT.CMAX)GO TO 20
GO TO 23
21 NU=NU+DN
IF(NU.GT.NBMAX)GO TO 24
GO TO 25
24 STOP
CLOSE(UNIT=2)
END
```

APPENDIX - D

```

C** STEADY STATE ANALYSIS OF SELF EXCITED IND. GEN.
C** PROGRAM FOR CASE (2) ASSUMING XC CONSTANT
C *****
C RS,RR=STATOR,ROTOR RESISTANCE(P.U)
C X1=STATOR/ROTOR REACTANCE(P.U)
C XC=CAPACITIVE REACTANCE(P.U)
C XT=SATURATED MAGNETIZING REACTANCE P.U)
C VG, VT=AIR GAP,TERMINAL VOLTAGES
C AIL,AIS=LOAD,STATOR CURRENT
C RL,XL=LOAD RESISTANCE,REACTANCE
C CVAR=CAPACITIVE VAR
C F=FREQUENCY(P.U)
C POUT,VAOUT=OUTPUT POWER IN WATTS,VA
C NO=ROTOR SPEED(P.U)
C IBASE,VBASE,FBASE=CURRENT,VOLTAGE,FREQUENCY BASE VALUE
C *****
DIMENSION RL(24)
COMPLEX Z1,ZT,AIL,ZLS,AIS,VTE,ZL,ALR
REAL J11,J12,J22,J21,PO,K
OPEN(UNIT=2,DEVICE='DISK',FILE='DILY.DAT')
PRINT 150
150 FORMAT(AX,'DILY.FOR')
READ(2,*)RS,RR,X1,FO,FP5,CMIN,XL,XMAX
READ(2,*)CT,CMAX,DOB,DOFAX,VBASE,VBASE,FBASE
READ(2,*)(RL(J),J=1,24)
WRITE(2,RS,RR,X1,FO,FP5,CMIN,XL,XMAX)
61 FORMAT(4X,'RS=',F6.4,4X,'RR=',F6.4,4X,'X1=',F6.4,4X,'FO=',F5.2
1X,'FPS=',E11.3,4X,'CMIN=',E12.5,4X,'XL=',F6.4,4X,'XMAX=',F6.4
25 C=CMIN
23 DO 81 J=1,24
F=FO
RL=RL(J)
X0=XMAX
PRINT6Z,RL,C,FO
62 FORMAT(4X,'RL=',F7.4,4X,'C=',E13.6,4X,'FO=',F8.6)
C *****
C NEWTON RAPHSON METHOD

```

```

I=1
XC=U./ (C1.*B1.*5^I.*C.*I10.4)
C1=-ER*lambda-X1*RL-X1*RH-X1*RS
C2=-lambda*X1*EB-ER*AL*X1-X1*RH*X1
C3=ER*RS*X1+ER*X1*RL+ER*AL*X1
C4=ER*X1*X1*RS+ER*X1*RH*X1
C5=RL*X1+C1.*C.*RS+ER*lambda
C6=ER*lambda*X1+C1.*ER*lambda*(1+R1)*ER*RL+XC.*lambda.*RS+ER*X1*X1
C7=-ER*AL.*XC.*ER*XC.*ER
C8=-ER*RL.*XC.*Y1-ER*XC.*AL.*ER
B1=-lambda.*Y1-X1.*X1
B2=-lambda.*X1.*X1
B3=ER*lambda.*X1.*ER*RH.*X1
B4=ER*lambda.*X1.*X1
B5=X1.*(X1+X1)+ER*RL+ER*RR+XC.*X1
F6=AL.*XC.*X1+ER*RS.*X1+XC.*XC.*X1+RS.*RL.*X1+ER*RL.*X1
F7=-ER*X1.*XC-ER*lambda.*X1-ER*RS.*RL-ER*XC.*X1
B6=-ER*lambda.*XC.*X1-ER*Y1.*XC.*X1-ER*ER*RL.*X1
F9=1.0
F10=-RL.*XC.*RR-XC+ER*RS
G11=C1.*F.*3+C3.*F.*2+C5.*F+C7
G12=B1.*(F.*2)*(C1.*lambda+C2)+2.*F*(C3.*AL+C4)+(C5.*X1+C6)
G21=B1.*(F.*4)+B3.*(F.*3)+B5.*(F.*2)+F7.*F+F9
G22=AL.*F.*3*(B1.*lambda+F2)+3.*(F.*2)*(B3.*X1+B4)+2.*F.*
1+(F7.*X1+B6)+(B7.*lambda+B8)
FX0F=(F.*3)*(C1.*X1+C2)+(F.*2)*(C3.*R1+C4)+F*(C5.*X1+C6)+(C7.*X1+C8)
GX0F=(F.*4)*(B1.*X1+B2)+(F.*3)*(B3.*X1+B4)+(F.*2)*(B5.*lambda+B6)
1+F*(B7.*X1+B8)+(B9.*X1+B10)
FXP=AL*B(FX0F)
GXP=AL*B(GX0F)
D5101A=G11.*G22-J(2.*G21)
L1(FAN,10,ER*RS)G01120
G01010
L1(GX0,10,ER*RS)G01010
G01010
L1=TR1
H=(-FX0F.*G22+GX0F.*G11)/D5101A

```

$$K = (-GX)^2 + (1 + FX + FX^2) / (D - TFE)$$

$$\lambda = \lambda + a$$

$$F = F + \lambda$$

IF (L, GR, 1.0) GO TO 4

GO TO 5

4 PRINT '3', B, A, F, P, X, A, B, X, Y

50 FOR A=1 (GA, 'XF=' , F, 'G, 'X, 'F=' , F, 'G, 'A, 'FX=' , F, 'G, 'X, 'GA=' ,
'A, 'B, 'A, 'X=' , X)

C *****

C DEKFORWARD OF DIFFERENTIALS

$$KSF = KS / F$$

$$KLF = KL / F$$

IF (X, GR, 1.0) GO TO 22

IF (X, GR, 3.75) GO TO 50

GO TO 60

5 VGF = 1.63 - .1733 * X

GO TO 51

6 VGF = 2.40 - .4 * X

51 A = F * ((K * F) ** 2 - (F ** 2 * X - ZC) ** 2)

$$ZS = (E1 * F ** 2 * X) / A + (C - F ** 2 * X) / (A * C * E1 + E1 * X * F ** 2) / A$$

$$ZL = (E1 * F ** 2 * X - ZC - F ** 2 * X * ZS ** 2 * A * C + F * X * A * C ** 2) / A$$

$$Z1 = C * P * A (E1, F, L)$$

$$Z1S = C * P * A (E1, Z1)$$

$$Z1L = C * P * A (Z1, X)$$

$$ZT = Z1 + Z1S$$

$$ALB = VGF / ZT$$

$$ALB = C * A * B (ALB)$$

$$ALB = ALB * X / SE$$

$$ALB = ALB * X / 1.732$$

$$VGF = VGF - Z1 * ALB$$

$$VGF = C * A * B (VGF)$$

$$VT = VGF * X$$

$$V1 = VT * SE / E1$$

$$A1B = V1 / X$$

$$A1B = C * A * B (A1B)$$

$$A1B = A1B * X / SE$$

$$A1B = A1B * X / 1.732$$

```

AIC=LBASE*VT*F/(XCI)
CVAR=3.*AIC*VTE
PBASE=LBASE*VBASE
VAOUT=3.*PBASE.*AITE*VT
RRF=RR/(CF*HI)
ZR=CF*DKU(RF,XI)
AIR=-VGF/RE
AIRP=ABS(AIR)
POUT=-3.*PBASE*(AIRI.**2*RRF*F)
P1=-BASE*F
POUT=3.*PBASE*(AIRI.**2*RI)
PRINTP64,VT,AIC,CVAR,POUT,VAOUT,AIR,VGF,P1,AISI,VSI,AISI
63  FORMAT(5X,'VT=',F6.4,4X,'AIC=',F7.4,4X,'CVAR=',
1F6.4,4X,'POUT=',F10.4,4X,'VAOUT=',F10.4,4X,'AIRP=',F6.4,4X,
2'VGF=',F6.4,4X,'P1=',F7.4,4X,'AISI=',F8.4,4X,'VSI=',F9.4
3,4X,'AISI=',F7.4)
IF(AISI.GT.1.9)GO TO 22
80  CONTINUE
22  C=C+CF
IF(C.GT.CFHAX)GO TO 21
GO TO 23
21  R0=R+D*U
IF(R0.GT.RUHAX)GO TO 24
GO TO 25
24  STOP
CLOSE(UNIT=2)
END

```

```

C STEADY STATE ANALYSIS OF SELF EXCITED IFO GENERATOR
C PROGRAM FOR CASE (3) KEEPING (VT) CONSTANT
C *****
C RS,RR=STATOR,ROTOR RESISTANCE(P.U)
C X1=STATOR/ROTOR REACTANCE(P.U)
C NU=ROTOR SPEED(P.U)
C XE=SATURATED MAGNETIZING REACTANCE (P.U)
C XC=CAPACITIVE REACTANCE(P.U)
C AIS,AIR,AII=STATOR,ROTOR,LOAD CURRENT
C VT,VG=TERMINAL,ALR GAP VOLTAGES.
C CVAR=CAPACITIVE VAR REQUIRED
C VADUT,PDUT=OUTPUT IN VA,WATTS
C *****
C DIMENSION RL1(24)
C COMPLEX Z1,ZR,AIR,ZLG,VGF,AIS,ZT,AIIS,ZL,AII
C REAL IBASE,J11,J12,J22,J21,NU,K,JDJAX
C OPEN(UNIT=2,DEVICE='LSK',FILE='DDEAIR.DAT')
C PRINT150
150 FORMAT(1X,'DDEAIR')
C READ(2,*)RS,RR,X1,NU,EPS,VTMIN,XCMAX,XI
C READ(2,*)IBASE,DVT,DMU,VTMAX,NUMAX,VBASE,FBASE
C READ(2,*)(RL1(J),J=1,24)
C PRINT161,RS,RR,X1,NU,EPS,VTMIN,XCMAX
161 FORMAT(4X,'RS=',F8.6,4X,'RR=',F8.6,4X,'X1=',F8.6,4X
1,'NU=',F8.6,4X,'EPS=',F8.6,4X,'VTMIN=',F8.6,4X,'XCMAX=',F8.6)
C SOLUTION FOR XC AND P USING NEWTON RAPHSON METHOD
171 VT=VTMIN
20 DO 100 J=1,24
F=NU
XC=XCMAX
RL=RL1(J)
PRINT6,NU,RL,XI
6 FORMAT(4X,'NU=',F5.3,4X,'RL=',F5.2,4X,'XI=',F5.2)
I=1
30 RSF=RS/F
VTF=VT/F
A=P*((RL*F)**2+(F**2*X1-XC)**2)

```

$$RE = (RL * F ** 2 * XL * XC - F ** 2 * XL * XC * RL + RL * XC ** 2) / A$$

$$PIA = (-RL ** 2 * F * XC - F ** 3 * XL ** 2 * XC + F * XL * XC ** 2) / A$$

$$Z1 = C * PLX(RE, PIA)$$

$$ZLS = C * PLX(RSF, X1)$$

$$AIS = VTF / Z1$$

$$VGF = VTF + AIS * ZLS$$

$$VGFA = CABS(VGF)$$

$$AIS * = CABS(AIS)$$

$$IF(VGFA.GT..98)GO TO 91$$

$$GO TO 92$$

$$91 \quad XM = (1.63 - VGFA) / .1733$$

$$92 \quad XN = (2.48 - VGFA) / .4$$

$$XM = (1.633 - VGFA) / .1733$$

$$C1 = -RR * XL - X1 * RL - X1 * RL - XL * RS$$

$$C2 = -X1 * X1 * RS - RR * XL * X1 - X1 * RL * X1$$

$$C3 = NU * RS * X1 + NU * X1 * RL + NU * RL * X1$$

$$C4 = NU * XL * X1 * RS + NU * X1 * RL * X1$$

$$C5 = RL * XC + XC * RS + RR * XC$$

$$C6 = RR * XL * XC + RL * XC * X1 + PL * RR * RS + XC * X1 * RS + RR * XC * X1$$

$$C7 = -PU * RL * XC - NU * XC * RS$$

$$C8 = -NU * RL * XC * X1 - NU * XC * X1 * RS$$

$$C11 = C1 * XM + C2$$

$$C12 = C3 * X1 + C4$$

$$C13 = (C5 * XM + C6 - RL * RR * RS) / XC$$

$$C14 = RL * RR * RS$$

$$C15 = (C7 + XM * C8) / XC$$

$$B1 = -X1 * X1 - XL * X1$$

$$B2 = -X1 * X1 * X1$$

$$B3 = NU * X1 * XL + NU * XL * X1$$

$$B4 = NU * X1 * X1 * X1$$

$$B7 = -NU * XL * XC - NU * X1 * XC - NU * RS * RL - NU * XC * X1$$

$$B8 = -NU * X1 * XC * X1 - NU * X1 * XC * X1 - NU * RS * RL * X1$$

$$B9 = 0.$$

$$E10 = -RL * XC * RR - XC * RR * RS$$

$$D11 = B1 * XM + B2$$

$$D12 = B3 * XM + B4$$

$$D13 = XL * (XM + X1) + X1 * (XL + X1) + XM * X1$$

APPENDIX - E

```

D14=RL*RR*X1+RR*RS*XL+RS*RH*(X0+X1)+PL*XM*RE
D15=(B7*X1+BU+BU*RS*RL*(X0+X1))/XC
D16=-FD*RS*RL*(X0+X1)
D17=(B9*XF+H10)/XC
J11=C13*F+C15
J12=3.*F**2*C11+2.*F**C12+C13*XC+C14
J21=F**2*D13+F*D15+J17
J22=4.*F**3*D11+3.*F**2*D12+2.*F*(D13*XC+D14)+D15*XC+D16
FXCF=(F**3)*C11+(F**2)*C12+F*(C13*XC+C14)+C15*XC
GXCF=(F**3)*D11+(F**2)*D12+(F)*D13*XC+D14
I+F*(D15*XC+D16)+D17*XC
FXC=ABS(FXCF)
GXC=ABS(GXCF)
DELTA=J11*J22-J12*J21
IF(FXC.LT.EPS)GOTO20
GOTO10
IF(GXC.LT.EPS)GOTO40
GO TO 10
I=I+1
H=(-FXCF*J22+GXCF*J12)/DELTA
K=(-GXCF*J11+FXCF*J21)/DELTA
XC=XC+H
F=F+K
IF(I.GT.200)GOTO40
GOTO30
PRINT41, XC, F, FXC, GXC, I, XM, VGFA, AISM
1  FORMAT(4X, 'XC=', F5.3, 4X, 'F=', F5.3, 4X, 'FXC=', F10.3, 4X
1, 'GXC=', F10.3, 4X, 'I', I3, 4X, 'XM=', F7.4, 4X, 'VGFA=', F8.4, 4X,
2 'AISM=', F8.4)
C=1./(2.*3.14*100.4*50.*XC)
RLF=RL/F
ZL=C*PLA(RLF, XL)
AID=VTF/ZL
AIDH=CABS(AID)
AXDP=AIDH*IBASE
AIDL=AIDH*1.732
PBASB=IBASE*VBASE

```

```

FOOT=3.*PI*BASE*(ALIP**2*RI)/1.732
Z1=Z1+Z1B5
AIS=VGF/Z1
AIS=CABS(AIS)
AISP=AIS*IBASE
AISL=AISP*1.732
AIC=VGF*(C**2)*IBASE/XC
RRF=RR/(F-DU)
ZR=CF*PLX(RRF,X1)
AIR=-VGF/ZR
AIR=CABS(AIR)
AIRP=AIR*IBASE
PGEN=-3.*PI*BASE*(AIR**2*RRF*F)
VT1=VGF*F*VBASE
VAOUT=1.732*AIRP*VT1
CVAR=3.*AIC*VT1
F1=PEASE*F
PRINT42,C,CVAR,AIC,AISL,VAOUT,FOOT,PGEN,F1,AIRP,AISL,VD1
2  FORMAT(4X,'C=',E12.5,4X,'CVAR=',F9.4,4X,'AIC=',F7.4,
14X,'AISL=',F9.4,4X,'VAOUT=',F10.4,4X,'FOOT=',F10.4,4X,'PGEN=',
2F10.4,4X,'F1=',F5.3,4X,'AIRP=',F7.4,4X,'AISL=',F8.4,4X,
3'VT1=',F1.4)
IF(AISL.GT.6.9)GO TO 101
10 CONTINUE
11 IF(V1.GT.VTMAX)GO TO 16
GO TO 101
12 VT=VT+DV**2
GO TO 91
13 IF(CU.LE.CUMAX) GO TO 100
GO TO 171
14 ND=ND+DU**2
GO TO 171
70 STOP
CLOSE(UNIT=2)
END

```

APPENDIX - F

```

C**  STEADY STATE ANALYSIS OF IND. GENERATOR
C**  PROGRAM FOR CASE(4) ASSUMING VG/F CONSTANT
*****
C    RS,RR=STATOR,ROTOR RESISTANCE(P.U)
C    X1=STATOR/ROTOR REACTANCE(P.U)
C    XC=CAPACITIVE REACTANCE(P.U)
C    XM=SATURATED MAGNETISING REACTANCE(P.U)
C    VG,VT=AIR GAP,TERMINAL VOLTAGES
C    AIL,AIS=LOAD,STATOR CURRENTS
C    RL,XL=LOAD RESISTANCE, REACTANCE
C    CVAR=CAPACITIVE VAR
C    F=FREQUENCY
C    NU=ROTOR SPEED
C    Z=IMPEDANCE
*****
      DIMENSION RL1(22)
      COMPLEX Z1,ZLS,ZT,AIS,VTF,ZL,AIL,AIR
      REAL J11,J12,J21,J22,K,NU,IBASE
      OPEN(UNIT=3,DEVICE='DSK',FILE='DLIR.DAT')
      PRINT150
150   FORMAT(IX,'DLIR')
      READ(3,*)RS,RR,X1,VGF,F,EPS,XCMAX,XLMIN
      READ(3,*)DF,FMAX,IBASE,VBASE,FBASE
      READ(3,*)(RL1(J),J=1,22)
      PRINT11,RS,RR,X1,VGF,F,EPS,XCMAX,XLMIN
11   FORMAT(4X,'RS=',F8.6,4X,'RR=',F8.6,4X,'X1=',F8.6,4X,'VGF='
1, F8.6,4X,'F=',F8.6,4X,'EPS=',E12.5,4X,'XCMAX=',F9.6,4X,'XLMIN='
2, F9.6)
110  XL=XLMIN
      DO 70 J=1,22
      IF(VGF.GT.0.98)GO TO 91
      GO TO 92
91   XM=(1.63-VGF)/.1733
92   XM=(2.48-VGF)/.4
      XC=XCMAX
      NU=F
      RL=RL1(J)

```

PRINT6, VGF, BL, XL, P

FORMAT(4X, 'VGF=' , F9.6, 4X, 'RL=' , F9.6, 4X, 'X1=' , F9.6, 4X, 'P=' , F(.4)

NEWTON RAPHSON METHOD

I=1

C1=(-BL+(XM+X1)-(XM+X1)*RS)

C2=(RR*XL*P+P*RI)*(XM+X1)+P*(XM+X1)*RS+RR*P*X1+XM*RR*P)

C3=P**2*XL*(XM+X1)*RS+P**2*X1*RL*(XM+X1)+P**2*XM*X1*RI

C4=-P**3*XL*(XM+X1)*RS+RL*P*RR*RS-P**3*RR*XL*X1-P**3*X1*RL

1*(XM+X1)-XM*RR*P+3*XL-P**3*XM*X1*RI

D1=-P*XL*(XM+X1)-P*XL*(XM+X1)-XM*XL*P

D2=-RI*P+P**2*XL*(XM+X1)+P**2*XL*(XM+X1)-RR*RS+P**2*XM*X1

D3=P**3*X1*XL*(XM+X1)-RS*RL*P*(XM+X1)+P**3*XL*XM*X1

D4=RL*P**2*RR*X1-P**4*X1*XL*(XM+X1)+P**2*XL*RR*RS

1+RS*RI*P**2*(XM+X1)+RR*RI*P**2*XM-P**4*XL*XM*X1

J11=C1*NU+C2

J12=C1*XC+C3

J21=D1*NU+D2

J22=D1*XC+D3

FXC=XC*(C1*NU+C2)+(C3*NU+C4)

GXC=XC*(D1*NU+D2)+(D3*NU+D4)

DELTA=J11*J22-J21*J12

FXC=ABS(FXC)

GXC=ABS(GXC)

IF(FXC.LT.EPS) GO TO 10

GO TO 2

IF(GXC.LT.EPS) GO TO 30

GO TO 2

I=I+1

H=(-FXC#J22+GXC#J12)/DELTA

K=(-GXC#J11+FXC#J21)/DELTA

XC=XC+H

NU=NU+K

IF(J.GT.100)GOTO30

GOTO40

PRINT7, XC, XM, NU, FXC, GXC, J

FORMAT(4X, 'XC=' , F9.6, 4X, 'XM=' , F9.6, 4X, 'NU=' , F10.6, 4X, 'FXC

APPENDIX - F

I='R12.5, AX, 'GXC='R12.5, IX, 'I='I)

PERFORMANCE OF THE MACHINE

C=1./(2.*B*.14*5*.1100.*X)

RSP=RS/F

RGF=RL/F

A=*((R1*7)**2+(F**2*X1+XC)**2)

RF=(RL**2*X1*XC+F**2*AL*XC*1+RD*XC**2)/A

PIA=(-RL**2+F*XC-F**2*X1**2*XC+F*AL*XC**2)/A

Z1=CMPLX(RF,PIA)

Z1S=CMPLX(RSP,X1)

Z1L=CMPLX(RGF,X1)

Z1=Z1+Z1S

ALS=VGF/Z1

ALSD=CABS(ALS)

ALSD=ALSD*IBASE

ALSD=ALSD*1.732

VTF=VGF-Z1S*ALS

VTF=CABS(VTF)

VT=VTF**F

VT1=VT*VBASE

ATL=VTF/Z1

ATL=CABS(ATL)

ATL=ATL*IBASE

ATL=ATL*1.732

AIC=IBASE*VTF/XC

CVAR=3.*AIC*VT1

PHASE=IBASE*VBASE

VAOBT=3.*PHASE*ATL*VT

RRF=RR/(CF-RC)

ZR=CMPLX(RRF,X1)

ARR=-VGF/ZR

ARR=CABS(ARR)

ARR=ARR*IBASE

PGS=-3.*PBAS.*(ARR**2+RRF**F)

POUT=3.*PBAS*(ATL**2*RL)

P1=F*PBAS

```
PRINTB,C,VT,PGEN,AIRP,VT1,AIC,ALLI,AISL,CVAR,VAGHT,POUT,F1
FORMAT(1X,'C=',E13.6,4X,'VT=',F9.6,4X,'PGEN=',F10.6,4X,'AIR ='
1,F11.6,4X,'VT1=',F13.6,4X,'AIC=',F10.6,4X,'ALLI=',F10.6,
24X,'AISL=',F10.6,4X,'CVAR=',F12.6,4X,'VAGHT=',F12.6
3,4X,'POUT=',F12.6,4X,'F1=',F7.4)
IF(AISL.GT.6.0)GO TO 71
CONTINUE
IF(F.LT.FMAX)GO TO 60
GO TO 61
F=F+DF
GO TO 119
STOP
CLOSE(UNIT=3)
END
```